arXiv:hep-th/0701156v2 12 Mar 2009

hep-th/0701156

The Refined Topological Vertex

Amer Iqbal[1], Can Kozçaz[2], Cumrun Vafa[3,4]

[1]Department of Mathematics,
University of Washington,
Seattle, WA, 98195, U.S.A.

[2]Department of Physics,
University of Washington,
Seattle, WA, 98195, U.S.A.

[3]Jefferson Physical Laboratory,
Harvard University,
Cambridge, MA, 02138, U.S.A.

[4]Center for Theoretical Physics,
Massachusetts Institute of Technology,
Cambridge, MA, 02139, U.S.A.

Abstract

We define a refined topological vertex which depends in addition on a parameter, which physically corresponds to extending the self-dual graviphoton field strength to a more general configuration. Using this refined topological vertex we compute, using geometric engineering, a two-parameter (equivariant) instanton expansion of gauge theories which reproduce the results of Nekrasov. The refined vertex is also expected to be related to Khovanov knot invariants.

Contents

1 Introduction **2**

2 GV Formulation and Topological Vertex **6**

2.1 Topological string amplitudes and GV reformulation 6

2.2 Partition function from the topological vertex 9

3 The Refined Topological Vertex **11**

4 Open String Partition Function and Sym$^\bullet(\mathbb{C})$ **13**

4.1 Stack of Branes 17

4.2 Refined vertex and open string partition function 18

4.3 Brane orientation and the gluing rule 21

5 Refined Partition Functions from the Refined Vertex **21**

5.1 $\mathcal{O}(-1) \oplus \mathcal{O}(-1) \mapsto \mathbb{P}^1$ 22

5.2 χ_y-genus, Sym$^\bullet(\mathbb{C}^2)$ and the refined topological vertex 24

5.3 $\mathcal{O}(0) \oplus \mathcal{O}(-2) \mapsto \mathbb{P}^1$ 26

5.4 Another toric geometry: $\mathbb{C}^3/\widetilde{\mathbb{Z}_2 \times \mathbb{Z}_2}$ 28

5.5 Local $\mathbb{P}^1 \times \mathbb{P}^1$ 29

5.5.1 Partition function from instanton calculation 31

5.5.2 Spin content of BPS states 32

5.6 Local $\mathbb{F}_m$ 33

5.6.1 Spin content of BPS states: local $\mathbb{F}_1$ 35

5.7 An $SU(3)$ geometry 38

5.8 An $SU(3)$, $N_f = 4$ geometry 39

5.9 Slicing independence of the partition function 41

6 Conclusion **42**

7 Appendix A: Derivation of the Refined Topological Vertex **43**

7.1 Young diagrams and skew partitions 43

7.2 Plane partitions and skew plane partitions 45

7.3 Transfer matrix approach and Schur functions 48

7.4 Partition function with an infinite number of parameters 51

7.5 Equivariant parameters, boundary of the Young diagram and instanton calculus 55

7.6 q, t slices and the boundary of the Young diagram 57

7.7 Framing factors 61

8 Appendix B: Gromov-Witten Theory and Refined Partition Function: The case of $\mathcal{O}(-1) \oplus \mathcal{O}(-1) \mapsto \mathbb{P}^1$ **62**

9 Appendix C: An Important Identity **64**

10 Appendix D: Schur Functions **65**

1 Introduction

The study of topological strings on Calabi-Yau manifolds has been the topic of intense research for many years now. There are a number of conjectures relating the topological string amplitudes with various generating functions of interest to both physicists and mathematicians.

The Calabi-Yau threefold (CY3-fold) X gives rise to the corresponding compactified theory via M-theory compactification. In this way gauge theories with certain gauge groups and matter content can be geometrically engineered using CY3-folds [1, 2]. The topological string partition function on such spaces is expected to be related to instanton sums in gauge theories. This conjecture has been sharpened, thanks to the work of Nekrasov [3], which provides the tool to directly compute the partition function of 5D supersymmetric gauge theory on $\mathbb{C}^2 \times S^1$.

On the other hand, using the topological vertex formalism [4, 5] the partition function of topological string can be evaluated on such backgrounds. In particular, for $U(N)$ gauge

theories with and without hypermultiplets, the equivalence of gauge theory and the corresponding topological string partition function has been proven using the topological vertex formalism [6–9]. However, as was noted in [8], the instanton calculus [3] which was used to calculate the gauge theory partition function has more refined information. Recall that on the gauge theory side the partition function is calculated using localization in equivariant K-theory [10, 11] with respect to an $r+2$ dimensional torus $\mathbb{T}^2 \times \mathbb{K}$, where $\mathbb{K}$ is the r dimensional maximal torus of the gauge group and $\mathbb{T}^2$ acts on the $\mathbb{C}^2$,

$$\mathbb{T}^2 : \ (z_1, z_2) \mapsto \ (e^{i\epsilon_1} z_1, e^{i\epsilon_2} z_2) \, . \tag{1}$$

The $\mathbb{T}^2$ action on $\mathbb{C}^2$ lifts to an action on the instanton moduli space such that the fixed points are labeled by the colored partitions (Young diagrams) of certain instanton charge [12].

The gauge theory partition function is a function of two equivariant parameters $\epsilon_{1,2}$. For $\epsilon_1 = -\epsilon_2 = g_s$, the gauge theory partition function reduces to the A-model topological string partition function with genus parameter g_s [6, 7]. In this limit ($\epsilon_1 + \epsilon_2 = 0$), the topological vertex formalism can be used to calculate the partition function from the toric geometry of the corresponding CY3-fold. However, the usual topological vertex formalism, needs to be extended to deal with the case $\epsilon_1 + \epsilon_2 \neq 0$.

Recall that the topological string partition function is the generating function of the Gromov-Witten invariants. Therefore a natural question to ask is whether the partition function with $\epsilon_1 + \epsilon_2 \neq 0$ is the generating function of some invariants more refined than the Gromov-Witten invariants. The Gopakumar-Vafa (GV) reformulation [13] of the topological string amplitudes suggests such a possibility which was explored in [8]. Given a CY3-fold X, the M-theory compactification on X gives (in an appropriate limit) a 5D supersymmetric gauge theory with eight supercharges. The BPS particles in the 5D theory have a geometric origin as the M2-branes wrapped on holomorphic curves in X. The mass of such a particle coming from the holomorphic curve $C \in H_2(X, \mathbb{Z})$ is given by $\int_C \omega$, where ω is the Kähler form on X. The spin of these particles is classified by the little group of massive particles which in 5D is $SO(4) \simeq SU(2)_L \times SU(2)_R$. Compactifying on a circle to get Type IIA on X, the wrapped M2-branes with some momentum in the compact direction become the bound states of D2-branes with D0-branes. The number of particles with charge $C \in H_2(X, \mathbb{Z})$ and $SU(2)_L \times SU(2)_R$ spin (j_L, j_R), $N_C^{(j_L, j_R)}$, is equal to the number of the cohomology classes of the moduli space of D2-brane wrapped on C. For generic CY3-folds, $N_C^{(j_L, j_R)}$ is not an invariant and can change as we change the complex structure. But $N_C^{j_L} = \sum_{j_R} (-1)^{2j_R} (2j_R +$

1)$N_C^{(j_L,j_R)}$, which sums over all j_R's with alternating signs, remains *invariant*. For the case of non-compact toric CY3-folds, there are no complex structure deformations. Therefore, one would expect no jumps in the $N_C^{(j_L,j_R)}$ degeneracies, and so one would hope to be able to compute these as well.

Because the D-brane has a $U(1)$ gauge field living on its worldvolume, the moduli space of supersymmetric configurations includes not only the curve moduli but also the moduli of the flat connections on the curve coming from the gauge field. Since the moduli space of flat connections on a smooth curve of genus g is T^{2g}, the moduli space of the D-brane is a T^{2g} fibration over the moduli space of the curve. The total space is a Kähler manifold and the Lefschetz action by the Kähler class is the diagonal $SU(2)_D \subset SU(2)_L \times SU(2)_R$ action on the moduli space. The $SU(2)_L \times SU(2)_R$ action on the moduli space is such that $SU(2)_L$ acts on the fiber direction and the $SU(2)_R$ acts in the base direction.

The topological string partition function is the generating function of the invariants $N_C^{j_L}$,

$$\begin{aligned} Z(\omega, g_s) &:= \exp\Big(\sum_{g\geq 0} g_s^{2g-2} F_g(\omega)\Big) \\ &= \prod_{C\in H_2(X,\mathbb{Z})} \prod_{j_L} \prod_{k_L=-j_L}^{+j_L} \prod_{m=0}^{\infty} \Big(1 - q^{2\,k+m+1}\, Q^C\Big)^{(-1)^{2j_L+1}(m+1)N_C^{j_L}} , \end{aligned} \tag{2}$$

where $q = e^{ig_s}$ and $Q^C = e^{-\int_C \omega}$. The parameters Q give the charge under $H_2(X,\mathbb{Z})$ whereas the parameter q couples with the $SU(2)_L$ spin.

As mentioned before, for Calabi-Yau manifolds which do not admit any complex structure deformations, such as non-compact toric threefolds, the multiplicities $N_C^{(j_L,j_R)}$ themselves are invariants. Using these multiplicities we can define a refined topological string partition function with a product structure similar to the one given above [8],

$$Z(\omega, q, t) := \prod_{C\in H_2(X,\mathbb{Z})} \prod_{j_L,j_R} \prod_{k_L=-j_L}^{+j_L} \prod_{k_R=-j_R}^{+j_R} \prod_{m_1,m_2=1}^{\infty} \Big(1 - t^{k_L+k_R+m_1-\frac{1}{2}}\, q^{k_L-k_R+m_2-\frac{1}{2}} Q^C\Big)^{M_C^{(j_L,j_R)}} , \tag{3}$$

$$M_C^{(j_L,j_R)} = (-1)^{2(j_L+j_R)+1} N_C^{(j_L,j_R)} ,$$

where the parameters $\sqrt{q\,t}$ and $\sqrt{\frac{t}{q}}$ couple with $SU(2)_L$ and $SU(2)_R$ spin, respectively.

It was argued in [8] that for Calabi-Yau manifolds which give rise to $\mathcal{N} = 2$ supersymmetric gauge theories via geometric engineering, the refined topological string partition function is

equal to the partition function of the compactified 5D gauge theory, *i.e.*, the K-theoretic version of the Nekrasov's instanton partition functions [10, 11, 14] with $q = e^{i\epsilon_1}, t = e^{-i\epsilon_2}$.

The topological vertex formalism [4] provides a powerful method to calculate the topological string partition function for non-compact toric CY3-folds. A similar formalism to calculate the refined partition functions will be very interesting providing a refinement of the Gromov-Witten and Donaldson-Thomas theories of toric CY3-folds. The purpose of this paper is to develop such a formalism. We will define a refined topological vertex $C_{\lambda\,\mu\,\nu}(t, q)$ which now depends on one extra parameter compared to the ordinary topological vertex, where together with the usual gluing algorithm for toric CY3-folds, gives the refined topological string partition. However, the refined vertex can be used to define the refined invariants only when the toric Calabi-Yau threefold is made of vertices, all of which contain a fixed locus (p, q) of vanishing cycle in T^2 (which is a subset of the T^3 fibration of toric geometries). This implies that we can compute the refined topological string amplitudes only for toric threefolds which are somewhat special. However, one can also obtain a generic toric case from the refined vertex by using analytic continuation and doing flops on the vertices. This in particular means that the refined vertex is not cyclically symmetric as the usual topological vertex. The toric CY3-folds for which the refined vertex works are exactly those which give rise to gauge theories via geometric engineering. This implies that the refined vertex contains no more information than the K-theoretic version of the instanton partition functions. However, the refined vertex provides a combinatorial interpretation of the instanton partitions functions. Since the refined vertex is not cyclically symmetric a certain choice of direction in the toric diagram of the CY3-fold has to be made.

The fact that the topological vertex has a combinatorial interpretation in terms of counting certain 3D partitions with fixed asymptotes is a well known fact [15]. *As a guiding principal in formulating the refined topological vertex we will demand a similar combinatorial interpretation in terms of 3D partitions for the refined vertex.*[1]

This paper is organized as follows. In section 2, we will review GV formulation of the topological string amplitudes and their computation using the topological vertex formalism. In section 3, we propose the refined topological vertex. In section 4, we discuss the connection between the refined vertex and stacks of branes, and motivate the gluing rules for the refined vertex. In section 5, we will calculate the refined partition functions for certain geometries

[1] For another attempt at defining a refined topological vertex see [16].

using the refined vertex. In particular, we show how one recovers Nekrasov's results using the refined vertex. We also compute the degeneracy of the BPS states in these geometries and explain the $SU(2)_L \times SU(2)_R$ content of the states. In Appendix A, we will give the complete derivation of the refined vertex in terms of 3D partitions. In Appendix B, we will show that the refined partition function of $\mathcal{O}(-1) \oplus \mathcal{O}(-1) \mapsto \mathbb{P}^1$ can be obtained by appropriately weighting the contribution of the holomorphic maps to the two fixed points of the geometry. We will also show that for $\mathbb{C}^3$ by appropriately weighting the contribution of the maps to the torus invariant fixed point gives a generalization of the MacMahon function which also has a combinatorial interpretation.

2 GV Formulation and Topological Vertex

In this section, we will briefly review the Gopakumar-Vafa reformulation of the topological string amplitudes and their calculation using the topological vertex.

2.1 Topological string amplitudes and GV reformulation

The topological string amplitudes F_g arise in the A-twisted topological theory as integrals over the genus g moduli space of Riemann surfaces and are related to the generating functions of the genus g Gromov-Witten invariants. The general form of these amplitudes is given by

$$\begin{aligned} F_0(\omega) &= \frac{1}{3!}\int_X \omega\wedge\omega\wedge\omega + \sum_{C\in H_2(X,\mathbb{Z})} \mathcal{N}_C^0\, e^{-\int_C \omega}\,, \\ F_1(\omega) &= -\frac{1}{24}\int_X \omega\wedge c_2(X) + \sum_{C\in H_2(X,\mathbb{Z})} \mathcal{N}_C^1\, e^{-\int_C \omega}, \\ F_{g\geq 2}(\omega) &= (-1)^g \frac{\chi(X)}{2}\int_{\overline{\mathcal{M}}_g} \lambda_{g-1}^3 + \sum_{C\in H_2(X,\mathbb{Z})} \mathcal{N}_C^g\, e^{-\int_C \omega}\,, \end{aligned} \tag{4}$$

where ω is the Kähler form, $\mathcal{N}_C^g$ is the genus g Gromov-Witten invariant of C, $\overline{\mathcal{M}}_g$ is the moduli space of genus g Riemann surfaces and λ_{g-1} is the g^{th} Chern class of the Hodge bundle over $\overline{\mathcal{M}}_g$ (see Appendix B). The topological string amplitudes can be compactly organized into the generating function, the topological string partition function

$$Z(\omega, g_s) = \exp\Big(\sum_{g=0}^{\infty} g_s^{2g-2} F_g(\omega)\Big)\,. \tag{5}$$

From the worldsheet perspective, the genus g amplitude, F_g, is the generating function of the "number" of maps from a genus g Riemann surface to CY3-fold X. However, the target space viewpoint provides a more physical interpretation of the generating function $F(\omega, g_s)$ [13]. We will briefly review this interpretation since it is crucial in understanding the refined partition functions. Recall that in M-theory compactification on CY3-fold X we get a 5D field theory with eight supercharges. The particles in this theory come from quantization of the moduli space of wrapped M2-branes on various 2-cycles of X. These particles carry $SU(2)_L \times SU(2)_R$ quantum numbers where $SU(2)_L \times SU(2)_R = SO(4)$ is the little group of massive particles in 5D. If we compactify one direction, then the particles can be interpreted as wrapped D2-branes and the Kaluza-Klein modes as bound D0-branes. These charged particles when integrated out give rise to the F-terms in the effective action. The contribution of a particle of mass m and in representation $\mathcal{R}$ of the $SU(2)_L \times SU(2)_R$ to F is given by

$$S = \log\det(\Delta + m^2 + 2e\,\sigma_L\mathcal{F}) \;= \int_\epsilon^\infty \frac{ds}{s}\frac{\mathrm{Tr}_{\mathcal{R}}(-1)^{\sigma_L+\sigma_R}e^{-sm^2}e^{-2se\sigma_L\mathcal{F}}}{(2\sinh(se\mathcal{F}/2))^2}\,, \tag{6}$$

where σ^L is the Cartan of $SU(2)_L$ and arises because the graviphoton field strength is self-dual. e is the charge of the particle, and is equal to its mass and we identify the graviphoton field strength $\mathcal{F} = g_s$. The mass of the particle is given by the area of the curve on which the D2-brane is wrapped. An extra subtlety arises due to D0-branes. In the lift to M-theory, we see that a wrapped M2-brane comes with momentum in the circle direction, and therefore, if we denote the mass of the M2-brane wrapping a curve class $C \in H_2(X,\mathbb{Z})$ by T_C then the mass of the M2-brane with momentum n is given by taking T_C to $T_C + 2\pi i n/g_s$. Let us denote by $N_C^{(j_L,j_R)}$ the number of BPS states coming from an M2-brane wrapped on the holomorphic curve C, and the left-right spin content under $SU(2)_L \times SU(2)_R$ given by (j_L, j_R). Then the total contribution coming from all particles is obtained by summing over the momentum, the holomorphic curves and the left-right spin content,

$$\begin{aligned}
F &= \sum_{C\in H_2(X,\mathbb{Z})}\sum_{n\in\mathbb{Z}}\sum_{j_L,j_R} N_C^{(j_L,j_R)}\int_\epsilon^\infty \frac{ds}{s}\frac{\mathrm{Tr}_{(j_L,j_R)}(-1)^{\sigma_L+\sigma_R}e^{-sT_C-2\pi i n}e^{-2s\sigma_L\lambda_s}}{(2\sinh(s\lambda_s/2))^2} \\
&= \sum_{C\in H_2(X,\mathbb{Z})}\sum_{k=1}^\infty\sum_{j_L,j_R} N_C^{(j_L,j_R)}e^{-kT_C}\frac{\mathrm{Tr}_{(j_L,j_R)}(-1)^{\sigma_L+\sigma_R}e^{-2k\lambda_s\sigma_L}}{k(2\sinh(k\lambda_s/2))^2} \\
&= \sum_{C\in H_2(X,\mathbb{Z})}\sum_{k=1}^\infty\sum_{j_L} N_C^{j_L}e^{-kT_C}\frac{\mathrm{Tr}_{j_L}(-1)^{\sigma_L}e^{-2k\lambda_s\sigma_L}}{k(2\sinh(k\lambda_s/2))^2}\,, \quad \text{where} \quad N_C^{j_L} = \sum_{j_R} N_C^{(j_L,j_R)}(-1)^{2j_R}(2j_R+1)\,.
\end{aligned} \tag{7}$$

In terms of these integers $N_C^{j_L}$ one can write F as

$$F = \sum_{C\in H_2(X,\mathbb{Z})} \sum_{k=1}^{\infty} \sum_{j_L} (-1)^{2j_L} N_C^{j_L} e^{-kT_C} \Big(\frac{q^{-2j_L k} + \cdots + q^{+2j_L k}}{k(q^{k/2} - q^{-k/2})^2} \Big) , \quad q = e^{ig_s} . \tag{8}$$

If we turn on a constant graviphoton field strength which is not self-dual $F = F_1\, dx^1 \wedge dx^2 + F_2\, dx^3 \wedge dx^4$, then we can write the contribution that comes from integrating out the particle in representation $\mathcal{R}$ of $SU(2)_L \times SU(2)_R$ as

$$S := \int_\epsilon^\infty \frac{ds}{s} \frac{\mathrm{Tr}_{\mathcal{R}} (-1)^{\sigma_L + \sigma_R} e^{-sm^2} e^{-2se(\sigma_L F_+ + \sigma_R F_-)}}{(2\sinh(seF_1/2))(-2\sinh(seF_2/2))} . \tag{9}$$

Summing over the contributions from all particles as before we get

$$F(\omega, t, q) = \sum_{C\in H_2(X,\mathbb{Z})} \sum_{n=1}^{\infty} \sum_{j_L, j_R} \frac{(-1)^{2j_L+2j_R}\, N_C^{(j_L,j_R)} \Big((t\,q)^{-nj_L} + \cdots + (t\,q)^{nj_L} \Big) \Big((\frac{t}{q})^{-nj_R} + \cdots + (\frac{t}{q})^{nj_R} \Big)}{n(t^{n/2} - t^{-n/2})(q^{n/2} - q^{-n/2})}\, e^{-nT_C} , \tag{10}$$

where $q = e^{F_1}, t = e^{F_2}$. The integers $N_C^{(j_L,j_R)}$ give the degeneracy of particles with spin content (j_L, j_R), and charge C and are the number of cohomology classes with spin (j_L, j_R) of the moduli space of a D-brane wrapped on a holomorphic curve in the class C [13].

As an example, consider the local $\mathbb{P}^1 \times \mathbb{P}^1$ which we will denote by X. M-theory compactification on $S^1 \times X$ gives $SU(2)$ gauge theory with eight supercharges. In this case, the gauge theory partition function was calculated in [3]. As we will show in the last section this partition function can be obtained from the refined topological vertex as well and is given by[2]

$$\begin{aligned}
Z(Q_b, Q_f, t, q) &= \sum_{\nu_1,\nu_2} Q_b^{|\nu_1|+|\nu_2|} Z(\nu_1, \nu_2; Q_f, t, q) \qquad (11)\\
Z(\nu_1, \nu_2; Q, t, q) &:= \Big(\frac{t}{q}\Big)^{|\nu_1|+|\nu_2|} q^{||\nu_1^t||^2}\, t^{||\nu_2||^2}\, \widetilde{Z}_{\nu_1^t}(t,q) \widetilde{Z}_{\nu_1}(q,t) \widetilde{Z}_{\nu_2^t}(t,q) \widetilde{Z}_{\nu_2}(q,t)\, G(\nu_1, \nu_2, Q, t, q)\\
G(\nu_1, \nu_2, Q, t, q) &= \prod_{i,j=1}^{\infty} \frac{(1 - Q\, q^{j-1} t^i)(1 - Q\, (q/t)\, q^{j-1} t^i)}{(1 - Q\, q^{-\nu_{2,i}^t + j - 1}\, t^{-\nu_{1,j} + i})(1 - Q\, (q/t)\, q^{-\nu_{2,i}^t + j - 1}\, t^{-\nu_{1,j} + i})}
\end{aligned}$$

$$\widetilde{Z}_\nu(t, a) = \prod_{(i,j)\in\nu} (1 - t^{a(i,j)+1} q^{\ell(i,j)})^{-1} , \quad a(i,j) = \nu_j^t - i\, , \ \ell(i,j) = \nu_i - j\, , \tag{12}$$

[2] $\nu_{1,2}$ are 2D partitions, ν^t is the transpose partition and $||\nu||^2 = \sum_i \nu_i^2$.

where $-\log(Q_{b,f}) = T_{b,f}$ are the Kähler parameters associated with the base and the fiber $\mathbb{P}^1$'s.

We can use the above partition function to calculate the BPS degeneracies of various states corresponding to charge $C \in H_2(X, \mathbb{Z})$. For example, consider the curve $2B + 2F$, the canonical class of the $\mathbb{P}^1 \times \mathbb{P}^1$. This is a genus one curve and therefore the corresponding moduli space will admit non-trivial $SU(2)_L$ action. The spin content can be extracted from the refined partition function and is given by

$$\sum_{j_L, j_R} N^{(j_L, j_R)}_{2B+2F}(j_L, j_R) = (\tfrac{1}{2}, 4) \oplus (0, \tfrac{7}{2}) \oplus (0, \tfrac{5}{2})\,. \tag{13}$$

To see that this is the correct result note that the moduli space of $2B + 2F$ together with its Jacobian is given by a $\mathbb{P}^7$ bundle over $\mathbb{P}^1 \times \mathbb{P}^1$: pick a point in $\mathbb{P}^1 \times \mathbb{P}^1$, the moduli space of curves passing through that point in the class $2B + 2F$ is given by $\mathbb{P}^7$. Thus the diagonal $SU(2)_L \times SU(2)_R$ action which is just the Lefshetz action is given by

$$(\tfrac{1}{2}) \otimes (\tfrac{1}{2}) \otimes (\tfrac{7}{2}) = (\tfrac{5}{2}) \oplus 2(\tfrac{7}{2}) \oplus (\tfrac{9}{2})\,. \tag{14}$$

Note that since $2B + 2F$ is a genus one curve, the corresponding Jacobian is also genus one, and therefore j_L can only be 0 or $\frac{1}{2}$. From this restriction on j_L and the above diagonal action, we see that the unique left-right spin content is given by

$$(\tfrac{1}{2}, 4) \oplus (0, \tfrac{7}{2}) \oplus (0, \tfrac{5}{2})\,, \tag{15}$$

exactly as predicted by the partition function calculation

2.2 Partition function from the topological vertex

The topological vertex formalism [4] completely solves the problem of calculating the topological string partitions for toric CY3-folds. Consider the topological A-model with a toric non-compact Calabi-Yau manifold X as its target space. The amplitude of this model is the sum over the holomorphic maps from a Riemann surface Σ_g of genus g to the target Calabi-Yau manifold X where each term is weighted by the area of the surface in X. One can use the so-called toric diagrams (or web diagrams) to encode the geometry of the target space as a tri-valent graph on the plane. These diagrams show the degeneration loci of the toric action on X, *i.e.*, along each edge of the web one of the 1-cycles of the fiber $\mathbb{T}^2$ shrinks

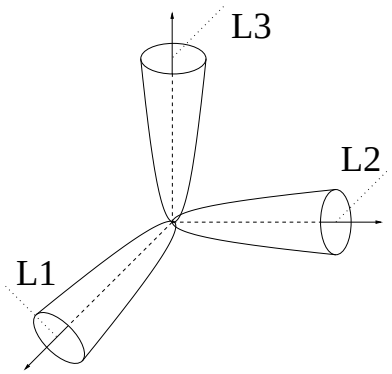

Figure 1: The holomorphic maps wrapping the disks along the degeneration loci with boundaries on the Lagrangian branes.

leaving the dual cycle S^1. The basic idea behind the topological vertex is to divide the corresponding toric diagram of X into tri-valent vertices, which, from physics point of view, should be considered as placing Lagrangian D-brane/anti-D-brane pairs to "cut" X. Each tri-valent vertex corresponds to a $\mathbb{C}^3$ patch.

The separation of the target space into $\mathbb{C}^3$ patches results in cuts in the holomorphic maps from the worldsheet to the target space as well. In other words, one ends up with Riemann surfaces (not to be confused with Σ_g) with boundaries over the point on the edge where the cut is made. The boundaries live on stack of D-branes (or anti-D-branes) along the three edges of the web. Closed string amplitudes on a given toric Calabi-Yau manifold are obtained by an appropriate gluing procedure. The rules to calculate the topological string amplitude on general toric, non-compact Calabi-Yau manifolds, given the toric diagram are the following:

- After dividing the toric diagram into vertices, associate each edge described by an integer vector v_i with a representation μ_i.
- The orientation of the vectors (v_i, v_j, v_k) describing the degeneration loci is important in order to write down correctly the associated vertex to each patch: if all vectors v_i are incoming then $C_{\mu_i\mu_j\mu_k}$ is the correct factor, otherwise we replace the partition with its transpose μ^t for any outgoing edge.
- Once we have set up all vertices and the associated factors $C_{\mu_i\mu_j\mu_k}$, we can glue them along their common edges. Assume that two vertices have the same v_i, we can take

one of the v_i's to be incoming on one vertex and outgoing on the other one. Then "gluing" turns out to be the following summation

$$\sum_{\mu_i}(-1)^{(n_i+1)\ell(\mu_i)}q^{-n_i\frac{\kappa(\mu_i)}{2}}e^{-\ell(\mu_i)t_i}C_{\mu_j\mu_k\mu_i}C_{\mu_i^t\mu_j'\mu_k'} \tag{16}$$

with the integer $n_i = |v_k' \wedge v_k|$. The appearance of this factor signals the equality of the framing along an edge on both vertices.

- The Kähler parameter T_i associated to an edge described by $v_i = (p_i, q_i)$ is given by $T_i = x_i/\sqrt{p_i^2+q_i^2}$ where x_i is the length in the plane.
- The partition μ along any non-compact direction is a trivial one and denoted by "$\emptyset$".

A useful representation of the vertex is given using the skew-Schur functions [15],

$$C_{\lambda\,\mu\,\nu}(q) = q^{\frac{\kappa(\mu)}{2}}s_{\nu^t}(q^{-\rho})\sum_{\eta}s_{\lambda^t/\eta}(q^{-\nu-\rho})s_{\mu/\eta}(q^{-\nu^t-\rho})\,, \tag{17}$$

where $q^{-\nu-\rho} = \{q^{-\nu_1+1/2}, q^{-\nu_2+3/2}, q^{-\nu_3+5/2}, \cdots\}$, and $s_{\mu/\eta}(x)$ is the skew-Schur function[3] defined, using the Littlewood-Richardson coefficients $c^{\mu}_{\eta\,\lambda}$, in terms of the Schur functions,

$$s_{\mu/\eta}(x) = \sum_{\lambda} c^{\mu}_{\eta\lambda}s_{\lambda}(x)\,. \tag{18}$$

3 The Refined Topological Vertex

In this section, we will explain the combinatorial interpretation of the refined vertex in terms of 3D partitions leaving the complete derivation to Appendix A where the relevant notation is also reviewed.

Recall that the generating function of the 3D partitions is given by the MacMahon function,

$$M(q) = \sum_{n\geq 0}C_n q^n = \prod_{k=1}^{\infty}(1-q^n)^{-n}\,. \tag{19}$$

The topological vertex $C_{\lambda\,\mu\,\nu}(q)$ has the following combinatorial interpretation [15]

$$M(q)C_{\lambda\,\mu\,\nu}(q) = \sum_{\pi(\lambda,\mu,\nu)} q^{|\pi(\lambda,\mu,\nu)|-|\pi_\bullet(\lambda,\mu,\nu)|}\,, \tag{20}$$

[3]For a brief overview see Appendix D

where $\pi(\lambda,\mu,\nu)$ is a 3D partition such that along the three axes it asymptotically approaches the three 2D partitions λ,μ and ν. $|\pi|$ is number of boxes (volume) of the 3D partition π and $\pi_\bullet$ is the 3D partition with the least number of boxes satisfying the same boundary condition[4].

The refined vertex also has a similar combinatorial interpretation in terms of 3D partitions which we will explain now. Recall that the diagonal slices of a 3D partition, π, are 2D partitions which interlace each other. These are the 2D partitions living on the planes $x-y=a$, where $a\in\mathbb{Z}$. We will denote these 2D partitions by π_a. For the usual vertex the a^{th} slice is weighted with $q^{|\pi_a|}$, where $|\pi_a|$ is the number of boxes cut by the slice (the number of boxes in the 2D partition π_a). The 3D partition is then weighted by

$$\prod_{a\in\mathbb{Z}} q^{|\pi_a|} = q^{\sum_{a\in\mathbb{Z}}|\pi_a|} = q^{\#\text{ of boxes in the }\pi} \tag{21}$$

In the case of the refined vertex, the 3D partition is weighted in a different manner. Given a 3D partition π and its diagonal slices π_a we weigh the slices for $a<0$ with parameter q and the slices with $a\geq 0$ with parameter t so that the measure associated with π is given by

$$\Big(\prod_{a<0} q^{|\pi_a|}\Big)\Big(\prod_{a\geq 0} t^{|\pi_a|}\Big) = q^{\sum_{i=1}^{\infty}|\pi(-i)|}\, t^{\sum_{j=1}^{\infty}|\pi(j-1)|}\,. \tag{22}$$

The generating function for this counting is a generalization of the MacMahon function and is given by

$$M(t,q) := \sum_{\pi} q^{\sum_{i=1}^{\infty}|\pi(-i)|}\, t^{\sum_{j=1}^{\infty}|\pi(j-1)|} = \prod_{i,j=1}^{\infty}(1-q^{i-1}t^j)^{-1}\,. \tag{23}$$

We can think of this assignment of q and t to the slices in the following way. If we start from large positive a and move towards the slice passing through the origin then everytime we move the slice towards the left we count it with t and everytime we move the slice up (which happens when we go from $a=i$ to $a=i-1$, $i=0,1,2\cdots$) we count it with q.

Since we are slicing the skew 3D partitions with planes $x-y=a$ we naturally have a preferred direction given by the z-axis. Let us take the 2D partition along the z-axis to be ν. The case we discussed above, obtaining the refined MacMahon function, corresponds to $\nu=\emptyset$. For a non-trivial, ν the assignment of q and t to various slices is different and depends on the shape of ν. As we go from $+\infty$ to $-\infty$ the slices are counted with t if we go towards the left and is counted with q if we move up. An example is shown in Fig. 2.

[4]Since even the partition with the least number of boxes has infinite number of boxes we need to regularize this by putting it in an $N\times N\times N$ box as discussed in [15].

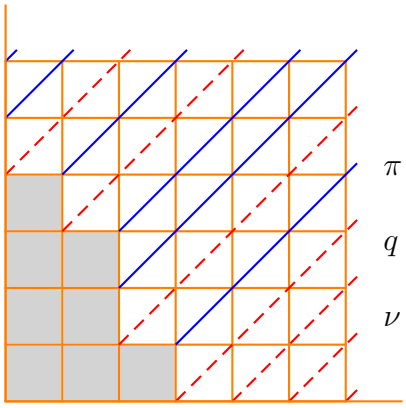

$\pi \rightarrow \prod_{a\in\mathbb{Z}} q_a^{|\pi(a)|} = q^{\sum_{i=1}^{\infty}|\pi(\nu_i^t-i)|}\, t^{\sum_{j=1}^{\infty}|\pi(-\nu_j+j-1)|}$

$q =$ blue (solid line), $t =$ red (dashed line)

$\nu = (4,3,1)$

Figure 2: Slices of the $3D$ partitions are counted with parameters t and q depending on the shape of ν.

After taking into account the framing and the fact that the slices relevant for the topological vertex are not the perpendicular slices [15] the generating function is given by

$$G_{\lambda\,\mu\,\nu}(t,q) = \left(\frac{q}{t}\right)^{\frac{||\mu||^2+||\nu||^2}{2}} t^{\frac{\kappa(\mu)}{2}}\, M(t,q) P_{\nu^t}(t^{-\rho};q,t) \sum_{\eta} \left(\frac{q}{t}\right)^{\frac{|\eta|+|\lambda|-|\mu|}{2}} s_{\lambda^t/\eta}(t^{-\rho}q^{-\nu}) s_{\mu/\eta}(t^{-\nu^t}q^{-\rho}),$$

and the refined vertex is given by

$$\begin{aligned} C_{\lambda\,\mu\,\nu}(t,q) &= \frac{G_{\lambda\,\mu\,\nu}(t,q)}{M(t,q)} \qquad (24)\\ &= \left(\frac{q}{t}\right)^{\frac{||\mu||^2+||\nu||^2}{2}} t^{\frac{\kappa(\mu)}{2}}\, P_{\nu^t}(t^{-\rho};q,t) \sum_{\eta} \left(\frac{q}{t}\right)^{\frac{|\eta|+|\lambda|-|\mu|}{2}} s_{\lambda^t/\eta}(t^{-\rho}q^{-\nu}) s_{\mu/\eta}(t^{-\nu^t}q^{-\rho}). \end{aligned}$$

In the above expression, $P_\nu(\mathbf{x};q,t)$ is the Macdonald function such that

$$\begin{aligned} P_{\nu^t}(t^{-\rho};q,t) &= t^{\frac{||\nu||^2}{2}}\, \widetilde{Z}_\nu(t,q)\,, \qquad (25)\\ \widetilde{Z}_\nu(t,q) &= \prod_{(i,j)\in\,\nu} (1-t^{a(i,j)+1}q^{\ell(i,j)})^{-1}\,, \quad a(i,j)=\nu_j^t-i\,, \quad \ell(i,j)=\nu_i-j\,. \end{aligned}$$

4 Open String Partition Function and $\mathrm{Sym}^\bullet(\mathbb{C})$

In order to gain some insight into the proposed refined vertex and its gluing rules (to be discussed below) it is useful to recall the connection between topological vertex and open string amplitudes in the presence of stack of A-branes.

Let us consider the connection between open string partition function and the topological vertex. When a stack of Lagrangian D-branes is ending on one of the legs of the $\mathbb{C}^3$ the partition function is given by

$$Z(q;V) = \sum_{\nu} C_{\emptyset\emptyset\nu}(q^{-1})\,\mathrm{Tr}_\nu V\,. \tag{26}$$

Since $\mathrm{Tr}_\nu V = s_\nu(\mathbf{x})$ where $\mathbf{x} = \{x_1, x_2, \cdots\}$ are the eigenvalues of the holonomy matrix V.

$$\begin{aligned} Z(q;V) &= \sum_{\nu} C_{\emptyset\emptyset\nu}(q^{-1})\, s_\nu(\mathbf{x}) \\ &= \sum_{\nu} s_{\nu^t}(q^\rho) s_\nu(\mathbf{x}) = \prod_{i,j=1}^{\infty}(1+q^{-i+\frac{1}{2}}x_j)\,. \end{aligned} \tag{27}$$

In the case of a single Lagrangian brane $\mathbf{x} = (-Q, 0, 0, 0, \cdots)$ we get the well known partition function

$$Z(q;Q) = \prod_{i=1}^{\infty}(1 - Q\,q^{-i+\frac{1}{2}})\,. \tag{28}$$

We will now show that the above partition function of a single Lagrangian brane can be interpreted in terms of the Hilbert series of the the symmetric product of $\mathbb{C}$.

Recall that the Schur functions have the property that

$$s_{\nu/\lambda}(Q) = \begin{cases} Q^{|\nu|-|\lambda|}, & \nu \succ \lambda \\ 0, & \text{otherwise.} \end{cases} \tag{29}$$

This implies that $s_\nu(Q)$ is non-zero only for those partitions for which $\ell(\nu) = 1$, *i.e.*, $\nu = (\nu_1, 0, 0, \cdots)$. These are exactly the partitions which label the fixed points of the symmetric product of $\mathbb{C}$, *i.e.*, $\mathrm{Sym}^k(\mathbb{C})$ has a single fixed point labelled by the partition $\nu = (k, 0, 0, \cdots)$. We can construct a generating function of the Hilbert series of the symmetric products [10],

$$G(\phi, q) := \sum_{k=0}^{\infty} \phi^k\, H[\,\mathrm{Sym}^k(\mathbb{C})](q) \tag{30}$$

Since the symmetric product $\mathrm{Sym}^k(\mathbb{C})$ can be identified with the ring $R_k := \mathbb{C}[z_1, z_2, \cdots, z_k]/S_k$ therefore the Hilbert series is given by [10]

$$\begin{aligned} H[R](q) &= \sum_{n=0}^{\infty} q^n\, r_n(R) \\ r_n(R) &= \#\text{ of monomials in } R \text{ of charge } n \end{aligned} \tag{31}$$

where on $\mathbb{C}$ q acts as a $\mathbb{C}^\times$ action $z \mapsto qz$. To determine $H[\,\mathrm{Sym}^k(\mathbb{C})](q)$ note that the R_k is just the ring of symmetric functions in the variables $(z_1, z_2, \cdots, z_k)$ and therefore the Schur functions provide a basis of R_k,

$$R_k =< \; s_\nu(z_1, \cdots, z_k) | \ell(\nu) \leq k \; >, \tag{32}$$

where the condition $\ell(\nu) \leq k$ is necessary since $s_\nu(z_1, \cdots, z_k) = 0$ for $\ell(\nu) > k$. R_k is isomorphic to the Hilbert space $\mathcal{H}_k$ generated by bosonic oscillator up to charge k. Recall that the bosonic oscillators satisfying the commutation relation

$$[\alpha_n, \alpha_m] = n\delta_{n+m,0} \tag{33}$$

generate the Hilbert space, $\mathcal{H}$, isomorphic to the ring of symmetric functions in infinite variables R . This essentially follows from the identification

$$p_\nu(\mathbf{x}) \leftarrow \quad \nu = 1^{m_1}2^{m_2}\cdots \quad \rightarrow (\alpha_{-1})^{m_1}(\alpha_{-2})^{m_2}\cdots|0\rangle. \tag{34}$$

Under the above identification

$$R_k \simeq \mathcal{H}_k =< (\alpha_{-1})^{m_1}\cdots(\alpha_{-k})^{m_k}|0\rangle \,|\, \{m_1, \cdots m_k \geq 0\} > \tag{35}$$

and the Hilbert spaces $\mathcal{H}_k$ form a nested sequence

$$\mathcal{H}_0 \subset \mathcal{H}_1 \subset \mathcal{H}_2 \subset \mathcal{H}_3 \subset \cdots \tag{36}$$

which corresponds to the nested sequence of Young diagrams of increasing number of rows.

The $\mathbb{C}^\times$ action, which lifts to an action on the $\mathrm{Sym}^\bullet(\mathbb{C})$ such that the Schur functions $s_\nu(z_1, \cdots, z_k)$ are eigenfunctions with eigenvalue $q^{|\nu|}$, becomes the action of q^{L_0} on the states in $\mathcal{H}$ ($L_0 = \sum_{n>0} \alpha_{-n}\alpha_n$),

$$H[R_k](q) = \mathrm{Tr}_{\mathcal{H}_k} q^{L_0} = \sum_{\nu|\ell(\nu)\leq k} q^{|\nu|} = \prod_{n=1}^{k}(1-q^n)^{-1}\,. \tag{37}$$

The Hilbert series of R_k in this case turns out to be the generating function of the number of partitions with at most k parts. We can express $H[R_k](q)$ in terms of the Schur functions,

$$H[R_k](q) = \prod_{n=1}^{k}(1-q^n)^{-1} = s_{(k)}(1, q, q^2, \cdots)\,. \tag{38}$$

The generating functions $G(\phi, q)$ is then given by

$$\begin{aligned} G(\phi,q) &= \sum_{k=0}^{\infty} \phi^k H[R_k](q) = \sum_{k=0}^{\infty} \phi^k \mathrm{Tr}_{\mathcal{H}_k} q^{L_0} \\ &= \sum_{k=0}^{\infty} \phi^k s_{(k)}(1, q, q^2, \cdots) \\ &= \sum_{k=0}^{\infty} s_{(k)}(\phi) s_{(k)}(1, q, q^2, \cdots) = \sum_{\nu} s_\nu(\phi) s_\nu(1, q, q^2, \cdots) \\ &= \sum_{\nu} s_\nu(q^{-\rho}) s_\nu(\phi\, q^{-\frac{1}{2}}) = \sum_{\nu} s_{\nu^t}(q^\rho)\, s_\nu(-q^{-\frac{1}{2}}\phi) \\ &= \sum_{\nu} C_{\emptyset\emptyset\nu}(q^{-1})\, \mathrm{Tr}_\nu V = Z(q; V), \end{aligned} \tag{39}$$

where $\mathrm{Tr}_\nu V = s_\nu(Q)$ and $Q = q^{-\frac{1}{2}}\phi$.

Thus we see that as we move the brane to infinity ($Q = e^{-t} \mapsto 0$) the contribution of the higher modes is suppressed. On the other hand as the brane moves towards the origin ($Q \mapsto 1$) higher oscillator modes starts contributing with equal weight to the partition function.

From the above discussion it also follows that the topological vertex $C_{\emptyset\emptyset(k)}(q)$ has an interpretation as counting the number of states of a given energy in the Hilbert space $\mathcal{H}_k$. It is tempting to conjecture that the topological vertex with all three partitions non-trivial has a similar interpretation. This is supported by the fact that topological vertex when expanded as a powers series in q has non-negative integer coefficients.

It is easy to see that the recursion relation

$$\mathrm{Tr}_{\mathcal{H}_k} q^{L_0} = \frac{1}{1-q^k} \mathrm{Tr}_{\mathcal{H}_{k-1}} q^{L_0} \tag{40}$$

implies that the partition function $Z(q; Q)$ satisfies the equation

$$(q^{-\partial_u} - 1 + q^{\frac{1}{2}}\, e^{-u}) Z(q; e^{-u}) = 0\,. \tag{41}$$

It is easy to determine the disk contribution using this differential equation. Since $Z(q; Q) = \exp(\frac{F_0}{g_s} + F_1 + g_s F_2 + \cdots)$ therefore

$$(g_s \partial_u)^n e^{\frac{F}{g_s}} = e^{F/g_s}\{(\partial_u F)^n + O(g_s)\} \tag{42}$$

Therefore

$$Z^{-1}(q;e^{-u})q^{-\partial_u}Z(q;e^{-u}) = e^{-(\partial_u F)} + O(g_s) \tag{43}$$

which implies in the limit $g_s \mapsto 0$

$$\partial_u F_0 = -\log(1-q^{1/2}e^{-u})\,. \tag{44}$$

This relation was noted in [17] where it was related to the non-commutative geometry of the coordinates on the local mirror geometry. Below we will obtain a similar equation in the context of the refined vertex, whose geometric understanding is an important open question.

4.1 Stack of Branes

In the previous subsection, we considered of a single Lagrangian brane ending on one of the legs. Now we will consider the case of multiple Lagrangian branes on the one of legs of $\mathbb{C}^3$.

The partition function is given by

$$\begin{aligned} Z(\mathbf{x},q) &= \sum_{\nu} C_{\emptyset\emptyset\nu}(q^{-1})\, s_\nu(\mathbf{x})\,, \quad \mathbf{x}=\{x_1,x_2,\cdots,x_N\}\,, \\ &= \prod_{i=1}^{N}\prod_{j=1}^{\infty}(1+q^{-j+\frac{1}{2}}\,x_i)\,. \end{aligned} \tag{45}$$

The above partition function is the generating function of the Hilbert series of product of symmetric products of $\mathbb{C}$. To see consider the following generating function

$$\begin{aligned} G(\varphi_1,\cdots,\varphi_N,q) = \sum_{k_1,\cdots,k_N} \varphi_1^{k_1}\varphi_2^{k_2}\cdots\varphi_N^{k_N}\, H[M_{k_1\cdots k_N}](q)\,, \\ M_{k_1k_2\cdots k_N} = \mathrm{Sym}^{k_1}(\mathbb{C})\times\cdots\times\mathrm{Sym}^{k_N}(\mathbb{C})\,. \end{aligned} \tag{46}$$

The ring of functions on $M_{k_1\cdots k_N}$ is spanned by

$$s_{\nu_1}(x_{1,1},\cdots,x_{1,k_1})s_{\nu_2}(x_{2,1},\cdots,x_{2,k_2})\cdots s_{\nu_N}(x_{N,1},\cdots,x_{N,k_N})\,, \quad \ell(\nu_a)\le k_a\,, a=1,2,\ldots,N.$$

In terms of the bosonic oscillators $\alpha_n^{(a)}$ satisfying the commutation relations

$$[\alpha_n^{(a)},\alpha_m^{(b)}] = n\,\delta_{a,b}\delta_{m+n,0}\,. \tag{47}$$

the above ring is isomorphic to the Hilbert space $\mathcal{H}_{k_1\cdots k_N}$ spanned by

$$\prod_{a=1}^{N}(\alpha_{-1}^{(a)})^{m_{a,1}}\cdots(\alpha_{-k_a}^{(a)})^{m_{a,k_a}}|0\rangle\,. \tag{48}$$

The Hilbert series of $M_{k_1\cdots k_N}$ is then given by the trace of $\mathcal{H}_{k_1\cdots k_N}$,

$$H[M_{k_1\cdots k_N}](q)=\mathrm{Tr}_{\mathcal{H}_{k_1\cdots k_N}}q^{L_0} \tag{49}$$

where $L_0=\sum_{a=1}^{N}\sum_{n>0}\alpha_{-n}^{(a)}\alpha_n^{(a)}$. This implies that

$$H[M_{k_1\cdots k_N}](q)=\sum_{m_{1,1},m_{1,2}\cdots m_{N,k_N}}q^{\sum_{a=1}^{N}\sum_{i=1}^{k_a}im_{a,i}}=\prod_{a=1}^{N}\sum_{m_{a,1},\cdots,m_{a,k_a}}q^{\sum_{i=1}^{k_a}im_{a,i}}=\prod_{a=1}^{N}\prod_{i=1}^{k_a}(1-q^i)^{-1}\,.$$

Since the Hilbert series is given by the product of the Hilbert series therefore

$$G(\varphi_1,\cdots,\varphi_N,q)=\prod_{a=1}^{N}G(\varphi_a,q)=\prod_{a=1}^{N}\prod_{i=1}^{\infty}(1-q^{-i}\varphi_a)=Z(q;\mathbf{x})\,,\quad x_a=-q^{-\frac{1}{2}}\,\varphi_a\,. \tag{50}$$

4.2 Refined vertex and open string partition function

It is natural to expect that the refined vertex also has an interpretation in terms of generalized open topological string amplitudes in the presence of stacks of A-brane. In fact the results of [26] suggests that the Khovanov knot invariants are related to this refinement of the open string amplitude. It thus suggests that we should view the refined vertex as building blocks for computation of Khovanov knot invariants that can be obtained from local toric Calabi-Yau manifolds. The first step in motivating this interpretation is to show that the stack of D-branes in the context of refined vertex can also be related to the symmetric product of $\mathbb{C}$, as it was possible in the context of ordinary vertex. This we will show here.

When using the refined vertex the open string partition function depends on the leg on which the stack of branes is put essentially because the refined vertex is not cyclically symmetric. Thus we have three choices corresponding to the three legs of $\mathbb{C}^3$. We will consider all three cases,

$$\begin{aligned}
C_{\lambda\,\emptyset\,\emptyset}(t,q) &= \left(\tfrac{q}{t}\right)^{\frac{|\lambda|}{2}}s_{\lambda^t}(t^{-\rho})\,, \\
C_{\emptyset\,\mu\,\emptyset}(t,q) &= \left(\tfrac{q}{t}\right)^{\frac{||\mu^t||^2-|\mu|}{2}}s_{\mu^t}(q^{-\rho})\,, \\
C_{\emptyset\,\emptyset\,\nu}(t,q) &= \frac{q^{||\nu||^2/2}}{\prod_{s\in\nu}(1-t^{1+a(s)}\,q^{\ell(s)})}\,.
\end{aligned} \tag{51}$$

$\mathbb{I}$**:** The open string partition function is given by

$$\begin{aligned} Z(t,q,x) &= \sum_{\lambda} C_{\lambda\,\emptyset\,\emptyset}(t^{-1},q^{-1}) s_\lambda(x) = \sum_{\lambda} \left(\tfrac{t}{q}\right)^{\frac{|\lambda|}{2}} s_{\lambda^t}(t^\rho) s_\lambda(x) \\ &= \prod_{i=1}^{\infty}(1+x\,\sqrt{\tfrac{t}{q}}\,t^{-i+\frac{1}{2}}) = \prod_{i=1}^{\infty}(1-Q\,t^{-i+\frac{1}{2}})\,, \quad Q=-x\sqrt{\tfrac{t}{q}}\,. \end{aligned} \tag{52}$$

$\mathbb{II}$**:** The open string partition function in this case is given by

$$\begin{aligned} Z(t,q,x) &= \sum_{\mu} C_{\emptyset\,\mu\,\emptyset}(t^{-1},q^{-1}) s_\mu(x) = \sum_{\mu} \left(\tfrac{t}{q}\right)^{\frac{||\mu^t||-|\mu|}{2}} s_{\mu^t}(q^\rho) s_\mu(x) \\ &= \prod_{i=1}^{\infty}(1+x\,q^{-i+\frac{1}{2}}) = \prod_{i=1}^{\infty}(1-Q\,q^{-i+\frac{1}{2}})\,, \quad Q=-x\,. \end{aligned} \tag{53}$$

Thus we see that in both these case the partition function is the same as the partition function obtained from the ordinary vertex except that the partition function depends on either t or q depending on the leg on which the brane ends.

$\mathbb{III}$**:** The more interesting case is the third one in which the brane ends on the prefered leg. In this case the open string amplitude using the refined vertex is given by

$$\begin{aligned} Z(V,t,q) &= \sum_{\nu} C_{\emptyset\,\emptyset\,\nu}(t^{-1},q^{-1}) \mathrm{Tr}_\nu V \\ &= \sum_{\nu} C_{\emptyset\,\emptyset\,\nu}(t^{-1},q^{-1}) s_\nu(\mathbf{x}) \end{aligned} \tag{54}$$

where $\mathbf{x}=\{x_1,x_2,\cdots\}$. Since

$$C_{\emptyset\,\emptyset\,\nu}(t,q) = \frac{q^{||\nu||^2/2}}{\prod_{s\in\nu}(1-t^{1+a(s)}\,q^{\ell(s)})}\,,\; C_{\emptyset\,\emptyset\,\nu}(t^{-1},q^{-1}) = \frac{(-1)^{|\nu|}\left(\frac{t}{q}\right)^{|\nu|/2} t^{||\nu^t||^2/2}}{\prod_{s\in\nu}(1-t^{1+a(s)}\,q^{\ell(s)})} \tag{55}$$

therefore for $\mathbf{x}=\{-Q,0,0,\cdots\}$ we get

$$\begin{aligned} Z(Q,t,q) &= \sum_{\nu} C_{\emptyset\,\emptyset\,\nu}(t^{-1},q^{-1})\, s_\nu(-Q) = \sum_{k=0}^{\infty} C_{\emptyset\,\emptyset\,(k)}(t^{-1},q^{-1})(-Q)^k \\ &= \sum_{k=0}^{\infty}\left(Q\frac{t}{\sqrt{k}}\right)^k \prod_{n=1}^{k}(1-t\,q^{n-1})^{-1}\,. \end{aligned} \tag{56}$$

The above partition function can also be written using a more refined Hilbert series of the symmetric product of $\mathbb{C}$. The Schur functions provide a basis of R_k. A Schur function $s_\nu(z_1, \cdots, z_k)$ has charge $q^{|\nu|}$ under the $\mathbb{C}^\times$ action for $\ell(\nu) \leq k$. We define a second $\mathbb{C}^\times$ action such that

$$\mathbb{C}^\times : \, s_\nu(z_1, z_2, \cdots, z_k) \mapsto \, \vartheta^{\ell(\nu^t)} \, s_\nu(z_1, z_2, \cdots, z_k) \,, \;\; \ell(\nu) \leq k \,. \tag{57}$$

Note that this second $\mathbb{C}^\times$ action has a simple interpretation in terms of the bosonic oscillators. On $\mathcal{H}_k$ this second $\mathbb{C}^\times$ acts as ϑ^N where $N = \sum_{n>0} \frac{\alpha_{-n}\alpha_n}{n}$ is the operator that counts the number of total number of particles in a given state $|\nu\rangle$. On a state $|\nu\rangle = |1^{m_1} 2^{m_2} \cdots\rangle$ the operator N acts as

$$N|1^{m_1} 2^{m_2} \cdots\rangle = (m_1 + m_2 + \cdots)|1^{m_1} 2^{m_2} \cdots\rangle \tag{58}$$

Using this second $\mathbb{C}^\times$ action the refined Hilbert series of R_k

$$H[R_k](q, \vartheta) = \mathrm{Tr}_{\mathcal{H}_k} q^{L_0} \vartheta^N = \sum_{\nu | \ell(\nu) \leq k} q^{|\nu|} \, \vartheta^{\ell(\nu^t)} \,. \tag{59}$$

For $\ell(\nu) \leq k$ the partition ν can be written as $\nu = 1^{m_1} 2^{m_2} 3^{m_3} \cdots k^{m_k}$ such that $|\nu| = \sum_{i=1}^k i m_i$ and $\ell(\nu^t) = \sum_{i=1}^k m_i$ therefore

$$\begin{aligned} H[R_k](q, \vartheta) \;\; &= \;\; \sum_{\nu | \ell(\nu) \leq k} q^{|\nu|} \vartheta^{\ell(\nu)} \\ &= \sum_{m_1, m_2, \cdots, m_k} q^{m_1 + 2m_2 + 3m_3 + \cdots + k m_k} \, \vartheta^{m_1 + m_2 + \cdots m_k} = \prod_{i=1}^k (1 - \vartheta \, q^i)^{-1} \,. \end{aligned} \tag{60}$$

Then the generating function of the refined Hilbert series is given by

$$\begin{aligned} G(\phi, q, \vartheta) \;\; &= \;\; \sum_{k=0}^\infty \phi^k \, H[R_k](q, \vartheta) = \sum_{k=0}^\infty \phi^k \, \prod_{i=1}^k (1 - \vartheta \, q^i)^{-1} \\ &= \;\; Z(\phi \frac{\sqrt{q}}{t}, \vartheta \, q, q) \,. \end{aligned} \tag{61}$$

The refined partition function also satisfies an equation similar to the one satisfied by the quantum dilogarithm,

$$(\vartheta \, q^{-\partial_u} - 1 + \vartheta \, q^{\frac{1}{2}} \, e^{-u} \,) Z(e^{-u}, \vartheta \, q, q) = \vartheta - 1 \,. \tag{62}$$

where $Q = e^{-u}$.

Understanding the geometric meaning of this relation is an open problem which is important for a deeper understanding of the refined vertex.

4.3 Brane orientation and the gluing rule

We have seen previously that both the topological vertex and its refinement can be understood in terms of symmetric products of $\mathbb{C}$. The appearance of the $\mathrm{Sym}^\bullet(\mathbb{C})$ can be understood if we embed the topological string in the physical Type IIA string theory [18]. In this case, the Lagrangian branes become the D4-branes wrapping the Lagrangian 3-cycle in the CY3-fold and filling up two dimensions of the transverse four dimensions. The appearance of the symmetric product can then be interpreted as counting particles in two dimensions.

The refined topological vertex depends on two parameters t, q which in the instanton calculus corresponds to the $U(1)$ rotation parameters of the two orthogonal planes in $\mathbb{C}^2$. For the branes on the two unpreffered directions the open topological string partition function depends only on either t or q. This suggests that branes on two unpreferred directions actually fill the two different orthogonal planes in $\mathbb{C}^2$. To obtain the closed string partition function we have to glue two edges of the $\mathbb{C}^3$ vertex. From the instanton calculus we know that the closed string partition function can be obtained by counting points in $\mathbb{C}^2$. Therefore the gluing to obtain the closed string expression must be such that the two stack of branes, on the two legs which are to be glued, fill up orthogonal two dimensional planes in the $\mathbb{C}^2$ transverse to the CY3-fold.

Even though this gluing rule is very natural and we will see that it works, a deeper explanation of this is needed. In particular the asymmetry of the refined vertex is a feature that has to be explained in terms of the orientation of the Lagrangian branes: the unpreferred directions have branes that fill two orthogonal subspaces of $\mathbb{C}^2$. But we also need to have an explanation of the Lagrangian brane on the preferred direction. This we leave for future work. This is also related to the Khovanov knot invariant interpretation of the refined vertex: It should be possible to compute the Khovanov invariants (for toric knots at least) using the refined vertex, as we noted above. This is currently under investigation [19].

5 Refined Partition Functions from the Refined Vertex

In this section, we will use the refined topological vertex to determine the generalized partition function for various local toric CY3-folds.

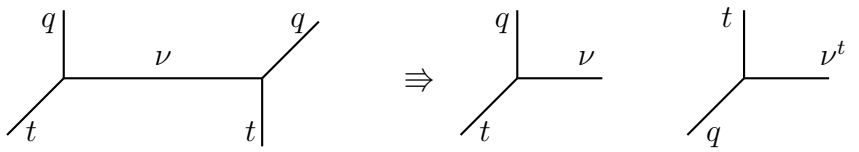

Figure 3: Toric diagram of $\mathcal{O}(-1)\oplus\mathcal{O}(-1)\mapsto\mathbb{P}^1$. The vertices are glued along the preferred direction ν.

5.1 $\mathcal{O}(-1)\oplus\mathcal{O}(-1)\mapsto\mathbb{P}^1$

The compactification of Type IIA string theory on the Calabi-Yau threefold $\mathcal{X}=\mathcal{O}(-1)\oplus\mathcal{O}(-1)\mapsto\mathbb{P}^1$ gives rise to $U(1)$ $\mathcal{N}=2$ gauge theory on the transverse $\mathbb{C}^2$ in a particular limit [1]. Using the topological vertex formalism, the topological string partition function is given by

$$\begin{aligned} Z(q,Q) &= \sum_{\nu} Q^{|\nu|}(-1)^{|\nu|}\, C_{\emptyset\emptyset\,\nu}(q)\, C_{\emptyset\emptyset\,\nu^t}(q) \\ &= \sum_{\nu} Q^{|\nu|}(-1)^{|\nu|} s_{\nu^t}(q^{-\rho}) s_{\nu}(q^{-\rho}) \\ &= \prod_{i,j=1}^{\infty}\left(1-Q\,q^{i+j-1}\right)=\prod_{k=1}^{\infty}\left(1-q^k\,Q\right)^k, \end{aligned} \tag{63}$$

where $T=-\ln(Q)$ is the Kähler parameter, the size of the $\mathbb{P}^1$.

We can use the refined topological vertex to determine the refined partition function. The toric diagram of $\mathcal{X}$ and the gluing of the refined vertex are shown in Fig. 3. From the gluing of the vertices in Fig. 3, we see that the refined topological string partition function is given by

$$Z(t,q,Q):=\sum_{\nu} Q^{|\nu|}(-1)^{|\nu|}\, C_{\emptyset\emptyset\,\nu}(t,q)\; C_{\emptyset\emptyset\,\nu^t}(q,t)\,. \tag{64}$$

Since

$$C_{\emptyset\emptyset\,\nu}(t,q)=q^{\frac{||\nu||^2}{2}}\,\widetilde{Z}_{\nu}(t,q)=q^{\frac{||\nu||^2}{2}}\,\prod_{s\in\nu}(1-t^{a(s)+1}q^{\ell(s)})^{-1}\,, \tag{65}$$

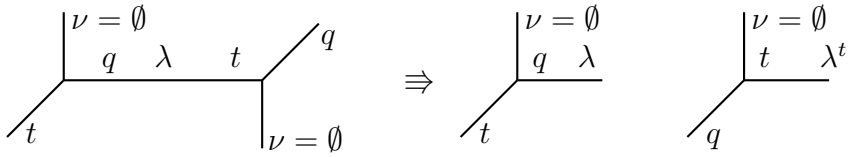

Figure 4: Toric diagram of $\mathcal{O}(-1) \oplus \mathcal{O}(-1) \mapsto \mathbb{P}^1$. The vertices are glued along the unpreferred direction λ

the refined partition function becomes[5]

$$Z(t,q,Q) \;=\; \sum_{\nu} \frac{Q^{|\nu|}(-1)^{|\nu|}\, q^{\frac{||\nu||^2}{2}}\, t^{\frac{||\nu^t||^2}{2}}}{\prod_{s\in\nu}(1-t^{a(s)+1}q^{\ell(s)})(1-t^{a(s)}q^{\ell(s)+1})}\,. \tag{66}$$

This is exactly the partition function given in Eq. (4.5) of [10] if we identify $(t_1, t_2, \mathfrak{q}) = (t, q^{-1}, Q\sqrt{\frac{t}{q}})$. A different representation of the partition function can be obtained by choosing different preferred directions as shown in Fig. 4.

The refined partition function with this choice is given by

$$\begin{aligned} Z(t,q,Q) \;&=\; \sum_{\lambda} Q^{|\lambda|}(-1)^{|\lambda|}\, C_{\lambda\,\emptyset\,\emptyset}(t,q)\, C_{\lambda^t\,\emptyset\,\emptyset}(q,t) \\ &=\; \sum_{\lambda} (-Q)^{|\lambda|} \left(\tfrac{q}{t}\right)^{\frac{|\lambda|}{2}} s_{\lambda^t}(t^{-\rho}) \left(\tfrac{t}{q}\right)^{\frac{|\lambda|}{2}} s_{\lambda}(q^{-\rho}) \\ &=\; \sum_{\lambda} (-Q)^{|\lambda|} s_{\lambda^t}(t^{-\rho})\, s_{\lambda}(q^{-\rho}) \;=\; \prod_{i,j=1}^{\infty} (1 - Q\, q^{i-\frac{1}{2}}\, t^{j-\frac{1}{2}}) \\ &=\; \mathrm{Exp}\left\{ -\sum_{n=1}^{\infty} \frac{Q^n}{n(q^{\frac{n}{2}} - q^{-\frac{n}{2}})(t^{\frac{n}{2}} - t^{-\frac{n}{2}})} \right\}. \end{aligned} \tag{67}$$

Identifying the above two representations of the partition function we get the following

[5] An equivalent expression obtained by $\nu \mapsto \nu^t$ is given by

$$\sum_{\nu} \frac{Q^{|\nu|}(-1)^{|\nu|}\, q^{\frac{||\nu^t||^2}{2}}\, t^{\frac{||\nu||^2}{2}}}{\prod_{s\in\nu}(1-t^{\ell(s)+1}q^{a(s)})(1-t^{\ell(s)}q^{a(s)+1})}$$

.

identity

$$\sum_{\nu} \frac{Q^{|\nu|}(-1)^{|\nu|}\, q^{\frac{||\nu||^2}{2}}\, t^{\frac{||\nu^t||^2}{2}}}{\prod_{s\in\nu}(1-t^{a(s)+1}q^{\ell(s)})(1-t^{a(s)}q^{\ell(s)+1})} = \mathrm{Exp}\left\{-\sum_{n=1}^{\infty}\frac{Q^n}{n(q^{\frac{n}{2}}-q^{-\frac{n}{2}})(t^{\frac{n}{2}}-t^{-\frac{n}{2}})}\right\} \tag{68}$$

which is a specialization of the identity Eq. (5.4) of [25] and was also derived in [10].

Note that in gluing the two vertices, we have have taken the parameters q or t be the different on the gluing edges as discussed in section 4.3. The parameter does not have to be the same as the vertices are actually an infinite distance apart. Actually, one can also check that a combinatorial description of the partition function requires that the parameters be different on the two gluing edges.

5.2 χ_y-genus, $\mathbf{Sym}^\bullet(\mathbb{C}^2)$ and the refined topological vertex

In [8], it was shown that the the generating function of the equivariant χ_y-genus of the Hilbert scheme of $\mathbb{C}^2$, denoted by $\mathrm{Hilb}^k[\mathbb{C}^2]$, is given by the topological string amplitude of a certain CY3-fold X_0, which is the partial compactification of $\mathcal{X}$. The equivariant action of $\mathbb{C}^2$ was given by $(z_1, z_2) \mapsto (q\, z_1, q^{-1}\, z_2)$. Here we will show that the refined partition function of X_0 is given by similar generating function for which the equivariant action is given by $(z_1, z_2) \mapsto (q\, z_1, t^{-1} z_2)$. The generating function is given by

$$G(\varphi, y, t, q) = \sum_{k=0}^{\infty} \varphi^k \chi_y(\mathrm{Hilb}^k[\mathbb{C}^2])\,. \tag{69}$$

and will be calculated using the localization. The fixed points of $\mathrm{Hilb}^k[\mathbb{C}^2]$ under the above two parameter action are labeled by the 2D partitions of n [12]. The weight at the fixed point labeled by the partition ν is given by [10, 27]

$$\sum_{i,j} e^{w_{i,j}} = \sum_{(i,j)\in\,\nu} (t^{1+a(i,j)}q^{\ell(i,j)} + t^{-a(i,j)}q^{-1-\ell(i,j)}) \tag{70}$$

Using these weights the χ_y-genus of $\mathrm{Hilb}^k[\mathbb{C}^2]$ is given by

$$\chi_y(\mathrm{Hilb}^k[\mathbb{C}^2]) = \sum_i \prod_{j=1}^{2k} \frac{1-ye^{-w_{i,j}}}{1-e^{-w_{i,j}}}\,, \tag{71}$$

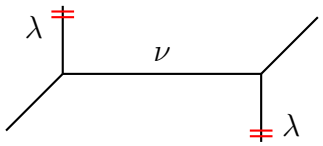

Figure 5: Toric diagram of partially compactified $\mathcal{O}(-1) \oplus \mathcal{O}(-1) \mapsto \mathbb{P}^1$.

where i label the fixed points (the partitions of k in this case) and j label the weights at a given fixed point,

$$\chi_y(\text{Hilb}^k[\mathbb{C}^2]) = \sum_{\nu,|\nu|=k} \prod_{(i,j)\in\nu} \frac{(1-yt^{1+a(i,j)}q^{\ell(i,j)})(1-yt^{-a(i,j)}q^{-1-\ell(i,j)})}{(1-t^{1+a(i,j)}q^{\ell(i,j)})(1-t^{-a(i,j)}q^{-1-\ell(i,j)})} \tag{72}$$

And the generating function is given by

$$G(\varphi, y, t, q) = \sum_{\nu} \varphi^{|\nu|} \prod_{(i,j)\in\nu} \frac{(1-yt^{1+a(i,j)}q^{\ell(i,j)})(1-yt^{-a(i,j)}q^{-1-\ell(i,j)})}{(1-t^{1+a(i,j)}q^{\ell(i,j)})(1-t^{-a(i,j)}q^{-1-\ell(i,j)})} \tag{73}$$

The above generating function can be simplified to an expression which can be compared with the refined vertex calculation more easily,

$$\begin{aligned} G(\varphi, y, t, q) &= \sum_{\nu} \varphi^{|\nu|} q^{\frac{||\nu||^2}{2}} t^{\frac{||\nu^t||^2}{2}} \widetilde{Z}_{\nu}(t,q)\widetilde{Z}_{\nu^t}(q,t) \\ &\quad \times \prod_{(i,j)\in\nu} (1-y\,t^{1+a(i,j)}q^{\ell(i,j)})(1-y\,t^{-a(i,j)}q^{-1-\ell(i,j)}) \end{aligned} \tag{74}$$

Now we will calculate the refined partition function of the CY3-fold X_0. The toric diagram of the CY3-fold X_0 is shown in Fig. 5. In this case the topological string partition function

is given by

$$\begin{aligned} Z(Q_1,Q_2) &:= \sum_{\lambda,\nu}(-Q_1)^{|\nu|}(-Q_2)^{|\lambda|}\, C_{\lambda\,\emptyset\,\nu}(t,q)\, C_{\lambda^t\,\emptyset\,\nu^t}(q,t) \\ &= \sum_{\nu,\lambda}(-Q_1)^{|\nu|}(-Q_2)^{|\lambda|}\, q^{\frac{||\nu||^2}{2}}\, \widetilde{Z}_\nu(t,q)\, s_{\lambda^t}(t^{-\rho}q^{-\nu})\, t^{\frac{||\nu^t||^2}{2}}\, \widetilde{Z}_{\nu^t}(q,t)\, s_\lambda(t^{-\nu^t}q^{-\rho}) \\ &= \sum_{\nu}(-Q_1)^{|\nu|}\, q^{\frac{||\nu||^2}{2}}\, t^{\frac{||\nu^t||^2}{2}}\, \widetilde{Z}_\nu(t,q)\, \widetilde{Z}_{\nu^t}(q,t) \sum_{\lambda}(-Q)^{|\lambda|} s_{\lambda^t}(t^{-\rho}q^{-\nu})\, s_\lambda(t^{-\nu^t}q^{-\rho}) \\ &= \sum_{\nu}(-Q_1)^{|\nu|}\, q^{\frac{||\nu||^2}{2}}\, t^{\frac{||\nu^t||^2}{2}}\, \widetilde{Z}_\nu(t,q)\, \widetilde{Z}_{\nu^t}(q,t) \prod_{i,j=1}^{\infty}(1-Q_2\, t^{i-\frac{1}{2}-\nu_j^t}\, q^{j-\frac{1}{2}-\nu_i})\,. \end{aligned}$$

For $Q_1 = 0$ we get the perturbative (in the gauge theory sense) contribution. The instanton part is then given by

$$\begin{aligned} \frac{Z(Q_1,Q_2)}{Z(0,Q_2)} &= \sum_{\nu}(-Q_1)^{|\nu|}\, q^{\frac{||\nu||^2}{2}}\, t^{\frac{||\nu^t||^2}{2}}\, \widetilde{Z}_\nu(t,q)\, \widetilde{Z}_{\nu^t}(q,t) \prod_{i,j=1}^{\infty}\Big(\frac{1-Q_2\, t^{i-\frac{1}{2}-\nu_j^t}\, q^{j-\frac{1}{2}-\nu_i}}{1-Q_2 t^{i-\frac{1}{2}} q^{j-\frac{1}{2}}}\Big) \\ &= \sum_{\nu}(-Q_1)^{|\nu|}\, q^{\frac{||\nu||^2}{2}}\, t^{\frac{||\nu^t||^2}{2}}\, \widetilde{Z}_\nu(t,q)\, \widetilde{Z}_{\nu^t}(q,t) \\ &\quad \times \prod_{(i,j)\in\nu}\Big(1-Q_2\, t^{i-\frac{1}{2}-\nu_j^t}\, q^{j-\frac{1}{2}-\nu_i}\Big)\Big(1-Q_2 t^{\nu_j^t-i+\frac{1}{2}} q^{\nu_i-j+\frac{1}{2}}\Big)\,. \end{aligned}$$

The above partition function is exactly the generating function of the χ_y-genus after the identification

$$\varphi = -Q_1\,,\;\; y = Q_2\sqrt{\tfrac{q}{t}}\,. \tag{75}$$

5.3 $\mathcal{O}(0)\oplus\mathcal{O}(-2)\mapsto\mathbb{P}^1$

This geometry can be obtained from local $\mathbb{P}^1\times\mathbb{P}^1$ by taking the size of one of the $\mathbb{P}^1$ very large. This limit gives two copies of $\mathcal{O}(0)\oplus\mathcal{O}(-2)\mapsto\mathbb{P}^1$.

a) b)

Figure 6: Two possible choices for the preferred direction, the internal line (a) and the parallel external lines (b).

In the usual topological vertex formalism the partition function is given by

$$
\begin{aligned}
Z(q,Q) &= \sum_{\nu} Q^{|\nu|}(-1)^{|\nu|} C_{\emptyset\emptyset\nu}(q)\,(-1)^{|\nu|}\,q^{\frac{\kappa(\nu)}{2}}\,C_{\emptyset\emptyset\nu^t}(q) \\
&= \sum_{\nu} Q^{|\nu|} s_{\nu^t}(q^{-\rho})\,q^{\frac{\kappa(\nu)}{2}}\,s_{\nu}(q^{-\rho}) = \sum_{\nu} Q^{|\nu|} s_{\nu^t}(q^{-\rho})\,s_{\nu^t}(q^{-\rho}) \\
&= \prod_{i,j=1}^{\infty}\left(1-Q\,q^{i+j-1}\right)^{-1} = \prod_{k=1}^{\infty}\left(1-Q\,q^{k}\right)^{-k} \\
&= \mathrm{Exp}\left\{\sum_{n=1}^{\infty}\frac{Q^n}{n(q^{\frac{n}{2}}-q^{-\frac{n}{2}})^2}\right\}.
\end{aligned}
\tag{76}
$$

In this case to define the refined partition function we have two choices for the preferred direction as shown in Fig. 6. The refined partition function for the case (a) of Fig. 6 is given by

$$
\begin{aligned}
Z(t,q,Q) &= \sum_{\nu} Q^{|\nu|}(-1)^{|\nu|}\,C_{\emptyset\emptyset\nu}(t,q)\,f_{\nu}(t,q)\,C_{\emptyset\emptyset\nu^t}(q,t) \\
&= \sum_{\nu}(-Q)^{|\nu|}\,\widetilde{Z}_{\nu}(t,q)\widetilde{Z}_{\nu^t}(q,t)\,q^{\frac{||\nu||^2}{2}}\,t^{\frac{||\nu^t||^2}{2}}\,f_{\nu}(t,q) \\
&= \sum_{\nu}\frac{(Q\sqrt{\frac{q}{t}})^{|\nu|}\,t^{||\nu^t||^2}}{\prod_{s\in\nu}(1-t^{a(s)+1}\,q^{\ell(s)})(1-t^{a(s)}\,q^{\ell(s)+1})}\,.
\end{aligned}
\tag{77}
$$

The partition function for case (b) of Fig. 6 is given by,

$$\begin{aligned} Z(t,q,Q) &= \sum_{\lambda} Q^{|\lambda|}(-1)^{|\lambda|}\, C_{\emptyset\,\lambda\,\emptyset}(t,q)\, f_\lambda(t,q)\; C_{\lambda^t\,\emptyset\,\emptyset}(t,q) \\ &= \sum_{\lambda}(-Q)^{|\lambda|}\Big(\frac{q}{t}\Big)^{\frac{||\lambda||^2}{2}} t^{\frac{\kappa(\lambda)}{2}}\, s_{\lambda^t}(q^{-\rho})\, f_\lambda(t,q)\, s_\lambda(t^{-\rho}) \\ &= \sum_{\lambda}(Q\sqrt{\tfrac{q}{t}})^{|\lambda|}\, s_{\lambda^t}(t^{-\rho})\, s_{\lambda^t}(q^{-\rho}) = \prod_{i,j=1}^{\infty}\Big(1-Q\,q^i\,t^{j-1}\Big)^{-1} \\ &= \mathrm{Exp}\left\{\sum_{n=1}^{\infty}\frac{Q^n\Big(\frac{q}{t}\Big)^{\frac{n}{2}}}{n(q^{\frac{n}{2}}-q^{-\frac{n}{2}})(t^{\frac{n}{2}}-t^{-\frac{n}{2}})}\right\}. \end{aligned} \tag{78}$$

The partition functions corresponding to the two choices are actually equal to each other (after scaling Q by $\sqrt{q/t}$) as can be seen by using the summation formulas for the Macdonald functions.

5.4 Another toric geometry: $\widetilde{\mathbb{C}^3/\mathbb{Z}_2\times\mathbb{Z}_2}$

The geometry in Fig. 7 is an interesting geometry consisting of a vertex with all non-trivial representations in the middle. In the limit of vanishing Q_1 and Q_3 (with $\lambda=\emptyset$), *i.e*, sending the lower and upper-most vertices to infinity, we recover our previous result for the conifold.

The refined partition function is given by

$$\begin{aligned} Z &= \sum_{\lambda,\mu,\nu}(-Q_1)^{|\lambda|}(-Q_2)^{|\mu|}(-Q_3)^{|\nu|} C_{\emptyset\,\emptyset\,\lambda}(t,q)\, C_{\mu\,\nu\,\lambda^t}(q,t)\, C_{\mu^t\,\emptyset\,\emptyset}(t,q)\, C_{\emptyset\,\nu^t\,\emptyset}(t,q) \\ &= \sum_{\lambda,\mu,\nu,\eta}(-Q_1)^{|\lambda|} q^{\frac{\|\lambda\|^2}{2}} t^{\frac{\|\lambda^t\|^2}{2}}\widetilde{Z}_\lambda(t,q)\widetilde{Z}_{\lambda^t}(q,t)\left(\frac{t}{q}\right)^{\frac{|\eta|}{2}} s_{\mu^t/\eta}(q^{-\rho}t^{-\lambda^t}) s_{\nu/\eta}(q^{-\lambda}t^{-\rho}) \\ &\times\; s_\mu(-Q_2 t^{-\rho}) s_{\nu^t}(-Q_3 q^{-\rho}) \\ &= \sum_{\lambda}(-Q_1)^{|\lambda|} q^{\frac{\|\lambda\|^2}{2}} t^{\frac{\|\lambda^t\|^2}{2}}\widetilde{Z}_\lambda(t,q)\widetilde{Z}_{\lambda^t}(q,t)\prod_{i,j=1}^{\infty}\frac{(1-Q_2\,q^{-\rho_j}t^{-\lambda_j^t-\rho_i})(1-Q_3\,q^{-\lambda_j-\rho_i}t^{-\rho_j})}{(1-Q_2Q_3\,q^{-\rho_i-1/2}t^{-\rho_i+1/2})} \end{aligned} \tag{79}$$

Note that for $Q_1=0$ the product representation of the refined partition function is consistent with having two $\mathbb{P}^1$'s with normal bundle $\mathcal{O}(-1)\oplus\mathcal{O}(-1)$ such that the sum of the two $\mathbb{P}^1$'s can be deformed into a $\mathbb{P}^1$ with normal bundle $\mathcal{O}(0)\oplus\mathcal{O}(-2)$.

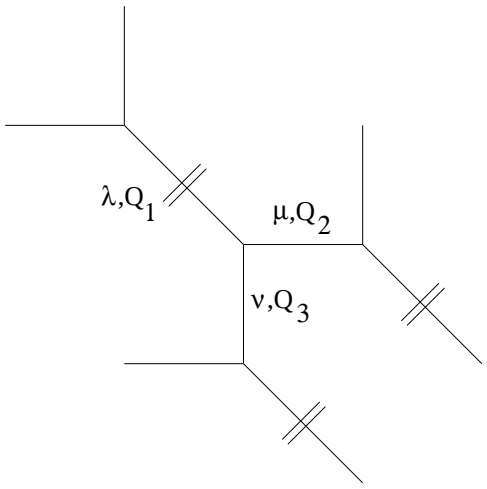

Figure 7: A toric geometry with three $\mathbb{P}^1$'s.

5.5 Local $\mathbb{P}^1 \times \mathbb{P}^1$

In this section, we will use the refined vertex to calculate the refined A-model partition function for the local $\mathbb{P}^1 \times \mathbb{P}^1$. The toric geometry for this case is shown in Fig. 8. The parallel horizontal edges in the rectangle correspond to the base $\mathbb{P}^1$. We cut the toric diagram perpendicular to these parallel lines following [6]. The 2D partitions on the parallel edges will be denoted by ν_1 and ν_2. The half of the toric diagram corresponds to a geometry $\mathcal{O}(0) \oplus \mathcal{O}(-2) \mapsto \mathbb{P}^1$ with a stack of D-branes on the two parallel edges in the representation ν_1, ν_2. We denote the open topological string partition function by $Z_{\nu_1,\nu_2}(t, q, Q_f)$ where $T_f = -\log Q_f$ is the Kähler parameter of the fiber $\mathbb{P}^1$. The two parts of the toric diagram are identical. This implies that the open topological string partition function associated with both sides is the same, $Z_{\nu_1,\nu_2}(t, q, Q_f)$. The only subtlety arises in how these two open string partition functions are "glued" together to form the closed string partition function. This gluing information is contained in the normal geometry of the base curve and determines the framing factors.

From the toric geometry, Fig. 8, it is clear that locally the two $\mathbb{P}^1$'s corresponding to the base curve (the upper and lower parallel edges) are $\mathcal{O}(0) \oplus \mathcal{O}(-2) \mapsto \mathbb{P}^1$ and $\mathcal{O}(-2) \oplus \mathcal{O}(0) \mapsto \mathbb{P}^1$. Therefore the framing factor with the top edge is $f_{\nu_1}(t, q)$ and with the lower edge is $f_{\nu_2}(q, t)$.

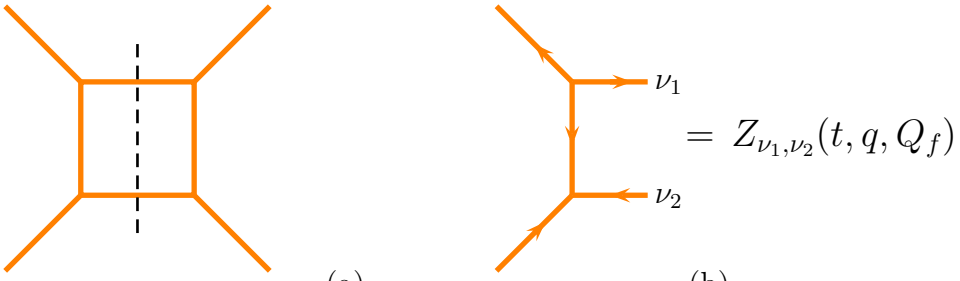

Figure 8: (a) Toric diagram of local $\mathbb{P}^1 \times \mathbb{P}^1$, (b) a slice of the toric diagram used to compute the partition function.

With this choice of framing factors the generalized partition function is given by

$$Z(Q_b, Q_f, t, q) := \sum_{\nu_1,\nu_2} (-Q_b)^{|\nu_1|+|\nu_2|} Z_{\nu_1,\nu_2}(t,q,Q_f)\, f_{\nu_1}(t,q)\, f_{\nu_2}(q,t)\, Z_{\nu_2,\nu_1}(q,t,Q_f), \tag{80}$$

where

$$f_{\nu_1}(t,q)\, f_{\nu_2}(q,t) \;=\; (-1)^{|\nu_1|}\Big(\frac{t}{q}\Big)^{\frac{||\nu_1^t||^2-|\nu_1|}{2}} q^{-\frac{\kappa(\nu_1)}{2}}\; (-1)^{|\nu_2|}\Big(\frac{q}{t}\Big)^{\frac{||\nu_2^t||^2-|\nu_2|}{2}} t^{-\frac{\kappa(\nu_2)}{2}}$$

and

$$\begin{aligned}
Z_{\nu_1,\nu_2}(t,q,Q_f) &= \sum_{\lambda} (-Q_f)^{|\lambda|} C_{\lambda^t\,\emptyset\,\nu_1}(t,q)\, f_\lambda(t,q)\, C_{\emptyset\,\lambda\,\nu_2^t}(t,q) \\
&= q^{\frac{||\nu_1||^2}{2}+\frac{||\nu_2^t||^2}{2}} \widetilde{Z}_{\nu_1}(t,q)\widetilde{Z}_{\nu_2^t}(t,q) \\
&\times \sum_{\lambda} (-Q_f)^{|\lambda|}\, s_\lambda(t^{-\rho}q^{-\nu_1})\, f_\lambda(t,q)\, \Big(\frac{q}{t}\Big)^{\frac{||\lambda||^2}{2}} t^{\frac{\kappa(\lambda)}{2}} s_\lambda(t^{-\nu_2}q^{-\rho}) \\
&= q^{\frac{||\nu_1||^2}{2}+\frac{||\nu_2^t||^2}{2}} \widetilde{Z}_{\nu_1}(t,q)\widetilde{Z}_{\nu_2^t}(t,q) \sum_{\lambda} (Q_f\sqrt{\tfrac{q}{t}})^{|\lambda|} s_\lambda(t^{-\rho}q^{-\nu_1})\, s_\lambda(t^{-\nu_2}q^{-\rho}) \\
&= q^{\frac{||\nu_1||^2}{2}+\frac{||\nu_2^t||^2}{2}} \widetilde{Z}_{\nu_1}(t,q)\widetilde{Z}_{\nu_2^t}(t,q) \prod_{i,j} \Big(1 - Q_f\, t^{i-1-\nu_{2,j}}\, q^{j-\nu_{1,i}}\Big)^{-1}.
\end{aligned} \tag{81}$$

$Z_{\emptyset,\emptyset}(t,q,Q_f)$ is the partition function of $\mathcal{O}(0)\oplus\mathcal{O}(-2) \mapsto \mathbb{P}^1$. We can separate out the

contribution which is independent of Q_b and write the above partition function as

$$\begin{aligned}
Z(Q_b,Q_f,t,q) &= Z_{pert}(Q_f,t,q)\, Z_{inst}(Q_b,Q_f,t,q) \\
Z_{pert}(Q_f,t,q) &= Z_{\emptyset,\emptyset}(t,q,Q_f)\, Z_{\emptyset,\emptyset}(q,t,Q_f) \\
Z_{inst}(Q_b,Q_f,t,q) &= \sum_{\nu_1,\nu_2} Q_b^{|\nu_1|+|\nu_2|}\, \frac{Z_{\nu_1,\nu_2}(t,q,Q_f)}{Z_{\emptyset,\emptyset}(t,q,Q_f)} \left(\left(\frac{t}{q}\right)^{\frac{||\nu_1^t||^2}{2}} q^{-\frac{\kappa(\nu_1)}{2}}\right) \left(\left(\frac{q}{t}\right)^{\frac{||\nu_2^t||^2}{2}} t^{-\frac{\kappa(\nu_2)}{2}}\right) \frac{Z_{\nu_2,\nu_1}(q,t,Q_f)}{Z_{\emptyset,\emptyset}(q,t,Q_f)} \\
&= \sum_{\nu_1,\nu_2} Q_b^{|\nu_1|+|\nu_2|}\, q^{||\nu_2^t||^2}\, t^{||\nu_1^t||^2}\, \widetilde{Z}_{\nu_1}(t,q)\widetilde{Z}_{\nu_2^t}(t,q)\, \widetilde{Z}_{\nu_2}(q,t)\widetilde{Z}_{\nu_1^t}(q,t) \\
&\times \prod_{i,j=1}^{\infty} \frac{(1-Q_f\, t^{i-1}q^j)(1-Q_f\, q^{i-1}t^j)}{(1-Q_f\, t^{i-1-\nu_{2,j}}q^{j-\nu_{1,i}})(1-Q_f\, q^{i-1-\nu_{1,j}}t^{j-\nu_{2,i}})}
\end{aligned}$$

5.5.1 Partition function from instanton calculation

The partition function of the 4D gauge theory was calculated by Nekrasov [3]. The 5D partition function which is the one A-model topological strings compute is a q-deformation of the 4D partition function [10, 11, 14].

The partition function can be calculated once the weights of the $U(1)\times U(1)$ action at the fixed points are determined. The fixed points are labelled by a set of N 2D partitions (in the $U(N)$ case), therefore, for a fixed point labelled by $\{\nu_1,\cdots,\nu_N\}$ the weight $W(\nu_1,\cdots,\nu_N)$ is given by

$$W(\nu_1,\cdots,\nu_N) = \prod_{a,b=1}^{N} N(\nu_a,\nu_b) \tag{82}$$

where

$$\begin{aligned}
N(\nu,\nu) &= \Big[\prod_{s\in\nu}(1-t^{a(s)}q^{\ell(s)+1})(1-t^{-a(s)-1}q^{-\ell(s)})\Big]^{-1} = t^{\frac{||\nu^t||^2+|\nu|}{2}}\, q^{\frac{||\nu||^2-|\nu|}{2}}\, \widetilde{Z}_{\nu}(t,q)\, \widetilde{Z}_{\nu^t}(q,t) \\
N(\nu_a,\nu_b) &= \Big[\prod_{(i,j)\in\nu_a}\Big(1-Q_{ba}t^{\nu_{b,j}^t-i}\, q^{\nu_{a,i}-j+1}\Big) \prod_{(i,j)\in\nu_b}\Big(1-Q_{ba}t^{-\nu_{a,j}^t+i-1}\, q^{-\nu_{b,i}+j}\Big)\Big]^{-1} \\
&= \prod_{i,j=1}^{\infty} \frac{1-Q_{ab}\, q^j\, t^{i-1}}{1-Q_{ab}\, q^{-\nu_{b,i}+j}\, t^{-\nu_{a,j}^t+i-1}}\,.
\end{aligned}$$

and $-\log Q_{ab}$ are the Kähler parameters. The partition function is then given by

$$Z^{U(N)}_{\text{gauge theory}} := \sum_{\nu_1,\nu_2,\cdots,\nu_N} \widehat{Q}^{|\nu_1|+|\nu_2|+\cdots+|\nu_N|} \prod_{a,b=1}^{N} N(\nu_a,\nu_b) \tag{83}$$

The above partition function computed from the gauge theory side is the A-model partition function of the Calabi-Yau threefold which gives rise to 5D supersymmetric gauge theory, via M-theory compactification, with zero Chern-Simons coefficient.

For $N = 2$ the partition function in Eq. (83) can be simplified to the following expression ($Q = Q_f, \widehat{Q}Q = \mathfrak{q}\frac{q}{t}$)

$$\begin{aligned} Z^{U(2)}_{\text{gauge theory}} &= \sum_{\nu_1,\nu_2} \mathfrak{q}^{|\nu_1|+|\nu_2|} Z(\nu_1^t, \nu_2^t; Q, t, q) \qquad (84) \\ Z(\nu_1, \nu_2; Q, t, q) &:= \left(\frac{q}{t}\right)^{|\nu_1|+|\nu_2|} q^{||\nu_1^t||^2} t^{||\nu_2||^2} \widetilde{Z}_{\nu_1^t}(t, q)\widetilde{Z}_{\nu_1}(q, t)\widetilde{Z}_{\nu_2^t}(t, q)\widetilde{Z}_{\nu_2}(q, t)\, G(\nu_1, \nu_2, Q, t, q) \\ G(\nu_1, \nu_2, Q, t, q) &= \prod_{i,j=1}^{\infty} \frac{(1 - Q\, q^{j-1}t^i)(1 - Q\, q^j t^{i-1})}{(1 - Q\, q^{-\nu_{2,i}^t+j-1}\, t^{-\nu_{1,j}+i})(1 - Q\, q^{-\nu_{2,i}^t+j}\, t^{-\nu_{1,j}+i-1})} \end{aligned}$$

$$\widetilde{Z}_\nu(t, a) = \prod_{s\in\nu}(1 - t^{a(s)+1}q^{\ell(s)})^{-1}\,, \quad \ell(i, j) = \nu_i - j\,, \quad a(i, j) = \nu_j^t - i \qquad (85)$$

It is easy to see that the above gauge theory partition function is the same as the refined partition function of the last section.

5.5.2 Spin content of BPS states

In this section, we list the spin content of various curves obtained from the refined partition function. A basis of $H_2(\mathbb{P}^1 \times \mathbb{P}^1)$ is given by $\{B, F\}$ such that

$$B \cdot B = F \cdot F = 0\,, \quad B \cdot F = 1\,. \qquad (86)$$

The class $nB + mF$ has a holomorphic representative if $n, m \geq 0$. The genus of such a curve is given by

$$g(nB + mF) = (n - 1)(m - 1)\,. \qquad (87)$$

From the refined partition function we can extract the spin content of the various states coming from $C \in H_2(X, \mathbb{Z})$. In the table below we list the spin content for certain $C_{n,m} = nB + mF$.

$C_{n,m}$	$\sum_{j_L,j_R} N_C^{(j_L,j_R)}(j_L,j_R)$
$B+mF,\ m\geq 0$	$(0,m+\frac{1}{2})$
$2B+2F$	$(\frac{1}{2},4)\oplus(0,\frac{7}{2})\oplus(0,\frac{5}{2})$
$2B+3F$	$(1,\frac{11}{2})\oplus(\frac{1}{2},5)\oplus(\frac{1}{2},4)\oplus 2(0,\frac{9}{2})\oplus(0,\frac{7}{2})\oplus(0,\frac{5}{2})$
$3B+3F$	$\left(2,\frac{15}{2}\right)\oplus\left(\frac{3}{2},7\right)\oplus\left(\frac{3}{2},6\right)\oplus 3\left(1,\frac{13}{2}\right)\oplus 2\left(1,\frac{11}{2}\right)\oplus(1,\frac{9}{2})$ $\oplus\left(\frac{1}{2},7\right)\oplus 3(\frac{1}{2},6)\oplus 3(\frac{1}{2},5)\oplus 2(\frac{1}{2},4)\oplus(\frac{1}{2},3)\oplus 4(0,\frac{11}{2})$ $\oplus 3(0,\frac{9}{2})\oplus 3(0,\frac{7}{2})\oplus(0,\frac{5}{2})\oplus(0,\frac{3}{2})$
$3B+4F$	$\left(3,\frac{19}{2}\right)\oplus\left(\frac{5}{2},9\right)\oplus\left(\frac{5}{2},8\right)\oplus 3\left(2,\frac{17}{2}\right)\oplus\left(\frac{3}{2},9\right)\oplus 2\left(2,\frac{15}{2}\right)$ $\oplus 4\left(\frac{3}{2},8\right)\oplus\left(1,\frac{17}{2}\right)\oplus\left(2,\frac{13}{2}\right)\oplus 4\left(\frac{3}{2},7\right)\oplus 7\left(1,\frac{15}{2}\right)\oplus 2\left(\frac{1}{2},8\right)$ $\oplus\left(0,\frac{17}{2}\right)\oplus 2\left(\frac{3}{2},6\right)\oplus 6\left(1,\frac{13}{2}\right)\oplus 7\left(\frac{1}{2},7\right)\oplus\left(0,\frac{15}{2}\right)\oplus\left(\frac{3}{2},5\right)$ $\oplus 5\left(1,\frac{11}{2}\right)\oplus 8\left(\frac{1}{2},6\right)\oplus 7\left(0,\frac{13}{2}\right)\oplus 2\left(1,\frac{9}{2}\right)\oplus 6\left(\frac{1}{2},5\right)$ $\oplus 6\left(0,\frac{11}{2}\right)\oplus\left(1,\frac{7}{2}\right)\oplus 4\left(\frac{1}{2},4\right)\oplus 7\left(0,\frac{9}{2}\right)\oplus 2\left(\frac{1}{2},3\right)$ $\oplus 4\left(0,\frac{7}{2}\right)\oplus\left(\frac{1}{2},2\right)\oplus 3\left(0,\frac{5}{2}\right)\oplus\left(0,\frac{3}{2}\right)\oplus\left(0,\frac{1}{2}\right)$

5.6 Local $\mathbb{F}_m$

In this section, we will use the refined vertex to calculate the refined partition function for the local $\mathbb{F}_m$, $m=0,1,2$. The case $m=0$ (local $\mathbb{P}^1\times\mathbb{P}^1$) has already been discussed in the last section. As we saw in [6], the partition function for local $\mathbb{F}_m$ differ just by framing factors along the edges which label the instanton charge (the edges corresponding to the base $\mathbb{P}^1$). This continues to be the case for the refined partition function for local $\mathbb{F}_m$.

The toric geometry for these cases is shown in Fig. 9. The parallel edges in the polygon correspond to the base $\mathbb{P}^1$. We cut the toric diagram perpendicular to these parallel lines as we did for the local $\mathbb{P}^1\times\mathbb{P}^1$. The 2D partitions on the parallel edges will be denoted by ν_1 and ν_2. The half of the toric diagram corresponds to a geometry $\mathcal{O}(0)\oplus\mathcal{O}(-2)\mapsto\mathbb{P}^1$ with a stack of D-branes on the two parallel edges in the representation ν_1,ν_2. We denote the open topological string partition function by $Z_{\nu_1,\nu_2}(t,q,Q_f)$ where $T_f=-\log Q_f$ is the Kähler parameter of the fiber $\mathbb{P}^1$. $Z_{\nu_1,\nu_2}(t,q,Q_f)$ was calculated in the last section and is given by Eq. (81). Although the two parts of the toric diagram look different (except for $m=0$ in which case they are identical) they are related to each other by an $SL(2,\mathbb{Z})$

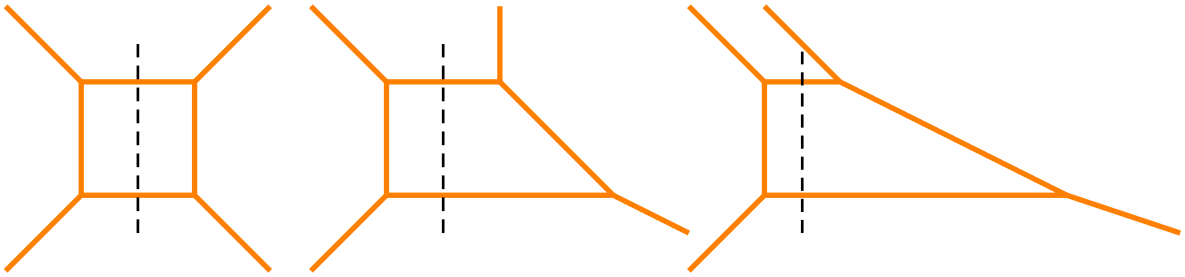

Figure 9: Local F_m : $m = 0$, $m = 1$, $m = 2$.

transformation. This implies that the open topological string partition function associated with each side is the same, $Z_{\nu_1,\nu_2}(t, q, Q_f)$. Thus the difference arises only in how these two open string partition functions are "glued" together to form the closed string partition function. This gluing information is contained in the normal geometry of the base curve and is what determines the framing factors.

From the toric geometry, Fig. 9, it is clear that locally the two $\mathbb{P}^1$'s corresponding to the base curve (the upper and lower parallel edges) are $\mathcal{O}(-m) \oplus \mathcal{O}(-2+m) \mapsto \mathbb{P}^1$ and $\mathcal{O}(-2-m) \oplus \mathcal{O}(m) \mapsto \mathbb{P}^1$. Therefore the framing factor with the top edge is $f_{\nu_1}^{-m+1}(t, q)$ and with the lower edge is $f_{\nu_2}^{m+1}(q, t)$.

Using the above framing factors the generalized partition function is given by

$$Z^{(m)}(Q_b, Q_f, t, q) = \sum_{\nu_1,\nu_2} (-Q_b)^{|\nu_1|+|\nu_2|} Q_f^{m\,|\nu_2|}\, Z_{\nu_1,\nu_2}(t, q, Q_f)\, f_{\nu_1}^{-m+1}(t, q)\, f_{\nu_2}^{m+1}(q, t)\, Z_{\nu_2,\nu_1}(q, t, Q_f).$$

We can write the above partition function as

$$Z^{(m)}(Q_b, Q_f, t, q) = Z^{(m)}_{pert}(Q_f, t, q)\, Z^{(m)}_{inst}(Q_b, Q_f, t, q) \tag{88}$$

where $Z^{(m)}_{pert}(Q_f, t, q)$ is a function only of Q_f and, in the field theory limit, it gives the perturbative prepotential of the theory. $Z^{(m)}_{inst}(Q_b, Q_f, t, q)$ depends on Q_b and gives the instanton correction to the prepotential in the field theory limit. Although Q_f and Q_b are on the same footing in the topological string theory we write the partition function this way to simplify the expressions and to be able to compare with the $m = 0$ case, which corresponds to Nekrasov's partition function.

$$Z^{(m)}_{pert}(Q_f,t,q) = Z_{\emptyset,\emptyset}(t,q,Q_f)\, Z_{\emptyset,\emptyset}(q,t,Q_f) = \prod_{i,j=1}^{\infty} (1-Q_f\, t^i\, q^{j-1})^{-1}\, (1-Q_f\, t^{i-1}\, q^j)^{-1}\,.$$

$$\begin{aligned} Z^{(m)}_{inst}(Q_b,Q_f,t,q) &= \sum_{\nu_1,\nu_2} Q_b^{|\nu_1|+|\nu_2|} Q_f^{m\,|\nu_2|}\, \frac{Z_{\nu_1,\nu_2}(t,q,Q_f)}{Z_{\emptyset,\emptyset}(t,q,Q_f)} \Big(\Big(\tfrac{t}{q}\Big)^{\frac{||\nu_1^t||^2}{2}}\, q^{-\frac{\kappa(\nu_1)}{2}}\Big)^{-m+1}\, \Big(\Big(\tfrac{q}{t}\Big)^{\frac{||\nu_2^t||^2}{2}}\, t^{-\frac{\kappa(\nu_2)}{2}}\Big)^{m+1} \\ &\times \quad (-1)^{m(|\nu_1|+|\nu_2|)}\, \frac{Z_{\nu_2,\nu_1}(q,t,Q_f)}{Z_{\emptyset,\emptyset}(q,t,Q_f)}\,, \end{aligned}$$

where

$$\frac{Z_{\nu_1,\nu_2}(t,q,Q_f)}{Z_{\emptyset,\emptyset}(t,q,Q_f)} = q^{\frac{||\nu_1||^2}{2}+\frac{||\nu_2^t||^2}{2}}\, \widetilde{Z}_{\nu_1}(t,q)\widetilde{Z}_{\nu_2^t}(t,q) \prod_{i,j=1}^{\infty} \frac{1-Q_f\, t^{i-1}q^j}{1-Q_f\, t^{i-1-\nu_{2,j}}\, q^{j-\nu_{1,i}}}\,. \tag{89}$$

The expression for the $Z^{(m)}_{inst}(Q_b,Q_f,t,q)$ can be simplified to become

$$\begin{aligned} Z_{inst}(Q_b,Q_f,t,q) &= \sum_{\nu_1,\nu_2} Q_b^{|\nu_1|+|\nu_2|} Q_f^{m|\nu_2|}\, (-1)^{m(|\nu_1|+|\nu_2|)} \left(\frac{q}{t}\right)^{\frac{m}{2}(||\nu_1||^2+||\nu_2^t||^2)}\, t^{\frac{m}{2}(\kappa(\nu_1)-\kappa(\nu_2))} \\ &\times \quad q^{||\nu_2^t||^2}\, t^{||\nu_1^t||^2}\, \widetilde{Z}_{\nu_1}(t,q)\widetilde{Z}_{\nu_2^t}(t,q)\, \widetilde{Z}_{\nu_2}(q,t)\widetilde{Z}_{\nu_1^t}(q,t) \\ &\times \quad \prod_{i,j=1}^{\infty} \frac{(1-Q_f\, t^i q^{j-1})(1-Q_f\, q^i t^{j-1})}{(1-Q_f\, t^{i-\nu_{2,j}} q^{j-1-\nu_{1,i}})(1-Q_f\, q^{i-\nu_{1,j}} t^{j-1-\nu_{2,i}})}. \end{aligned} \tag{90}$$

5.6.1 Spin content of BPS states: local $\mathbb{F}_1$

In this section, we list the spin content of some curves obtained from the refined partition function given in Eq. (90) for the case $m = 1$. $\mathbb{F}_1$ has a two dimensional $H_2(\mathbb{F}_1)$ with a basis given by B and F such that

$$B\cdot B = -1\,,\ F\cdot F = 0\,,\ \ B\cdot F = 1\,. \tag{91}$$

A class $nB + mF$ has a holomorphic curve in it if $m - n, n \geq 0$. The arithmetic genus of such a curve, $C = nB + mF$, is given by the adjunction formula,

$$g(nB+(n+k)F) = \frac{(n-1)(n-2)}{2} + k(n-1)\,. \tag{92}$$

Since $\mathbb{F}_1$ is the one point blowup of $\mathbb{P}^2$ there is a different basis $\{H, E\}$ of $H_2(\mathbb{F}_1)$ which will be useful for us later,

$$\begin{aligned} H &= B+F,\ E = B \\ H\cdot H &= 1\,,\ E\cdot E = -1\,,\ H\cdot E = 0\,, \end{aligned} \tag{93}$$

where E is the exceptional curve obtained by the blowup and H is the basic class of $\mathbb{P}^1$ in $\mathbb{P}^2$ given by linear polynomials. It is clear that the invariants of the curves $B+F, 2(B+F), 3(B+F), \cdots$ will be the same as the invariants of the curves $H, 2H, 3H, \cdots$ in local $\mathbb{P}^2$.

- $\underline{B+k\,F}$**:** These curves are of genus zero for all $k \geq 0$. The moduli space of such curves is given by $\mathbb{P}^{d-1}$ where $d = -C \cdot K_{F_1} = 2k+1$. Therefore, the left spin $j_L = 0$ and right spin $j_R = k$,

$$N^{(j_L,j_R)}_{B+k\,F} = \delta_{j_L,0}\,\delta_{j_R,k}\,. \tag{94}$$

  This is exactly what we get from the refined partition function.

- $\underline{2B+2F}$**:** This curve is also of genus zero, and since $2(B+F) = 2H$ the moduli space is given by $\mathbb{P}^5$, the space of quadratic polynomials in $\mathbb{P}^2$ (up to overall scaling). Thus

$$N^{(j_L,j_R)}_{2B+2F} = \delta_{j_L,0}\,\delta_{j_R,\frac{5}{2}}\,. \tag{95}$$

  This is exactly what we get from the refined partition function once multicovering has been taken into account.

- $\underline{2B+3F}$**:** This curve is of genus one. The spin content from the refined partition function is

$$(\tfrac{1}{2},4) \oplus (0,\tfrac{7}{2}) \oplus (0,\tfrac{5}{2})\,.$$

- $\underline{2B+4F}$**:** This curve is of genus 2. The spin content from the refined partition function is

$$\left(1,\tfrac{11}{2}\right) \oplus \left(\tfrac{1}{2},5\right) \oplus \left(\tfrac{1}{2},4\right) \oplus 2\left(0,\tfrac{9}{2}\right) \oplus \left(0,\tfrac{7}{2}\right) \oplus \left(0,\tfrac{5}{2}\right).$$

- $\underline{2B+5F}$**:** This curve is of genus 3. The spin content is given by

$$\left(\tfrac{3}{2},7\right) \oplus \left(1,\tfrac{13}{2}\right) \oplus \left(1,\tfrac{11}{2}\right) \oplus 2\left(\tfrac{1}{2},6\right) \oplus \left(\tfrac{1}{2},5\right) \oplus 2\left(0,\tfrac{11}{2}\right) \oplus \left(\tfrac{1}{2},4\right) \oplus 2\left(0,\tfrac{9}{2}\right) \oplus \left(0,\tfrac{7}{2}\right) \oplus \left(0,\tfrac{5}{2}\right).$$

- $\underline{3B+3F}$**:** This curve is of genus 1. The spin content is given by

$$\left(\tfrac{1}{2},\tfrac{9}{2}\right) \oplus (0,3)\,.$$

  Note that this is also the spin content of the curve $3H$ in local $\mathbb{P}^2$.

- $\underline{3B+4F}$**:** This curve is of genus 3. The spin content is given by

$$\left(\tfrac{3}{2},\tfrac{13}{2}\right)\oplus(1,6)\oplus(1,5)\oplus 2\left(\tfrac{1}{2},\tfrac{11}{2}\right)\oplus(0,6)\oplus 2\left(\tfrac{1}{2},\tfrac{9}{2}\right)\oplus(0,5)\oplus\left(\tfrac{1}{2},\tfrac{7}{2}\right)\oplus(0,4)\oplus(0,3)\oplus(0,2)$$

- $\underline{3B+5F}$**:** This curve is of genus 5. The spin content is given by

$$\begin{aligned}&\left(\tfrac{5}{2},\tfrac{17}{2}\right)\oplus(2,8)\oplus(2,7)\oplus 3\left(\tfrac{3}{2},\tfrac{15}{2}\right)\oplus(1,8)\oplus 2\left(\tfrac{3}{2},\tfrac{13}{2}\right)\oplus 3\,(1,7)\oplus\left(\tfrac{1}{2},\tfrac{15}{2}\right)\oplus\left(\tfrac{3}{2},\tfrac{11}{2}\right)\\&\oplus 4\,(1,6)\oplus 5\left(\tfrac{1}{2},\tfrac{13}{2}\right)\oplus 2\,(0,7)\oplus 2\,(1,5)\oplus 5\left(\tfrac{1}{2},\tfrac{11}{2}\right)\oplus 3\,(0,6)\oplus(1,4)\oplus 4\left(\tfrac{1}{2},\tfrac{9}{2}\right)\oplus 5\,(0,5)\\&\oplus 2\left(\tfrac{1}{2},\tfrac{7}{2}\right)\oplus 3\,(0,4)\oplus\left(\tfrac{1}{2},\tfrac{5}{2}\right)\oplus 3\,(0,3)\oplus(0,2)\oplus(0,1)\,.\end{aligned}$$

- $\underline{4B+4F}$**:** This curve has genus 3. The spin content is given by

$$\left(\tfrac{3}{2},7\right)\oplus\left(1,\tfrac{11}{2}\right)\oplus\left(\tfrac{1}{2},6\right)\oplus\left(\tfrac{1}{2},5\right)\oplus\left(\tfrac{1}{2},4\right)\oplus\left(0,\tfrac{13}{2}\right)\oplus\left(0,\tfrac{9}{2}\right)\oplus\left(0,\tfrac{5}{2}\right)$$

  This is also the spin content of the curve $4H$ in local $\mathbb{P}^2$.

- $\underline{5B+5F}$**:** This curve has genus 6. The spin content is given by

$$\begin{aligned}&(3,10)+\left(\tfrac{5}{2},\tfrac{17}{2}\right)\oplus(2,9)\oplus(2,8)\oplus(2,7)\oplus\left(\tfrac{3}{2},\tfrac{19}{2}\right)\oplus\left(\tfrac{3}{2},\tfrac{17}{2}\right)\oplus 2\left(\tfrac{3}{2},\tfrac{15}{2}\right)\\&\oplus\left(\tfrac{3}{2},\tfrac{13}{2}\right)\oplus\left(\tfrac{3}{2},\tfrac{11}{2}\right)\oplus(1,9)\oplus 2(1,8)\oplus 2(1,7)\oplus 2(1,6)\oplus(1,5)\oplus(1,4)\\&\oplus\left(\tfrac{1}{2},\tfrac{17}{2}\right)\oplus 2\left(\tfrac{1}{2},\tfrac{15}{2}\right)\oplus 3\left(\tfrac{1}{2},\tfrac{13}{2}\right)\oplus 2\left(\tfrac{1}{2},\tfrac{11}{2}\right)\oplus\left(\tfrac{1}{2},\tfrac{7}{2}\right)\oplus\left(\tfrac{1}{2},\tfrac{5}{2}\right)\oplus(0,8)\\&\oplus 2(0,7)\oplus 2(0,6)\oplus 2(0,5)\oplus(0,4)\oplus(0,3)\oplus(0,1)\,.\end{aligned}$$

  This is also the spin content of the curve $5H$ in local $\mathbb{P}^2$

From this example it is clear that although the refined vertex can only be used for a certain kind of geometries (those giving rise to gauge theories) the spin content of BPS states for any toric CY3-fold can be obtained by embedding this toric CY3-fold in another toric CY3-fold which does have a gauge theory interpretation. For example, the refined vertex can not be used to determine the refined partition function for local $\mathbb{P}^2$ but since one point blowup of local $\mathbb{P}^2$ is local $\mathbb{F}_1$ which does have a gauge theory interpretation therefore spin content of BPS states coming from local $\mathbb{P}^2$ can be obtained from the refined partition function of local $\mathbb{F}_1$. We list the spin content of first few BPS states for local $\mathbb{P}^2$ in the table below.

$C_n = nH$	$\sum_{j_L,j_R} N_C^{(j_L,j_R)}(j_L,j_R)$
H	$(0,1)$
$2H$	$(0,\frac{5}{2})$
$3H$	$\left(\frac{1}{2},\frac{9}{2}\right)\oplus(0,3)$
$4H$	$\left(\frac{3}{2},7\right)\oplus\left(1,\frac{11}{2}\right)\oplus\left(\frac{1}{2},6\right)\oplus\left(\frac{1}{2},5\right)$ $\oplus\left(\frac{1}{2},4\right)\oplus\left(0,\frac{13}{2}\right)\oplus\left(0,\frac{9}{2}\right)\oplus\left(0,\frac{5}{2}\right)$
$5H$	$(3,10)+\left(\frac{5}{2},\frac{17}{2}\right)\oplus(2,9)\oplus(2,8)\oplus(2,7)\oplus\left(\frac{3}{2},\frac{19}{2}\right)$ $\oplus\left(\frac{3}{2},\frac{17}{2}\right)\oplus 2\left(\frac{3}{2},\frac{15}{2}\right)\oplus\left(\frac{3}{2},\frac{13}{2}\right)\oplus\left(\frac{3}{2},\frac{11}{2}\right)\oplus(1,9)\oplus 2(1,8)$ $\oplus 2(1,7)\oplus 2(1,6)\oplus(1,5)\oplus(1,4)\oplus\left(\frac{1}{2},\frac{17}{2}\right)\oplus 2\left(\frac{1}{2},\frac{15}{2}\right)$ $\oplus 3\left(\frac{1}{2},\frac{13}{2}\right)\oplus 2\left(\frac{1}{2},\frac{11}{2}\right)\oplus\left(\frac{1}{2},\frac{7}{2}\right)\oplus\left(\frac{1}{2},\frac{5}{2}\right)\oplus(0,8)\oplus 2(0,7)$ $\oplus 2(0,6)\oplus 2(0,5)\oplus(0,4)\oplus(0,3)\oplus(0,1)$

5.7 An $SU(3)$ geometry

In this section, we will use the refined vertex to calculate the partition function of a certain CY3-fold which gives rise to compactified 5D supersymmetric $SU(3)$ gauge theory with Chern-Simons coefficient m.

The refined partition function is given by

$$Z=\sum_{\nu_1,\nu_2,\nu_3} Q_{b1}^{|\nu_1|}Q_{b_2}^{|\nu_2|}Q_{b3}^{|\nu_3|}Z_{\nu_1,\nu_2,\nu_3}(t,q)\left(f_{\nu_1}^{m+2}(t,q)\,f_{\nu_2}^{-m}(q,t)\,f_{\nu_3}^{-m+2}(t,q)\right)Z_{\nu_3,\nu_2,\nu_1}(q,t), \quad (96)$$

where

$$
\begin{aligned}
Z_{\nu_1,\nu_2,\nu_3} &:= \sum_{\lambda,\mu}(-Q_1)^{|\lambda|}(-Q_2)^{|\mu|}C_{\emptyset\,\lambda\,\nu_1}(t,q)f_\lambda(t,q)C_{\lambda^t\,\mu\,\nu_2}(t,q)f_\mu(t,q)C_{\mu^t\,\emptyset\,\nu_3}(t,q)\\
&= (-Q_1)^{|\lambda|}(-Q_2)^{|\mu|}\Big[(\tfrac{q}{t})^{\frac{||\lambda||^2-|\lambda|}{2}}t^{\frac{\kappa(\lambda)}{2}}\,q^{\frac{||\nu_1||^2}{2}}\widetilde{Z}_{\nu_1}(t,q)s_\lambda(t^{-\nu_1^t}q^{-\rho})\Big]f_\lambda(t,q)\\
&\times \Big[(\tfrac{q}{t})^{\frac{||\mu||^2-|\mu|}{2}}t^{\frac{\kappa(\mu)}{2}}\,q^{\frac{||\nu_2||^2}{2}}\widetilde{Z}_{\nu_2}(t,q)\sum_\eta s_{\lambda/\eta}(t^{-\rho}q^{-\nu_2})s_{\mu/\eta}(t^{-\nu_2^t}q^{-\rho})\Big]\,f_\mu(t,q)\\
&\times \Big[q^{\frac{||\nu_3||^2}{2}}\widetilde{Z}_{\nu_3}(t,q)s_\mu(t^{-\rho}q^{-\nu_3})\Big]\\
&= q^{\frac{||\nu_1||^2+||\nu_2||^2+||\nu_3||^2}{2}}\widetilde{Z}_{\nu_1}(t,q)\widetilde{Z}_{\nu_2}(t,q)\widetilde{Z}_{\nu_3}(t,q)\\
&\times \sum_\eta(\tfrac{q}{t})^{\frac{|\eta|}{2}}\Big(\sum_\lambda s_\lambda(-Q_1q^{-\rho}t^{-\nu_1^t})\,s_{\lambda/\eta}(t^{-\rho}q^{-\nu_2})\Big)\Big(\sum_\mu s_\mu(-Q_2t^{-\rho}q^{-\nu_3})\,s_{\mu/\eta}(q^{-\rho}q^{-\nu_2^t}\Big)\\
&= q^{\frac{||\nu_1||^2+||\nu_2||^2+||\nu_3||^2}{2}}\widetilde{Z}_{\nu_1}(t,q)\widetilde{Z}_{\nu_2}(t,q)\widetilde{Z}_{\nu_3}(t,q)\prod_{i,j=1}^{\infty}(1-Q_1\,t^{j-1/2-\nu_{1,i}^t}q^{i-1/2-\nu_{2,j}})^{-1}\\
&\times (1-Q_2\,t^{j-1/2-\nu_{2,i}^t}q^{i-1/2-\nu_{3,j}})^{-1}(1-Q_1Q_2\,t^{j-1/2-\nu_{1,i}^t}q^{i-1/2-\nu_{3,j}})^{-1}
\end{aligned}
$$

In the above expression $-\log Q_1$ and $-\log Q_2$ are the Kähler classes of the $\mathbb{P}^1$'s in the fiber and $Q_{b1,b2,b3}$ are given by [7]

$$
\begin{aligned}
Q_{b1} &= Q_bQ_1^{m+1}Q_2^{(m-1)(1-\delta_{m,0})}\\
Q_{b2} &= Q_bQ_2^{(m-1)(1-\delta_{m,0})}\\
Q_{b3} &= Q_bQ_2^{\delta_{m,0}}\,.
\end{aligned}
\tag{97}
$$

This is exactly the K-theoretic version of the Nekrasov's partition function as can be verified by using the weights of the torus action given in [10].

5.8 An $SU(3)$, $N_f = 4$ geometry

In this section, we will compute the refined partition function for the CY3-fold which gives rise to $SU(3)$ gauge theory with adjoint matter via geometric engineering. This CY3-fold is a blowup of a resolved A_2 singularity fibered over $\mathbb{P}^1$. The toric diagram of this geometry and the choice of the preferred direction for each vertex is shown in Fig. 10.

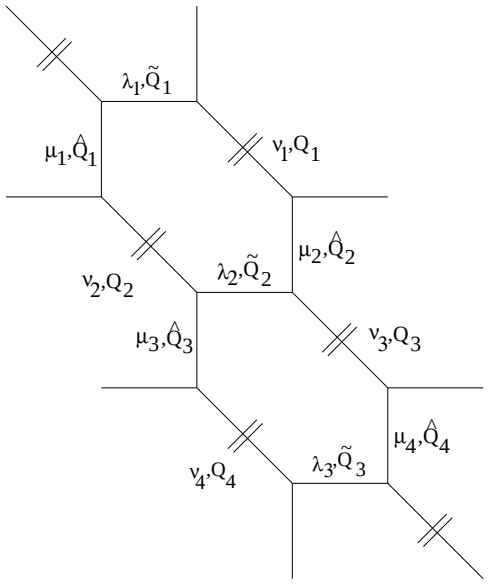

Figure 10: The web diagram of the CY3-fold giving rise to $SU(3)$ gauge theory with $N_f = 4$.

The refined partition function for this geometry is given by

$$
\begin{aligned}
Z &= \sum_{\{\mu_i\},\{\nu_i\},\{\lambda_i\}} (-\hat{Q}_1)^{|\mu_1|}\dots(-\hat{Q}_4)^{|\mu_4|}(-Q_1)^{|\nu_1|}\dots(-Q_4)^{|\nu_4|}(-\tilde{Q}_1)^{|\lambda_1|}\dots(-\tilde{Q}_3)^{|\lambda_3|} \\
&\times\ C_{\lambda_1\mu_1\emptyset}(t,q)C_{\lambda_1^t\emptyset\nu_1}(q,t)C_{\emptyset\mu_1^t\nu_2}(q,t)C_{\emptyset\mu_2\nu_1^t}(t,q)C_{\lambda_2\mu_3\nu_2^t}(t,q)C_{\lambda_2^t\mu_2^t\nu_3}(q,t)C_{\emptyset\mu_3^t\nu_4}(q,t) \\
&\times\ C_{\emptyset\mu_4\nu_3^t}(t,q)C_{\lambda_3\emptyset\nu_4^t}(t,q)C_{\lambda_3^t\mu_4^t\emptyset}(q,t) \\
&= \sum_{\{\mu_i\},\{\nu_i\},\{\lambda_i\},\{\eta_i\}} (-\hat{Q}_1)^{|\mu_1|}\dots(-\hat{Q}_4)^{|\mu_4|}(-Q_1)^{|\nu_1|}\dots(-Q_4)^{|\nu_4|}(-\tilde{Q}_1)^{|\lambda_1|}\dots(-\tilde{Q}_3)^{|\lambda_3|} \\
&\times\ q^{\frac{\|\nu_1^t\|^2+\dots+\|\nu_4^t\|^2}{2}} t^{\frac{\|\nu_1\|^2+\dots+\|\nu_4\|^2}{2}} \left(\frac{q}{t}\right)^{\frac{|\eta_1|+|\eta_2|-|\eta_3|-|\eta_4|}{2}} \widetilde{Z}_{\nu_1}(q,t)\widetilde{Z}_{\nu_1^t}(t,q)\dots\widetilde{Z}_{\nu_4}(q,t)\widetilde{Z}_{\nu_4^t}(t,q) \\
&\times\ s_{\lambda_1^t/\eta_1}(t^{-\rho})s_{\mu_1/\eta_1}(q^{-\rho})s_{\lambda_1}(q^{-\rho}t^{-\nu_1})s_{\mu_1^t}(q^{-\nu_2^t}t^{-\rho})s_{\mu_2}(t^{-\nu_1}q^{-\rho})s_{\lambda_2^t/\eta_2}(t^{-\rho}q^{-\nu_2^t})s_{\mu_3/\eta_2}(t^{-\nu_2}q^{-\rho}) \\
&\times\ s_{\lambda_2/\eta_3}(q^{-\rho}t^{-\nu_3})s_{\mu_2^t/\eta_3}(q^{-\nu_3^t}t^{-\rho})s_{\mu_3^t}(q^{-\nu_4^t}t^{-\rho})s_{\mu_4}(t^{-\nu_3}q^{-\rho})s_{\lambda_3^t}(t^{-\rho}q^{-\nu_4^t})s_{\lambda_3/\eta_4}(q^{-\rho})s_{\mu_4^t/\eta_4}(t^{-\rho}) \\
&= \sum_{\{\nu_i\}} (-Q_1)^{|\nu_1|}\dots(-Q_4)^{|\nu_4|} q^{\frac{\|\nu_1^t\|^2+\dots+\|\nu_4^t\|^2}{2}} t^{\frac{\|\nu_1\|^2+\dots+\|\nu_4\|^2}{2}} \widetilde{Z}_{\nu_1}(q,t)\widetilde{Z}_{\nu_1^t}(t,q)\dots\widetilde{Z}_{\nu_4}(q,t)\widetilde{Z}_{\nu_4^t}(t,q) \\
&\times\ \prod_{i,j=1}^{\infty} \frac{(1-\tilde{Q}_1 q^{-\rho_i}t^{-\nu_{1,i}-\rho_j})(1-\hat{Q}_1 q^{-\nu_{2,i}^t-\rho_j}t^{-\rho_i})(1-\hat{Q}_2 q^{-\nu_{3,j}^t-\rho_i}t^{-\nu_{1,i}-\rho_j})(1-\hat{Q}_3 q^{-\nu_{4,i}^t-\rho_j}t^{-\nu_{2,j}-\rho_i})}{(1-\tilde{Q}_1\hat{Q}_1 q^{-\nu_{2,j}^t-\rho_i+1/2}t^{-\nu_{1,i}-\rho_j-1/2})(1-\tilde{Q}_3\hat{Q}_4 q^{-\nu_{4,j}^t-\rho_i-1/2}t^{-\nu_{3,i}-\rho_j+1/2})} \\
&\times\ \frac{(1-\hat{Q}_4 q^{-\rho_i}t^{-\nu_{3,i}-\rho_j})(1-\tilde{Q}_3 q^{-\nu_{4,i}^t-\rho_j}t^{-\rho_i})(1-\tilde{Q}_2 q^{-\nu_{2,i}^t-\rho_j}t^{-\nu_{3,j}-\rho_i})(1-\tilde{Q}_2\hat{Q}_2\hat{Q}_3 q^{-\nu_{4,j}^t-\rho_i}t^{-\nu_{1,i}-\rho_j})}{(1-\tilde{Q}_2\hat{Q}_3 q^{-\nu_{4,i}^t-\rho_j+1/2}t^{-\nu_{3,j}-\rho_i-1/2})(1-\tilde{Q}_2\hat{Q}_2 q^{-\nu_{2,j}^t-\rho_i-1/2}t^{-\nu_{1,i}-\rho_j+1/2})}
\end{aligned}
$$

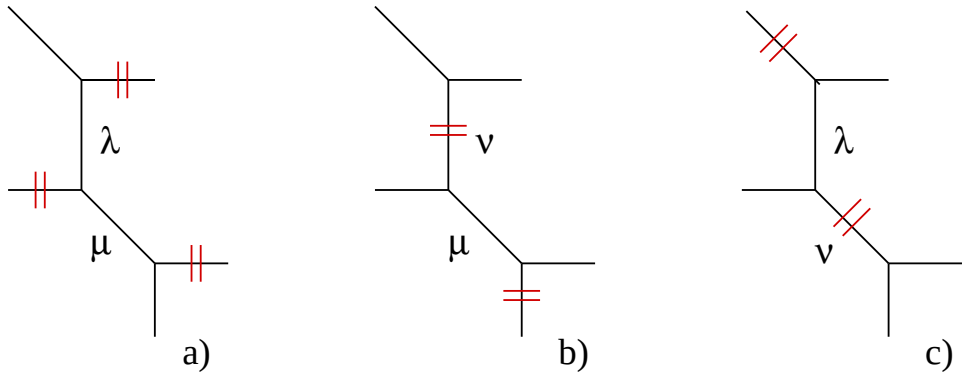

Figure 11: Three different slicings of the same toric diagram. Short red lines indicate the "instanton" direction.

Using the results of [3], it is easy to show that the above partition function is the same as the compactified 5D gauge theory partition function.

5.9 Slicing independence of the partition function

To show that the partition functions defined by the refined vertex are independent of the chosen "instanton" or the preferred direction consider the toric diagrams shown in Fig. 11. For this diagram we can choose the preferred direction in three different ways. Partition function for Fig. 11(a) is given by

$$
\begin{aligned}
Z &= \sum_{\lambda,\mu} (-Q_1)^{|\lambda|}(-Q_2)^{|\mu|} C_{\emptyset\,\lambda\,\emptyset}(t,q)\, C_{\mu\,\lambda^t\,\emptyset}(q,t)\, C_{\mu^t\,\emptyset\,\emptyset}(t,q) \qquad (98)\\
&= \sum_{\lambda,\mu} (-Q_1)^{|\lambda|}(-Q_2)^{|\mu|} s_\lambda(q^{-\rho}) \left(\sum_\eta \left(\frac{t}{q}\right)^{\frac{|\eta|}{2}} s_{\mu^t/\eta}(q^{-\rho}) s_{\lambda^t/\eta}(t^{-\rho}) \right) s_\mu(t^{-\rho}) \\
&= \sum_\eta \left(\frac{t}{q}\right)^{\frac{|\eta|}{2}} \left(\sum_\lambda s_\lambda(-Q_1 q^{-\rho}) s_{\lambda^t/\eta}(t^{-\rho}) \right) \left(\sum_\mu s_\mu(-Q_2 t^{-\rho}) s_{\mu^t/\eta}(q^{-\rho}) \right) \\
&= \prod_{i,j=1}^{\infty} (1 - Q_1\, q^{-\rho_i} t^{-\rho_j})(1 - Q_2\, q^{-\rho_i} t^{-\rho_j}) \sum_\eta \left(\frac{t}{q}\right)^{\frac{|\eta|}{2}} s_{\eta^t}(-Q_1 q^{-\rho}) s_{\eta^t}(-Q_2 t^{-\rho}) \\
&= \prod_{i,j=1}^{\infty} \frac{(1 - Q_1\, q^{-\rho_i} t^{-\rho_j})(1 - Q_2\, q^{-\rho_i} t^{-\rho_j})}{1 - Q_1 Q_2 \sqrt{\frac{t}{q}}\, q^{-\rho_i} t^{-\rho_j}}.
\end{aligned}
$$

The partition function for Fig. 11(b) is given by

$$
\begin{aligned}
Z &= \sum_{\nu,\lambda}(-Q_1)^{|\nu|}(-Q_2)^{|\lambda|}C_{\emptyset\emptyset\nu}(t,q)\,C_{\emptyset\,\lambda\,\nu^t}(q,t)C_{\emptyset\,\lambda^t\,\emptyset}(t,q) \qquad (99)\\
&= \sum_{\nu}(-Q_1)^{|\nu|}\,q^{\frac{||\nu||^2}{2}}\,t^{\frac{||\nu^t||^2}{2}}\,\widetilde{Z}_\nu(t,q)\,\widetilde{Z}_{\nu^t}(q,t)\,\Big(\sum_{\lambda}(-Q_2)^{|\lambda|}s_\lambda(t^{-\rho}\,q^{-\nu})s_{\lambda^t}(q^{-\rho})\Big)\\
&= \sum_{\nu}(-Q_1)^{|\nu|}\,q^{\frac{||\nu||^2}{2}}\,t^{\frac{||\nu^t||^2}{2}}\,\widetilde{Z}_\nu(t,q)\,\widetilde{Z}_{\nu^t}(q,t)\,\prod_{i,j=1}^{\infty}(1-Q_2t^{-\rho_i}q^{-\rho_j-\nu_i})\\
&= \prod_{i,j=1}^{\infty}(1-Q_2\,q^{\rho_i}\,t^{-\rho_j})\,\sum_{\nu}(-Q_1)^{|\nu|}\,q^{\frac{||\nu||^2}{2}}\,t^{\frac{||\nu^t||^2}{2}}\,\widetilde{Z}_\nu(t,q)\,\widetilde{Z}_{\nu^t}(q,t)\,\prod_{(i,j)\in\nu}(1-Q_2t^{-\rho_i}q^{-\rho_j-\nu_i}).
\end{aligned}
$$

The partition function for Fig. 11(c) is the same as that of Fig. 11(b) after changing $\nu \mapsto \nu^t$.

Thus for the partition function to be independent of the preferred direction requires the following identity:

$$
\sum_{\nu}(-Q_1)^{|\nu|}\,q^{\frac{||\nu||^2}{2}}\,t^{\frac{||\nu^t||^2}{2}}\,\widetilde{Z}_\nu(t,q)\,\widetilde{Z}_{\nu^t}(q,t)\,\prod_{(i,j)\in\nu}(1-Q_2\,t^{-\rho_i}q^{-\rho_j-\nu_i}) = \prod_{i,j=1}^{\infty}\frac{1-Q_1\,q^{-\rho_i}t^{-\rho_j}}{1-Q_1Q_2\,\sqrt{\frac{t}{q}}\,q^{-\rho_i}t^{-\rho_j}}
$$

which can be written in terms of Macdonald function $P_\nu(\mathbf{x};t,q)$ as

$$
\sum_{\nu}P_\nu(-Q_1\,t^{-\rho};q,t)\,P_{\nu^t}(q^{-\rho};t,q)\,\prod_{(i,j)\in\nu}(1-Q_2\,t^{-\rho_i}q^{-\rho_j-\nu_i}) = \prod_{i,j=1}^{\infty}\frac{1-Q_1\,q^{-\rho_i}t^{-\rho_j}}{1-Q_1Q_2\,\sqrt{\frac{t}{q}}\,q^{-\rho_i}t^{-\rho_j}}
$$

For $Q_2 = 0$ this is a well known identity (Example 6, page 352 of [25]). For $Q_2 \neq 0$ we have verified the above identity up to Q_1^3. This irrelevance of the chosen preferred direction is the manifestation of duality between supersymmetric $\mathcal{N} = 2$ gauge theories with gauge groups $SU(M)^{N-1}$ and $SU(N)^{M-1}$ as conjectured in [2].

6 Conclusion

In this paper we constructed a refined topological vertex which was used to determine the generalized partition function encoding left-right spin content information. The derivation of the refined topological vertex depended upon insights from the instanton calculus. From

the very beginning it was clear that the cyclic symmetry of the topological vertex will have to be sacrificed in order to obtain a refined vertex if the instanton calculus is to be our guide. Whether a refined vertex exists which is cyclically symmetric and can be used for all toric geometries, unlike the refined vertex which is not suitable for geometries that do not give rise to gauge theories, remains to be seen.

Acknowledgments

We would like to thank Sergei Gukov and Sheldon Katz for many valuable discussions. AI would also like to thank Charles Doran, Andreas Karch and Matthew Strassler for many valuable discussions. CK would also like to thank Andrew O'Bannon for many valuable discussions. We all would also like to thank the Stony Brook physics department and fourth Simons Workshop in Mathematics and Physics for their hospitality while this project was in progress. The research of C.V. is supported in part by NSF grants PHY-0244821 and DMS-0244464

7 Appendix A: Derivation of the Refined Topological Vertex

In this section, we will review the correspondence between the 3D partition and the topological vertex following [15, 22] and use the formalism of 3D partitions to define a "vertex" which depends on infinitely many parameters. A specialization of this "vertex" will be the refined vertex.

7.1 Young diagrams and skew partitions

Let $\nu = \{\nu_1 \geq \nu_2 \geq \nu_3 \geq \cdots \,|\, \nu_i \geq 0\}$ be a Young diagram, *i.e.*, a 2D partition. We denote by $|\nu|$ the size of the partition, $|\nu| = \sum_i \nu_i$, and by $\ell(\nu)$ the number of non-zero ν_i. A pictorial representation can be obtained by placing ν_i boxes at the i^{th} position, as shown in Fig. 12 for $\nu = \{4, 3, 3, 2, 1\}$. The height of the columns either stays the same or decreases as we

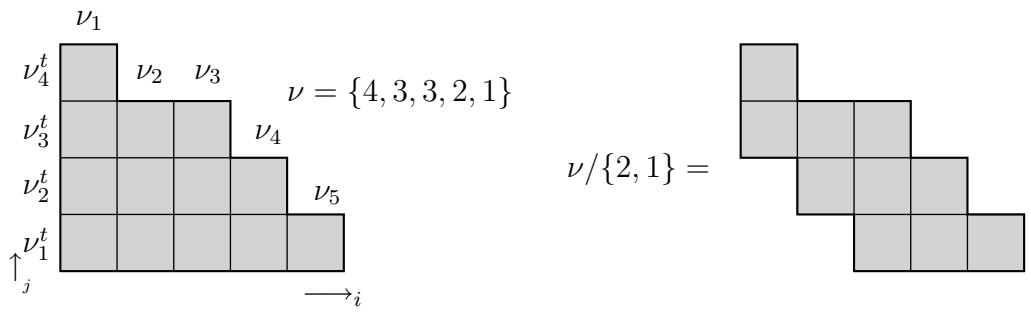

Figure 12: (a) Young diagram of the partition $\{4,3,3,2,1\}$. (b) The skew Young diagram of $\{4,3,3,2,1\}/\{2,1\}$.

move to the right. The transpose of ν is denoted by ν^t,

$$\nu^t = \{\nu_1^t, \nu_2^t, \cdots\}\,, \quad \nu_j^t = \#\{i \,|\, \nu_i \geq j\}\,. \tag{100}$$

We denote by $(i,j) \in \nu$ the box whose upper right corner has coordinates (i,j). If $(i,j) \in \nu$, then it is clear that $(j,i) \in \nu^t$. Given two partitions λ and ν we say $\lambda \subseteq \nu$, if $(i,j) \in \lambda$ implies $(i,j) \in \nu$.

Given two partitions λ and ν such that $\lambda \subseteq \nu$ a skew partition denoted by ν/λ consists of all boxes of ν which are not in λ,

$$\nu/\lambda = \{(i,j) \in \nu \,|\, (i,j) \notin \lambda\}. \tag{101}$$

A skew partition ν/λ for $\nu = \{4,3,2,2,1\}$ and $\lambda = \{2,1\}$ is shown in Fig. 12(b).

In general, ν/λ is not a 2D partition, *i.e.*, not a Young diagram. But if ν is such that it has N boxes in each row and N rows then for $N \geq \max(\lambda_1, \lambda_1^t)$ the skew diagram ν/λ is a 2D partition. We will denote by $\sigma(N)$ the 2D partition for which $\ell(\sigma(N)) = N$ and $\sigma_1(N) = \sigma_2(N) = \cdots \sigma_N(N) = N$. In this paper, we will only consider skew partitions of the form $\sigma(N)/\nu$ and will denote this 2D partition by ν^c,

$$\nu_i^c = N - \nu_{N-i+1}\,,\ i = 1,2,\cdots,N \tag{102}$$

For $\nu = \{3,2,2\}$ and $\sigma(6) = \{6,6,6,6,6,6\}$, Fig. 13 shows the skew partition $\sigma(6)/\nu$.

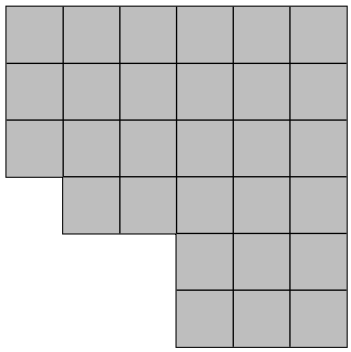

Figure 13: For a partition $\sigma(N)$ and an arbitrary $2D$ partition ν, the skew partition $\sigma(N)/\nu$ is always a 2D partition, provided $N \geq max(\nu_1, \nu_1^t)$.

7.2 Plane partitions and skew plane partitions

A *plane partition* is an array of non-negative integers $\{\pi_{i,j} \,|\, i,j \geq 1\}$ such that

$$\pi_{i,j} \geq \pi_{i+r,j+s}\,, \quad r,s \geq 0 \tag{103}$$

Placing $\pi_{i,j}$ cubes at the (i,j) position gives a pictorial representation of the plane partition. In this sense, plane partitions can be regarded as a 3 dimensional generalization of the Young diagrams, and they are also known as 3D partitions. The total number of cubes is given by $|\pi| = \sum_{i,j} \pi_{i,j}$. Fig. 14(a) shows an example of a 3D partition.

A skew 3D partition of shape ν/λ is an array of non-negative integers $\{\pi_{i,j} \mid (i,j) \in \nu/\lambda\}$ such that

$$\pi_{i,j} \geq \pi_{i+r,j+s}\,, \quad r,s \geq 0. \tag{104}$$

An example of a skew plane partition is shown in Fig. 14(b)

A skew plane partition of shape ν^c will be denoted by $\pi(\nu)$. It is clear that $\pi(\nu)$ is just a semi-standard Young tableau (SSYT) of shape ν^c except that we have to subtract the minimal semi-standard Young tableau of the same shape. Since the sum of entries of a minimal semi-standard Young diagram of shape λ is given by $m(\lambda) = \sum_i i\lambda_i$, the generating

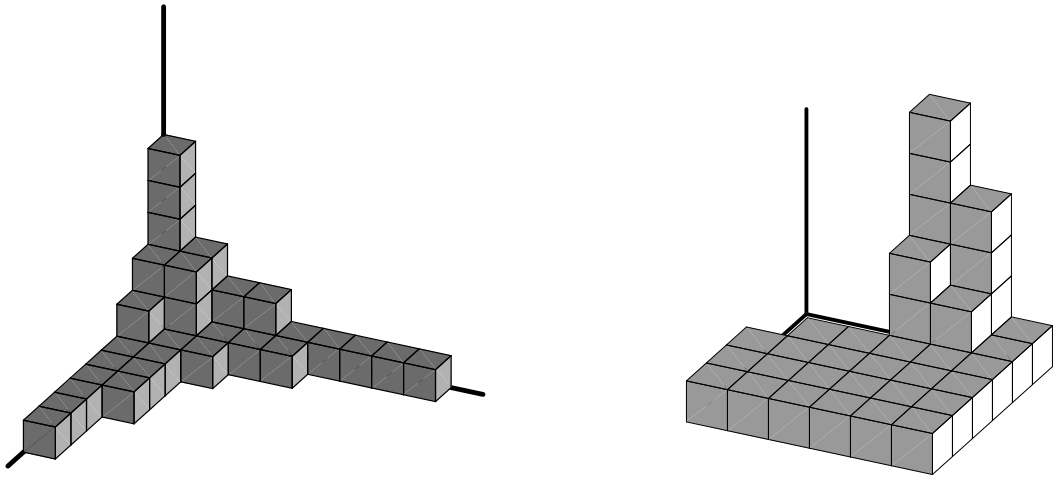

(a) (b)

Figure 14: (a) A 3D partition, (b) a skew 3D partition.

function for the number of skew plane partitions of shape ν^c is given by

$$\begin{aligned} Z_\nu(q) := \sum_{\pi(\nu)} q^{|\pi|} &= q^{-m(\nu^c)} \sum_{SSYT,T} x_1^{\#\text{of 1's}} x_2^{\#\text{of 2's}} \cdots \\ &= q^{-m(\nu^c)} s_{\nu^c}(x_1, x_2, \cdots), \;\; x_i = q^i \\ &= q^{-m(\nu^c)} s_{\nu^c}(q, q^2, q^3, \cdots) \\ &= \prod_{(i,j)\in\,\nu^c} (1 - q^{\widehat{h}(i,j)})^{-1} \end{aligned} \tag{105}$$

Where $\widehat{h}(i,j) = j - \nu_i + i - \nu_j^t - 1$ is the hook length. For $\nu = \emptyset$ we get the number of 3D partitions in a box of size $N \times N \times \infty$. In the limit $N \mapsto \infty$ this becomes the MacMahon function, $\prod_{k=1}^{\infty}(1-q^k)^{-k}$ [6]. From now on we will take the limit $N \mapsto \infty$. In this limit the function

$$\widetilde{Z}_\nu(q) := \frac{Z_\nu(q)}{Z_\emptyset(q)} \tag{106}$$

[6]The generating function of 3D partitions is given by the product of q-deformed hook length, $[h(s)]_q := (1-q^{h(s)})^{-1}$, over the infinite 2D partition, $\sigma(\infty)$. It is easy to see that the generating function of 2D partitions $\prod_{k=1}^{\infty}(1-q^k)^{-1}$ is given by the product of q-deformed hook lengths over the infinite 1D partition. However, the product of q-deformed hook lengths over the infinite 3D partition is not the generating function of 4D partitions.

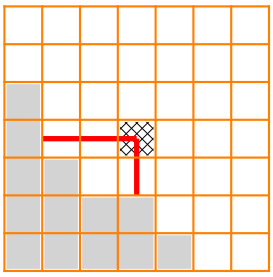

(a) The hook length of a box $(i,j) \in \nu^c$, $\widehat{h}(i,j) = j - \nu_i + i - \nu_j^t - 1$

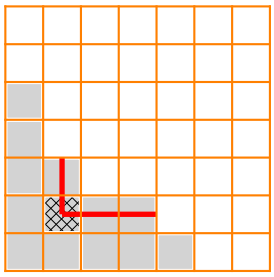

(b) The hook length of a box $(i,j) \in \nu$, $h(i,j) = \nu_i - j + \nu_j^t - i + 1$

Figure 15: The hook length for ν and ν^c is defined in the usual way. Note that the orientation of the hook in ν and ν^c agree if we rotate ν^c by 180°

can be written as a product over ν of q-deformed hook lengths[7],

$$\begin{aligned} \widetilde{Z}_\nu(q) &= \prod_{(i,j)\in\nu} (1-q^{h(i,j)})^{-1}\,, \quad h(i,j) = \nu_i - j + \nu_j^t - i + 1 \\ &= q^{-m(\nu)} s_\nu(q,q^2,q^3,\cdots) = q^{-\frac{||\nu||^2}{2}} s_{\nu^t}(q^{1/2},q^{3/2},q^{5/2}\cdots)\,. \end{aligned} \tag{107}$$

Apart from the framing factor $q^{\frac{||\nu||^2}{2}}$, the function $\widetilde{Z}_\nu(q)$ is just the one-partition topological vertex,

$$C_{\emptyset\emptyset\nu}(q) = q^{\frac{||\nu||^2}{2}} \widetilde{Z}_\nu(q)\,. \tag{108}$$

As discussed in [15], the topological vertex with all three non-empty partitions is related to the combinatorics of skew 3D partitions in which the "hole" in the partition is along all three axes. More specifically, we imagine that the region behind the asymptotic 2D partition in all three directions is excised.

The boxes are placed in the positive octant O^+ of $\mathbb{R}^3$ whose coordinates we are going to denote by (x,y,z). Let us associate the (x,y) plane with the (i,j) plane. Given a 3D partition π as a stack of cubes in the positive octant O^+ of R^3 we can reconstruct the array of non-negative numbers $\pi_{i,j}$ as the height of the stack of cubes, *i.e.*, as a height function defined on the (x,y) plane. However, we can obtain a different array of non-negative numbers $\pi^t_{j,k}$ ($\pi^{tt}_{i,k}$) by considering the height of the stack relative to the (y,z) ((x,z)) plane. This transformation is the analog of the transpose for the 2D partitions.

[7]Proof of this is given in Appendix C for the two parameter generalization, this identity follows by setting $q = t$.

We can define a generalized skew plane partition $\pi(\lambda,\mu,\nu)$ as an ordinary 3D partition from which cubes at (i,j,k) are removed if $(i,j)\in\nu$, or $(j,k)\in\mu$ or $(k,i)\in\lambda$,

$$\pi(\lambda,\mu,\nu)=\pi\smallsetminus\{(i,j,k)|(i,j)\in\nu\}\cup\{(i,j,k)|(j,k)\in\mu\}\cup\{(i,j,k)|(k,i)\in\lambda\}\,. \quad (109)$$

Then we can define the generating function for the number of generalized skew plane partitions of shape (λ,μ,ν),

$$Z_{\lambda\,\mu\,\nu}(q)=\sum_{\pi(\lambda,\mu,\nu)}q^{|\pi(\lambda,\mu,\nu)|}\,. \quad (110)$$

It is clear that $Z_{\lambda\,\mu\,\nu}(q)=Z_{\mu\,\lambda\,\nu^t}(q)$. The cyclic symmetry of the function is related to the transpose of the 3D partition,

$$\begin{aligned}\pi(\lambda,\mu,\nu) &= \pi^t(\mu,\nu,\lambda)\;\Rightarrow\; Z_{\lambda\,\mu\,\nu}(q)=Z_{\mu\,\nu\,\lambda}(q) \quad (111)\\ \pi(\lambda,\mu,\nu) &= \pi^{tt}(\nu,\lambda,\mu)\;\Rightarrow\; Z_{\lambda\,\mu\,\nu}(q)=Z_{\nu\,\lambda\,\mu}(q)\end{aligned}$$

Apart from the framing factors $Z_{\lambda\,\mu\,\nu}(q)/Z_{\emptyset\,\emptyset\,\emptyset}(q)$ is equal to the topological vertex [15]. To calculate $Z_{\lambda\,\mu\,\nu}(q)$ we use the transfer matrix approach following [15, 22].

7.3 Transfer matrix approach and Schur functions

To a 3D partition π we can associate a sequence of 2D partitions, $\{\eta(a)\,|\,a\in\mathbb{Z}\}$, by taking diagonal slices of π as shown in Fig. 16(a),

$$\eta(a)=\{\pi_{i+a,i}\,|\,i\geq max(1,-a+1)\}\,. \quad (112)$$

These diagonal slices are perpendicular to the (x,y) plane and their projections on the base are given by a set of equations parameterized by $a\in\mathbb{Z}$: $x-y=a$.

Each slice obtained from the plane partition will be a 2D partition. Since these 2D partitions come from a plane partition, they satisfy the interlacing condition. Two 2D partitions μ and ν interlace, $\mu\succ\nu$, if:

$$\mu_1\geq\nu_1\geq\mu_2\geq\nu_2\geq\dots \quad (113)$$

The diagonal slices $\{\eta(a)\,|\,a\in\mathbb{Z}\}$ of a 3D partition π are such that

$$\begin{aligned}\eta(a+1) &\succ \eta(a)\,,\quad a<0\,, \quad (114)\\ \eta(a) &\succ \eta(a+1)\,,\; a\geq 0\,.\end{aligned}$$

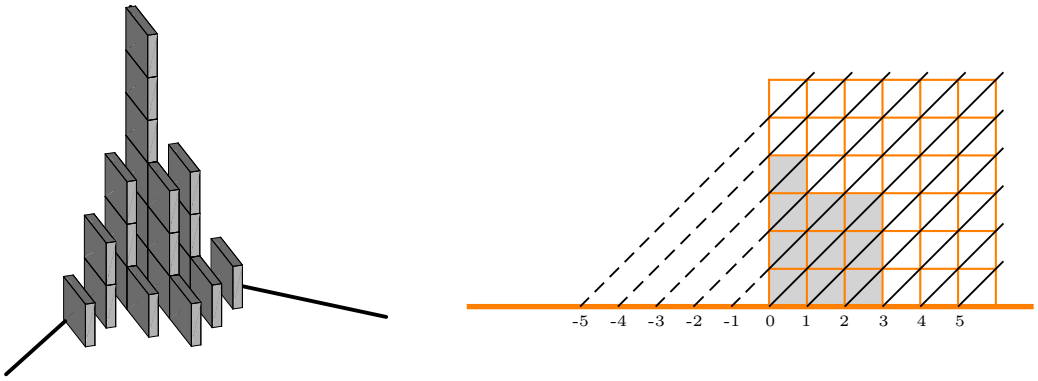

(a) (b)

Figure 16: (a) The diagonal slicing of the plane partition: we end up with a series of 2D partitions that obey the interlacing condition Eq. (114), (b) The slices are parametrized by integers

There exists a very useful set of coordinates to describe the 2D partitions called the *Frobenius coordinates*:

$$a_i = \mu_i - i + \frac{1}{2}\,, \quad b_i = \mu_i^t - i + \frac{1}{2}\,, \quad i = 1, 2, \cdots, d(\mu) \tag{115}$$

where $d(\mu)$ is the number of squares along the diagonal of μ. In terms of Frobenius coordinates, one can relate certain fermionic states to the 2D partition

$$|\mu\rangle = \prod_{i=1}^{d} \psi_{a_i}^* \psi_{b_i} |0\rangle \tag{116}$$

where ψ_a, ψ_a^*, $a \in \mathbb{Z} + 1/2$ are the generators of the Clifford algebra satisfying the following anti-commutation relations:

$$\{\psi_a, \psi_b\} = 0, \ \{\psi_a^*, \psi_b^*\} = 0, \ \{\psi_a, \psi_b^*\} = \delta_{ab}. \tag{117}$$

One can define operators analogous to creation and annihilation operators which can be written in terms of the modes J_n of the fermionic current $\psi^*\psi$,

$$\Gamma_\pm(z) = \exp\left(\sum_{n>0} \frac{z^n J_{\pm n}}{n}\right). \tag{118}$$

The modes J_n of the fermionic bilinear are such that

$$J_n \;=\; \sum_{k\in\mathbb{Z}+\frac{1}{2}} \psi_{k+n}\psi_k^*\,,\;\; n=\pm1,\pm2,\cdots\,, \tag{119}$$

and satisfying the commutation relations

$$[J_n,J_m]=-n\delta_{n+m,0}\,,\;\; [J_n,\psi_k]=\psi_{k+n}\,,\;\; [J_n,\psi_k^*]=-\psi^*_{k-n}\,. \tag{120}$$

The operators $\Gamma_\pm(x)$ satisfy the following commutation relation,

$$\Gamma_+(x)\Gamma_-(y)=(1-xy)\Gamma_-(y)\Gamma_+(x) \tag{121}$$

The relevance to the creation and annihilation operators becomes more evident if their action on a state corresponding to a 2D partition is considered:

$$\begin{aligned}\prod_i \Gamma_+(x_i)|\lambda\rangle &= \sum_\mu s_{\mu/\lambda}(x_1,x_2,\cdots)|\mu\rangle \\ \prod_i \Gamma_-(x_i)|\lambda\rangle &= \sum_\mu s_{\lambda/\mu}(x_1,x_2,\cdots)|\mu\rangle\end{aligned} \tag{122}$$

Since

$$s_{\lambda/\mu}(1)=\left\{\begin{array}{ll} 1, & \text{if}\,\lambda\succ\mu \\ 0, & \text{otherwise.}\end{array}\right\}\,, \tag{123}$$

it follows from Eq. (122) that

$$\begin{aligned}\Gamma_+(1)|\lambda\rangle &= \sum_{\mu\succ\lambda}|\mu\rangle, \\ \Gamma_-(1)|\lambda\rangle &= \sum_{\lambda\succ\mu}|\mu\rangle.\end{aligned} \tag{124}$$

The generating function of the number of plane partitions $Z_{3D}(q):=Z_{\emptyset\emptyset\emptyset}(q)$ can be now expressed using $\Gamma_\pm$ as

$$Z_{\emptyset\emptyset\emptyset}(q)=\langle\emptyset|\left(\prod_{t=0}^{\infty}q^{L_0}\Gamma_-(1)\right)q^{L_0}\left(\prod_{t=-\infty}^{-1}\Gamma_+(1)q^{L_0}\right)|\emptyset\rangle \tag{125}$$

where L_0 is the Hamiltonian such that the operator q^{L_0} moves a diagonal slice by one unit. The action of the operator q^{L_0} on a state corresponding to a 2D partition is defined as

$$q^{L_0}|\mu\rangle=q^{|\mu|}|\mu\rangle \tag{126}$$

The intuitive way of understanding the form of the partition function in terms of the creation and annihilation operators is straightforward: we start with the slice at $a = -\infty$ with the empty set and act on this slice with $\Gamma_+(1)$ to create all possible partitions as a sum. On the next slice (as we go from $a = -\infty$ to 0), we apply the creation operator on this sum, we again create all possible partitions such that they interlace the partitions in the previous slice. We keep acting with $\Gamma_+(1)$, until we hit the main slice $a = 0$. The main slice is where we start applying the annihilation operator $\Gamma_-(1)$ which destroys the previously created partitions, essentially by "creating" 2D partitions on the slice a that are interlaced by the partitions on the previous slice $a - 1$, for positive a's. This procedure, with the operators q^{L_0}'s, gives the sum of $q^{|\pi|}$ over all possible 3D partitions satisfying the interlacing condition that we stated before. Note that Γ_- acting on the vacuum gives zero, so we can move the Γ_-'s to the right to act on the vacuum, and use the commutation relations between $\Gamma_\pm$'s each time we pass them through each other. In [15], it is shown that $Z_{3D}(q)$ is actually the McMahon function;

$$Z_{3D}(q) = \prod_{n>0} \frac{1}{(1-q^n)^n}. \tag{127}$$

7.4 Partition function with an infinite number of parameters

In the previous section, we briefly outlined the systematic way to compute the partition function $Z_{3D}(q)$. We assumed that the partition at each slice is counted with the same parameter q. In this section, following [22] we want to describe the generalization of this to an infinite number of parameters and show that this generalization gives the same partition function when the different parameters on each slice are set to be equal to each other. Let us begin with the case when $\lambda = \mu = \emptyset$ and then we will allow λ and μ to be non-trivial. We keep our convention from the previous section that an integer a is used to describe each slice and we associate the parameter q_a to each slice. For a 2D partition ν, we can divide the corners of the pictorial representation of the corresponding partition into two groups: inner and outer corners. We parametrize the inner and outer corners by their coordinates, v_i and u_i respectively, of their projection onto the real line as shown in Fig. 17. It is easy to see that [22]

$$\sum_{i=0}^{M} v_i = \sum_{i=0}^{M-1} u_i\,, \quad M = \#\text{ of outer corners}\,. \tag{128}$$

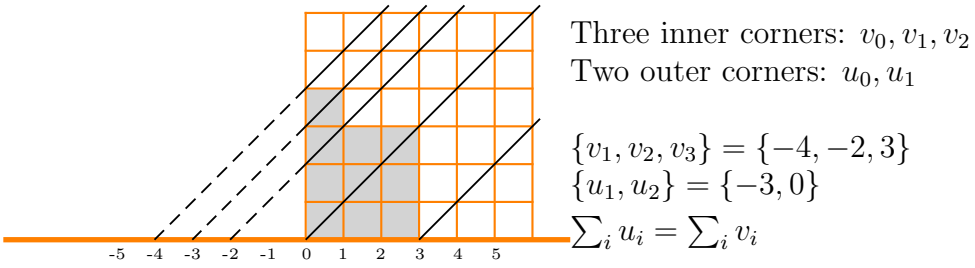

Figure 17: Inner and Outer corners of the partition $\nu = (4, 3, 3)$.

It is convenient to introduce another set of parameters $\{x_m^{\pm} \,|\, m \in \mathbb{Z} + \frac{1}{2}\}$ and identify them with q_a's in the following shape dependent way [22],

$$\begin{aligned} \frac{x^+_{m+1}}{x^+_m} &= q_{m+\frac{1}{2}}\,, \quad m > v_M \text{ or } u_i - 1 > m > v_i\,, \\ x^+_{u_i-\frac{1}{2}} x^-_{u_i+\frac{1}{2}} &= q_{u_i}^{-1}\,, \\ x^-_{v_i-\frac{1}{2}} x^+_{v_i+\frac{1}{2}} &= q_{v_i}\,, \\ \frac{x^-_m}{x^-_{m+1}} &= q_{m+\frac{1}{2}}\,, \; m < v_1 \text{ or } v_{i+1} - 1 > m > u_i\,. \end{aligned} \tag{129}$$

The generating function of the 3D partitions is then given by [22]

$$\begin{aligned} Z_{3D}(\mathbf{q}) = \sum_{\pi} \prod_{a\in\mathbb{Z}} q_a^{|\eta_a|} &= \langle 0| \prod_{k=-\infty}^{0} \Gamma_-(x^+_{-k+\frac{1}{2}}) \prod_{k=1}^{\infty} \Gamma_+(x^-_{-k+\frac{1}{2}}) |0\rangle \\ &= \prod_{k_1=1}^{\infty}\prod_{k_2=1}^{\infty} \left(1 - x^+_{k_1-\frac{1}{2}} x^-_{-k_2+\frac{1}{2}}\right)^{-1} \end{aligned} \tag{130}$$

$$\begin{aligned} x^+_{k-\frac{1}{2}} &= \prod_{i=0}^{k-1} q_i\,, \; k \geq 1\,, \\ x^-_{-\frac{1}{2}} &= 1\,, \; x^-_{-k+\frac{1}{2}} = \prod_{i=1}^{k-1} q_{-i}\,, \; k \geq 2\,. \end{aligned} \tag{131}$$

$$Z_{3D}(\mathbf{q}) = \prod_{k_1=1}^{\infty}\prod_{k_2=1}^{\infty} \left(1 - \prod_{i=0}^{k_1-1} q_i \prod_{j=1}^{k_2-1} q_{-j}\right)^{-1} \tag{132}$$

For $q_i = q\,,\, i \in \mathbb{Z}$ we get

$$Z_{3D}(q) = \prod_{k=1}^{\infty} (1 - q^k)^{-k}\,. \tag{133}$$

Having shown that setting all parameters equal to each other agrees with what we originally obtained, we can continue to develop the generalization to non-trivial λ and μ. The partition function with $\lambda = \mu = \emptyset$ is given by (ν being the 2D partition in the preferred direction)

$$\begin{aligned} Z_\nu(\mathbf{q}) &= P_{\emptyset\,\emptyset\,\nu}(\mathbf{q}) = \prod_{(i,j)\in\nu^c} (1 - q_{(i,j)})^{-1}\,, \\ q_{(i,j)} &= \prod_{(a,b)\in H(i,j)} q_{b-a}\,, \end{aligned} \tag{134}$$

where $H(i,j)$ is the set of boxes which form the hook of (i,j).

The partition function $Z_{3D}(\mathbf{q})$ can be written as a product over boxes of $\sigma(\infty)$ such that each box contributes a factor of $(1-x)^{-1}$ where x is the product of parameters q_i intersected by the hook length[8]. A similar interpretation in terms of hook length exists for the generating function of skew plane partitions.

We define $P_{\lambda\mu\nu}(\mathbf{q})$ as [22]

$$P_{\lambda\mu\nu}(\mathbf{q}) = \sum_{\pi \searrow \pi_0} \prod_{k\in\mathbf{Z}} q_k^{|\lambda(k)|} \tag{135}$$

Where the sum is over all 3D partitions π such that π asymptotically approaches λ, μ and ν along the three axes and π_0 is a 3D partition with the least number of boxes. Each such partition π can be sliced along the diagonal such that we get a 2D partition $\pi(a)$ along the diagonal passing through $(0,a)$. In defining $P_{\lambda\mu\nu}(\mathbf{q})$ we weight each slice with a different parameter q_a.

For non-trivial λ and μ the partition function is given by [22]

$$P_{\lambda\mu\nu}(\mathbf{q}) = Z_\nu(\mathbf{q}) \sum_\eta s_{\lambda^t/\eta}(\mathbf{x}^+)\, s_{\mu/\eta}(\mathbf{x}^-)\,, \tag{136}$$

where $\mathbf{x}^\pm = \{x_m^\pm \,|\, m \in \mathbb{Z} + \frac{1}{2}\}$. This is the most general partition function in which each diagonal slice is counted with a different parameter.

At the end of this section, we would like to start talking about how to assign q and t to the slices depending on the shape of ν to get the generalized partition function from the generalized plane partitions. We will leave the physical motivation for the particular choice and the details to the next section.

[8] $Z_{3D}(\mathbf{q}) = \prod_{i,j=1}^\infty (1 - (\prod_{a=1}^i q_{a-j})(\prod_{b=1}^{j-1} q_{i-b}))^{-1}$.

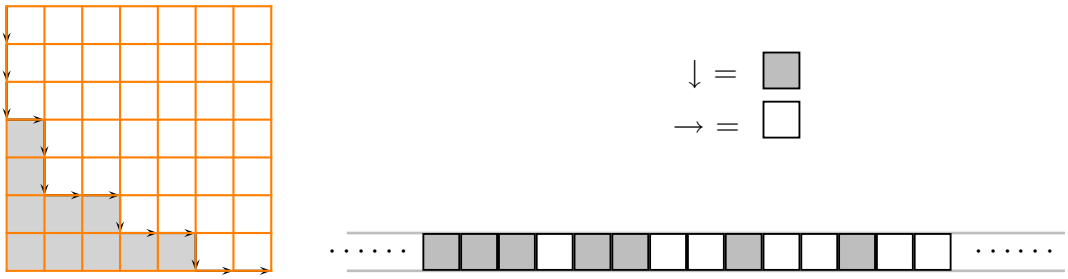

Figure 18: a) We can trace the profile of a particular 2D partition starting at $j = \infty$ and going to $i = \infty$ as depicted in the figure. b) To each vertical pass we associate a black box, and a white one to each horizontal pass. If we put these boxes in a row, then we get a unique "finger print" to a partition. The coordinates of the centers are given by the sets $D^{\pm}$.

Fig. 18 illustrates the idea behind our choice: while following the arrows on the boundary of the 2D partition, every time we have an arrow pointing down, we assign a black box (Fig. 18(b), and every time we have an arrow pointing to the right, we assign a white box. The coordinates of the center of these boxes are given by

$$\begin{aligned} \text{Black Boxes}: \ & \{\mu_i - i + \frac{1}{2} \,|\, i = 1, 2, \cdots\} \\ \text{White Boxes}: \ & \{j - \mu_j^t - \frac{1}{2} \,|\, j = 1, 2, \cdots\} \end{aligned} \tag{137}$$

These coordinates are closely related to the Frobenius coordinates. Note that if we count the number of black boxes to the left of the i^{th} white box, we get ν_i. Similarly, if we count the number of white boxes to the right of the j^{th} black box, we get ν_j^t.

We can divide the half-integers into two sets using the function $\epsilon(n)$ defined as

$$\begin{aligned} \epsilon(n) &= + \text{ if } v_i < n < u_i \\ \epsilon(n) &= - \text{ if } u_i < n < v_{i+1} \end{aligned} \tag{138}$$

for $0 \leq i \leq M - 1$[9]: $D^+ = \{n|\epsilon(n) = +\}$ and similarly $D^- = \{n|\epsilon(n) = -\}$. The sets D^+ and D^- are actually the same as the sets consisting of the coordinates of the center of the black and white boxes, respectively.

[9] M is the number of outer corners.

7.5 Equivariant parameters, boundary of the Young diagram and instanton calculus

The vertex we have obtained so far counts each slice with a different parameter and therefore depends on infinitely many parameters. The usual vertex can be obtained by setting all the parameters equal to q [15, 22]. It is clear that we can obtain the vertex which depends on two parameters by some choice of identification between q_a and t, q. It is not clear a priori what the map $\{q_a \,|\, a \in \mathbb{Z}\} \mapsto \{t, q\}$ should be.

However, the relation between the instanton partition functions and A-model topological string partition function, via geometric engineering, provides some insight into the possible map between the parameters. Recall that the partition function of the 5D compactified $U(1)$ theory can be written as [14]

$$Z(\epsilon_1, \epsilon_2, \beta) = \sum_{\nu} \exp\Big(-\frac{1}{4} \int_{x \neq y} f''_\nu(\epsilon_1, \epsilon_2|x) f''_\nu(\epsilon_1, \epsilon_2|y) \gamma_{\epsilon_1,\epsilon_2}(x-y|\beta, \Lambda) \Big), \tag{139}$$

where

$$\gamma_{\epsilon_1,\epsilon_2}(x|\beta,\Lambda) = \frac{1}{2\epsilon_1\epsilon_2}\Big[-\frac{\beta}{6}\Big(x + \frac{1}{2}(\epsilon_1+\epsilon_2)\Big)^3 + x^2 \log(\beta\Lambda)\Big] + \sum_{n=1}^{\infty} \frac{1}{n} \frac{e^{-\beta n x}}{(1-e^{\beta n \epsilon_1})(1-e^{\beta n \epsilon_2})}$$

and $f_\nu(\epsilon_1, \epsilon_2|x)$ is the profile of the partition ν ($\epsilon_2 > 0 > \epsilon_1$),

$$f_\nu(x|\epsilon_1,\epsilon_2) = |x| + \sum_{i=1}^{\infty} \Big(|x + \epsilon_1 - \epsilon_2 \nu_i - \epsilon_1\, i| - |x - \epsilon_1 - \epsilon_1\, i| - |x - \epsilon_2 \nu_i - \epsilon_1 i| + |x - \epsilon_1 i| \Big).$$

The profile of the partition controls the contribution of the partition to the partition function. The parameters $-\epsilon_1$ and ϵ_2 are the height and the width of the boxes in the partition as shown in Fig. 19. Since these 2D partitions on the edges are the boundaries of the 3D partitions therefore the height and the width of the 3D box is exactly $-\epsilon_1, \epsilon_2$ as shown in Fig. 20.

Hence in constructing the 3D partition from the diagonal slices as we move the slice towards the left we move it an amount $-\epsilon_1$ and as we move it upward we move it an amount ϵ_2. In the transfer matrix formalism this implies that different diagonal slices are counted with different parameters $e^{-\epsilon_1}$ and e^{ϵ_2}. Since the shape of the partition ν in the z direction determines the left-ward and upward motion of the slice therefore slices are counted with $e^{-\epsilon_1}$ and e^{ϵ_2} according to the shape of the partition ν.

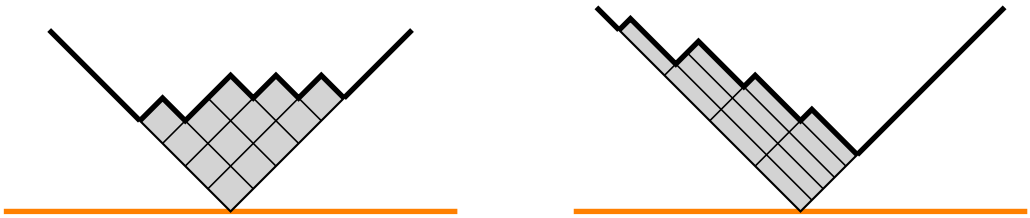

(a) (b)

Figure 19: The profile of the partition is drawn bold; a) shows the 2D partition for the self-dual case $\epsilon_2 = -\epsilon_1$, whereas b) shows the same partition for the non self-dual case $\epsilon_1 \neq \epsilon_2$ ($\epsilon_2 = -2\epsilon_1$)

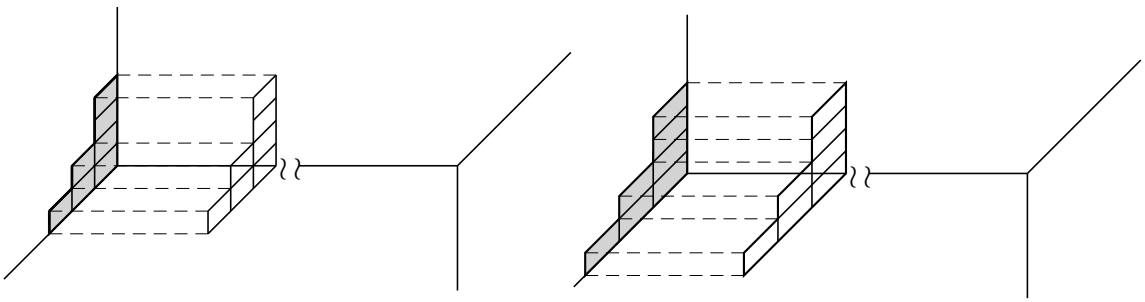

$\epsilon_2 = -\epsilon_1$ $\epsilon_2 = -2\epsilon_1$

(a) (b)

Figure 20: a) The figure shows the partition along the preffered direction for the self-dual case for the toric diagram $\mathcal{O}(-1) \oplus \mathcal{O}(-1) \mapsto \mathbb{P}^1$. b) the same as in a) but for $\epsilon_2 = -2\epsilon_1$.

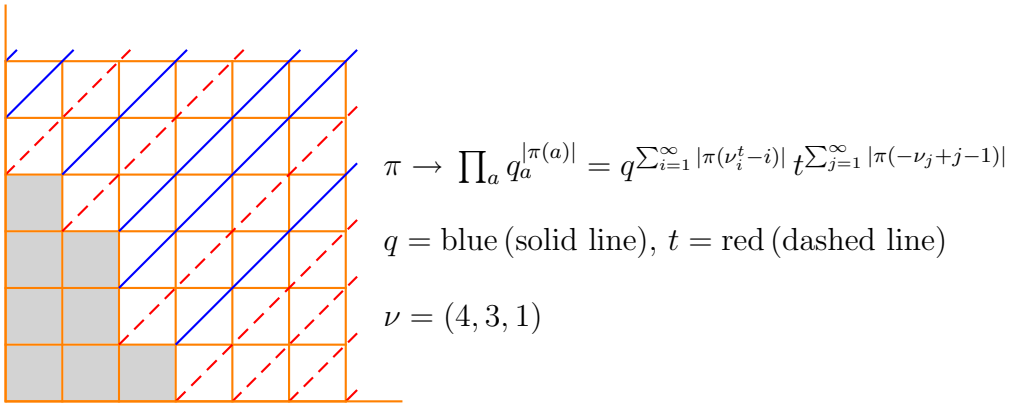

Figure 21: Slices of the 3D partitions are counted with parameters t and q depending on the shape of ν.

7.6 q, t slices and the boundary of the Young diagram

The generating function of 3D partitions is not difficult to calculate since we need only to specialize the parameters q_a. From the discussion in the previous discussion it follows that for $\nu = \emptyset$,

$$q_a = \begin{cases} t, & a \geq 0 \\ q, & a < 0\,. \end{cases} \tag{140}$$

The partition function $Z_{3D}(\mathbf{q})$ becomes

$$Z_{3D}(t, q) = \prod_{i,j=1}^{\infty} (1 - t^i q^{j-1})\,. \tag{141}$$

But, in general, the shape of ν will determine whether a slice is counted with parameter t or parameter q.

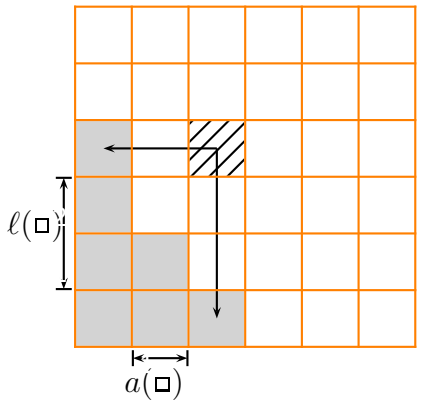

$h(\square) = a(\square) + \ell(\square) + 1$

$a(\square) = \#$ of boxes on the left
$\ell(\square) = \#$ of boxes below

$Z_\nu(t,q) = \prod_{\square \notin \nu}(1 - t^{a(\square)+1} q^{\ell(\square)})^{-1}$

Figure 22: $Z_\nu(t,q)$ is the Hook series of the complement of ν.

For a non-trivial ν, the map between $\{x_m^\pm \,|\, m \in \mathbb{Z} + \frac{1}{2}\}$ and $\{t, q\}$ is given by

$$\begin{aligned} \{x_m^+ | m \in D^+\} &= \{t^i q^{-\nu_i} | i = 1, 2, 3, \cdots\}, \\ \{x_m^- | m \in D^-\} &= \{q^{j-1} t^{-\nu_j^t} | j = 1, 2, 3, \cdots\}, \end{aligned} \tag{142}$$

where D^+ is the set of black boxes and D^- is the set of white boxes in the Maya diagram (Fig. 18(b)) of ν. If we consider the i^{th} white box from the left side, the number of black boxes to the right of this box is given by ν_i. This implies that there is one to one correspondence,

$$\{(m_1, m_2) | m_1 \in D^-, m_2 \in D^+, m_1 \geq m_2\} \mapsto \{(i,j) \in \nu\}, \tag{143}$$

and therefore

$$\{(m_1, m_2) | m_1 \in D^-, m_2 \in D^+, m_1 < m_2\} \simeq \{(i,j) \notin \nu\}, \tag{144}$$

which implies that

$$Z_\nu = \prod_{m_1 < m_2, m_{1,2} \in D^\pm} (1 - x_{m_2}^+ x_{m_1}^-)^{-1} = \prod_{(i,j) \notin \nu} (1 - q^{j-\nu_i - 1} t^{i - \nu_j^t})^{-1} \tag{145}$$

For $\nu = \emptyset$,

$$Z_\emptyset(t,q) := M(t,q) = \prod_{i,j=1}^{\infty} (1 - t^i q^{j-1})^{-1}. \tag{146}$$

$M(t,q)$ is a two parameter generalization of the MacMahon function.

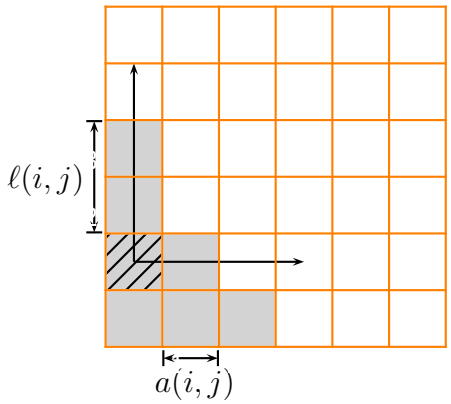

$h(\square) = a(\square) + \ell(\square) + 1$

$a(\square) = \#$ of boxes on the right
$\ell(\square) = \#$ of boxes on top

$\prod_{\square\in\nu}(1-q^{h(\square)})^{-1} \;\to = \prod_{\square\in\nu}(1-t^{a(\square)+1}q^{\ell(\square)})^{-1}$

$s_{(4\,2\,1)}(q) = \frac{1}{(1-q)^3(1-q^2)(1-q^3)(1-q^4)(1-q^6)}$
$\widetilde{Z}_{(4\,2\,1)}(t,q) = \frac{1}{(1-t)^3(1-t\,q)(1-t^2\,q^2)(1-t^3\,q^3)}$

Figure 23: A Young diagram $\nu = (4\,2\,1)$.

If we define $q = e^{i\epsilon_1}, t = e^{-i\epsilon_2}$ then $\log M(t,q)$ is symmetric in ϵ_1, ϵ_2 (upto an infinite constant)

$$\begin{aligned}\log M(t,q) &= \frac{\zeta(3)}{\epsilon_1\epsilon_2} - i\frac{\zeta(2)}{2}\Big(\frac{\epsilon_1+\epsilon_2}{\epsilon_1\epsilon_2}\Big) + \frac{\zeta(1)}{12}\Big(\frac{(\epsilon_1+\epsilon_2)^2+\epsilon_1\epsilon_2}{\epsilon_1\epsilon_2}\Big) + i\frac{\zeta(0)}{24}(\epsilon_1+\epsilon_2) \\ &+ \sum_{g_1+g_2\geq 2}(-1)^{g_1+g_2}\frac{B_{2g_1}B_{2g_2}B_{2g_1+2g_2-2}}{(2g_1)!(2g_2)!(2g_1+2g_2-2)}\,\epsilon_1^{2g_1-1}\epsilon_2^{2g_2-1}\,.\end{aligned}$$

It is easy to show that (Appendix C) if we define

$$\widetilde{Z}_\nu(t,q) \;:=\; \frac{Z_\nu(t,q)}{Z_\emptyset(t,q)}\,, \tag{147}$$

then $\widetilde{Z}_\nu(t,q)$ can be written as a product over boxes of ν,

$$\widetilde{Z}_\nu(t,q) = \prod_{s\in\nu}(1-t^{a(s)+1}q^{\ell(s)})^{-1} = \prod_{s\in\nu^t}(1-t^{\ell(s)+1}q^{a(s)})^{-1}\,. \tag{148}$$

The function $\widetilde{Z}_\nu(t,q)$ is a specialization of the Macdonald symmetric function $P(\mathbf{x};q,t)$ [25],

$$\widetilde{Z}_\nu(t,q) = t^{-\frac{||\nu||^2}{2}}\,P_{\nu^t}(t^{-\rho};q,t)\,. \tag{149}$$

Thus we see that this particular specialization of the Macdonald function can be interpreted as counting skew plane partitions such that the shape of ν determines whether to count a box with t or q.

When all three partitions (λ,μ,ν) are non-trivial, the partition function (in diagonal slicing)

is given by

$$
\begin{aligned}
P_{diag}(\lambda\mu\nu) &= \langle\lambda^t| \prod_{m\in Z+\frac{1}{2}} \Gamma_{-\epsilon(m)}(x_m^{\epsilon(m)})|\mu\rangle\,, \qquad (150)\\
&= \langle\lambda^t| \prod_{m\in D^+} \Gamma_-(x_m^+) \prod_{m\in D^-} \Gamma_+(x_m^-)|\mu\rangle \prod_{m_1<m_2, m_1\in D^-, m_2\in D^+} (1-x_{m_2}^+ x_{m_1}^-)^{-1}\,,\\
&= t^{-|\lambda|}\, Z_\nu(t,q) \sum_\eta s_{\lambda^t/\eta}(\mathbf{x}^+) s_{\mu/\eta}(\mathbf{x}^-)\\
&= t^{-\frac{|\lambda|}{2}}\, q^{-\frac{|\mu|}{2}} Z_\nu(t,q) \sum_\eta \left(\frac{q}{t}\right)^{|\eta|/2} s_{\lambda^t/\eta}(t^{-\rho}q^{-\nu}) s_{\mu/\eta}(t^{-\nu^t}q^{-\rho}),
\end{aligned}
$$

where $\rho = \{-\frac{1}{2}, -\frac{3}{2}, -\frac{5}{2}, \cdots\}$.

To convert the above partition function in the diagonal slicing to the partition function in the perpendicular slicing we multiply by $q^{-n(\lambda^t)}\, t^{-n(\mu)}$ [15]. The perpendicular partition function is then given by

$$
\begin{aligned}
P_{\lambda\mu\nu}(t,q) &= q^{-n(\lambda^t)-\frac{|\mu|}{2}}\, t^{-n(\mu)-\frac{|\lambda|}{2}}\, Z_\nu(t,q) \sum_\eta \left(\frac{q}{t}\right)^{|\eta|/2} s_{\lambda^t/\eta}(t^{-\rho}q^{-\nu}) s_{\mu/\eta}(t^{-\nu^t}q^{-\rho}) \qquad (151)\\
&= q^{-\frac{||\lambda||^2}{2}}\, t^{-\frac{||\mu^t||^2}{2}}\, Z_\nu(t,q) \sum_\eta \left(\frac{q}{t}\right)^{\frac{|\eta|+|\lambda|-|\mu|}{2}} s_{\lambda^t/\eta}(t^{-\rho}q^{-\nu}) s_{\mu/\eta}(t^{-\nu^t}q^{-\rho}).
\end{aligned}
$$

The refined topological vertex is given by

$$
\begin{aligned}
C_{\lambda\mu\nu}(t,q) &= q^{f(\nu)}\, t^{g(\nu)}\, q^{\frac{||\lambda||^2}{2}+\frac{||\mu||^2}{2}} \frac{P_{\lambda\mu\nu}(t,q)}{M(t,q)} \qquad (152)\\
&= q^{f(\nu)}\, t^{g(\nu)} \left(\frac{q}{t}\right)^{\frac{||\mu||^2}{2}} t^{\frac{\kappa(\mu)}{2}} \frac{Z_\nu(t,q)}{M(t,q)} \sum_\eta \left(\frac{q}{t}\right)^{\frac{|\eta|+|\lambda|-|\mu|}{2}} s_{\lambda^t/\eta}(t^{-\rho}q^{-\nu}) s_{\mu/\eta}(t^{-\nu^t}q^{-\rho})\\
&= q^{f(\nu)}\, t^{g(\nu)} \left(\frac{q}{t}\right)^{\frac{||\mu||^2}{2}} t^{\frac{\kappa(\mu)}{2}} \widetilde{Z}_\nu(t,q) \sum_\eta \left(\frac{q}{t}\right)^{\frac{|\eta|+|\lambda|-|\mu|}{2}} s_{\lambda^t/\eta}(t^{-\rho}q^{-\nu}) s_{\mu/\eta}(t^{-\nu^t}q^{-\rho}).
\end{aligned}
$$

The functions $f(\nu)$ and $g(\nu)$ are such that

$$
f(\nu) + g(\nu) = \tfrac{||\nu||^2}{2}\,. \qquad (153)
$$

This one relation is not enough to fix the two functions $f(\nu)$ and $g(\nu)$ therefore we will make a choice here and take $g(\nu) = 0$. The one partition topological vertex is equal to

a specialization of the Schur function, $s_{\nu^t}(q^{-\rho})$, and with the above choice of $g(\nu)$ the one partition refined topological vertex is equal to the generalization of the Schur function,

$$C_{\emptyset\emptyset\nu}(t,q) = q^{\frac{||\nu||^2}{2}}\,\widetilde{Z}_\nu(t,q) \begin{cases} = q^{\frac{\kappa(\nu)}{2}} Q_\nu(q^{-\rho};t,q), \\ = \left(\frac{q}{t}\right)^{\frac{||\nu||^2}{2}} P_{\nu^t}(t^{-\rho};q,t)\,. \end{cases} \tag{154}$$

where $P_\nu(\mathbf{x};q,t)$ is the Macdonald function and $Q_\nu(\mathbf{x};q,t)$ is dual of the Macdonald function. As we will show in the next section this choice gives correct A-model partition functions. The refined vertex becomes,

$$\boxed{C_{\lambda\,\mu\,\nu}(t,q) = \left(\frac{q}{t}\right)^{\frac{||\mu||^2+||\nu||^2}{2}} t^{\frac{\kappa(\mu)}{2}}\, P_{\nu^t}(t^{-\rho};q,t)\, \sum_\eta \left(\frac{q}{t}\right)^{\frac{|\eta|+|\lambda|-|\mu|}{2}} s_{\lambda^t/\eta}(t^{-\rho}q^{-\nu}) s_{\mu/\eta}(t^{-\nu^t}q^{-\rho})}$$

For $t=q$ the above reduces to the usual topological vertex since $P_\nu(q^{-\rho};q,q) = s_\nu(q^{-\rho})$.

7.7 Framing factors

Recall that the framing factor arises whenever the $\mathbb{P}^1$ along which the two vertices are glued has a global geometry other than $\mathcal{O}(-1)\oplus\mathcal{O}(-1)\mapsto\mathbb{P}^1$. For $q=t$ the framing factor is given by $q^{-\frac{\kappa(\mu)}{2}}$.

Since the two directions orthogonal to the preferred direction correspond to the parameters t and q therefore rotations along these directions will be counted with these two parameters. Rotating the ν diagram along the first row gives $n(\nu)$ extra boxes which we count with the parameter t. Then, rotating the diagram along the first column gives $n(\nu^t)$ boxes which we count with the parameter q. Thus, the framing factor along the preferred direction is given by

$$f_\nu(t,q) := (-1)^{|\nu|}\, t^{n(\nu)}\, q^{-n(\nu^t)} = (-1)^{|\nu|} \left(\frac{t}{q}\right)^{n(\nu)} q^{-\frac{\kappa(\nu)}{2}}\,, \tag{155}$$

where we have introduced a factor of $(-1)^{|\nu|}$ for later convenience.

The framing factor when $t\neq q$ can also be calculated from the geometry of instanton moduli spaces following [28]. The simplest case is to take the $U(1)$ theory with the charge k instanton moduli space given by $\mathrm{Sym}^k(\mathbb{C}^2)$ and consider a supersymmetric quantum mechanics on this moduli space with coupling to an external gauge field. A shown in [28] the effect of this

extra coupling is to introduce an extra term, which is the framing factor, in the partition function given by

$$\begin{aligned} e^{\sum_{(i,j)\in\nu}(\epsilon_1(i-1)+\epsilon_2(j-1))} &= t^{\sum_{(i,j)\in\nu}(i-1)}\, q^{-\sum_{(i,j)\in\nu}(j-1)} \\ &= t^{n(\nu)} q^{-n(\nu^t)}\,. \end{aligned} \tag{156}$$

This is exactly the framing factor one gets from the combinatorics of 3D partitions.

8 Appendix B: Gromov-Witten Theory and Refined Partition Function: The case of $\mathcal{O}(-1)\oplus\mathcal{O}(-1)\mapsto\mathbb{P}^1$

It is interesting to consider the case of $\mathcal{O}(-1)\oplus\mathcal{O}(-1)\mapsto\mathbb{P}^1$ from the point of view of Gromov-Witten theory [20]. In this case the refined partition function can be obtained from the Gromov-Witten theory and has a interesting interpretation from the localization point of view which might be useful for other toric CY3-folds.

The multi-cover contribution is given by [20]

$$\begin{aligned} C(g,d) &= \int_{[\overline{\mathcal{M}}_{g,0}(\mathbb{P}^1,d)]^{vir}} c_{top}(R^1\pi_*\mu^*N) \\ &= d^{2g-3}\,\frac{|B_{2g}(2g-1)|}{(2g)!}\,,\;\; g\geq 0\,. \end{aligned} \tag{157}$$

Where B_n are Bernoulli numbers defined as $\sum_{m\geq 0}\frac{B_m}{m!}t^m=\frac{t}{e^t-1}$.

The partition function can be calculated using the multicover contribution and is given by

$$Z=\mathrm{Exp}\Big(\sum_{g\geq 0}\sum_{d\geq 1}\lambda_s^{2g-2}Q^d C(g,d)\Big)=\prod_{n=1}^{\infty}(1-q^n\,Q)^{-n}\,,\;\; q=e^{-\lambda_s}\,. \tag{158}$$

However, using localization $C(g,d)$ can also be written as [20, 21]

$$\begin{aligned} C(g,d) &= d^{2g-3}\sum_{g_1+g_2=g, g_{1,2}\geq 0} C_{g_1,g_2}\,,\quad C_{g_1,g_2}=b_{g_1}b_{g_2} \\ b_g &= \begin{cases} 1, & \text{for } g=0 \\ \int_{\overline{\mathcal{M}}_{g,1}}\psi_1^{2g-2}\lambda_g=\frac{2^{2g-1}-1}{2^{2g-1}}\,\frac{|B_{2g}|}{(2g)!}, & \text{for } g\geq 1\,. \end{cases} \end{aligned} \tag{159}$$

Essentially the contribution $b_{g_1} b_{g_2}$ is from degenerate worldsheets of genus $g_1 + g_2$ such that the two components of genus g_1 and g_2 map to the two fixed points of X. By weighing the contribution the two fixed points differently we get

$$\begin{aligned} \widehat{Z} &= \mathrm{Exp}\Big(\sum_{g_1,g_2 \geq 0} \lambda_1^{2g_1-1} \lambda_2^{2g_2-1} Q^d \, d^{2g-3} \, b_{g_1} b_{g_2} \Big) \\ &= \prod_{n,m=1}^{\infty} \Big(1 - q^{n-\frac{1}{2}} t^{m-\frac{1}{2}} \, Q \Big) \,, \;\; q = e^{-\lambda_1} \,, t = e^{-\lambda_2} \,. \end{aligned} \tag{160}$$

Which is exactly the refined topological string partition function.

A similar calculation for the case of target space $\mathbb{C}^3$ gives the constant map contribution to the topological string partition function, *i.e.*, the MacMahon function.

$$\begin{aligned} C_g := \int_{\overline{\mathcal{M}}_g} \lambda_{g-1}^3 &= \frac{|B_{2g-2}|}{2g-2} \sum_{g_1+g_2=g} b_{g_1} b_{g_2} \\ &= |\zeta(3-2g)| \sum_{g_1+g_2=g} b_{g_1} b_{g_2} = \sum_{g_1+g_2=g} \widehat{C}_{g_1,g_2} \,, \\ \widehat{C}_{g_1,g_2} &= |\zeta(3-2g_1-2g_2)| \, b_{g_1} \, b_{g_2} \end{aligned} \tag{161}$$

where B_n is the n^{th} Bernoulli number and we have used the identity $B_n = (-1)^{n+1} n \, \zeta(1-n)$.

$$M(q) = \mathrm{Exp}\Big(\sum_{g \geq 0} \lambda^{2g-2} C_g \Big) = \prod_{n \geq 1} (1-q^n)^{-n} \quad \Rightarrow \quad \begin{aligned} \widetilde{M}(t,q) &= \mathrm{Exp}\Big(\sum_{g_1,g_2 \geq 0} \lambda_1^{2g_1-1} \lambda_2^{2g_2-1} \widehat{C}_{g_1,g_2} \Big) \\ &= \prod_{n,m \geq 1} (1 - q^{n-\frac{1}{2}} t^{m-\frac{1}{2}})^{-1} \,. \end{aligned}$$

The function $M(q)$ is the MacMahon function and is the generating function of the number of 3D partitions,

$$\begin{aligned} M(q) &= \sum_{n=0}^{\infty} p(n) \, q^n \\ p(n) &= \#\text{ of plane partitions of } n \,. \end{aligned} \tag{162}$$

The function $\widetilde{M}(t,q)$ also has a combinatorial interpretation in terms of 3D partitions,

$$\widetilde{M}(t,q) = \sum_{\pi} p(|\pi_+|, |\pi_-|) t^{|\pi_+|} q^{|\pi_-|} \,, \tag{163}$$

where π_+ and π_- are two parts of the 3D partition π obtained by cutting π by the plane $x = y$. $|\pi_+|$ and $|\pi_-|$ are the volumes of the two parts such that $|\pi_+| + |\pi_-| = |\pi|$ and $p(n,m)$ is the number of 3D partitions with $(|\pi_+|, |\pi_-|) = (n,m)$.

9 Appendix C: An Important Identity

In this appendix we prove the identity

$$\widetilde{Z}_\nu(t,q) = \frac{Z_\nu(t,q)}{M(t,q)}. \tag{164}$$

Proof: Consider the following identity [10]

$$\sum_{i,j=1}^{\infty}\left(t^{i-\nu_{1,j}}q^{j-\nu^t_{2,i}-1} - t^i q^{j-1}\right) = \sum_{s\in\nu_1} t^{-\ell_{\nu_1}(s)}q^{-a_{\nu_2}(s)-1} + \sum_{s\in\nu_2} t^{\ell_{\nu_2}(s)+1}q^{a_{\nu_1}(s)}. \tag{165}$$

Let us set $\nu_1 = \nu_2 = \nu^t$

$$\begin{aligned}\sum_{i,j=1}^{\infty}\left(t^{i-\nu^t_j}q^{j-\nu_i-1} - t^i q^{j-1}\right) &= \sum_{s\in\nu^t}\left(t^{-\ell_{\nu^t}(s)}q^{-a_{\nu^t}(s)-1} + t^{\ell_{\nu^t}(s)+1}q^{a_{\nu^t}(s)}\right)\\ &= \sum_{s\in\nu}\left(t^{-a_\nu(s)}q^{-\ell_\nu(s)-1} + t^{a_\nu(s)+1}q^{\ell_\nu(s)}\right).\end{aligned} \tag{166}$$

The substitutions $q\to q^m$ and $t\to t^m$ will allow us to find a formal expansion of log:

$$\begin{aligned}\sum_{m=1}^{\infty}\frac{1}{m}\sum_{i,j=1}^{\infty}t^{m(i-\nu^t_j)}q^{m(j-\nu_i-1)} &- \sum_{m=1}^{\infty}\frac{1}{m}\sum_{(i,j)\in\nu}t^{m(i-\nu^t_j)}q^{m(j-\nu_i-1)}\\ &= \sum_{m=1}^{\infty}\frac{1}{m}\sum_{i,j=1}^{\infty}t^{mi}q^{m(j-1)} + \sum_{m=1}^{\infty}\frac{1}{m}\sum_{s\in\nu}t^{m(a_\nu(s)+1)}q^{m\ell_\nu(s)}.\end{aligned} \tag{167}$$

If the order of the $m-$summation is changed with the one following it, one actually gets the identity we are trying to prove:

$$\begin{aligned}\sum_{i,j=1}^{\infty}\log\left(1-t^{i-\nu^t_j}q^{j-\nu_i-1}\right) &- \sum_{(i,j)\in\nu}\log\left(1-t^{i-\nu^t_j}q^{j-\nu_i-1}\right)\\ &= \sum_{i,j=1}^{\infty}\log\left(1-t^iq^{j-1}\right) + \sum_{s\in\nu}\log\left(1-t^{a_\nu(s)+1}q^{\ell_\nu(s)}\right).\end{aligned} \tag{168}$$

This can be put in a more suggestive form by exponentiating both sides and taking the inverse

$$\begin{aligned}\frac{\prod_{i,j=1}^{\infty}\left(1-t^{i-\nu^t_j}q^{j-\nu_i-1}\right)^{-1}}{\prod_{(i,j)\in\nu}\left(1-t^{i-\nu^t_j}q^{j-\nu_i-1}\right)^{-1}} &= \prod_{(i,j)\notin\nu}\left(1-t^{i-\nu^t_j}q^{j-\nu_i-1}\right)^{-1}\\ &= \prod_{i,j=1}^{\infty}\left(1-t^iq^{j-1}\right)^{-1}\prod_{s\in\nu}\left(1-t^{a_\nu(s)+1}q^{\ell_\nu(s)}\right)^{-1}.\end{aligned} \tag{169}$$

10 Appendix D: Schur Functions

This appendix should serve as a review of the definition and some properties we have used of the Schur functions. Before defining the Schur function, let us introduce the antisymmetric polynomial a_α of a finite number of variables $\{x_i\}_{i=1}^n$:

$$a_\alpha(x_1,\ldots,x_n) = \sum_{\omega\in S_n} \epsilon(\omega)\ \omega(x^\alpha) \tag{170}$$

where $\epsilon(\omega)$ serves as the antisymmetrizer for an element ω of the symmetric group S_n and x^α is a shorthand notation for the monomial $x_1^{\alpha_1}\ldots x_n^{\alpha_n}$. We have a non-vanishing polynomial $a_\alpha(x_i)$ only if all α_i's are different. That allows us to put the exponents of the variables, without loss of generality, into a particular ordering: $\alpha_1 > \alpha_2 > \cdots > \alpha_n \geq 0$. The freedom of choosing such an ordering among α_i's enables us to connect the polynomials $a_\alpha(x_i)$ to partitions, so we can write $\alpha = \lambda + \delta$ for a partition λ with length $\ell(\lambda) \leq n$ and $\delta = (n-1, n-2, \ldots, 1, 0)$. The polynomial $a_\alpha(x_i)$ can be now rewritten in terms of the partition λ as

$$a_{\lambda+\delta}(x_1,\ldots,x_n) = \sum_{\omega} \epsilon(\omega)\ \omega(x^{\lambda+\delta}). \tag{171}$$

This particular form of the polynomial $a_\alpha(x_i)$ makes it more evident to express this sum as a determinant

$$a_{\lambda+\delta}(x_1,\ldots,x_n) = det\left(x_i^{\lambda_j+n-j}\right)_{1\leq i,j\leq n}. \tag{172}$$

This form of $a_\alpha(x_i)$ makes it evident that it is divisible in the ring of polynomials in the variables $\{x_i\}_{i=1}^n$ with integer coefficients, $\mathbb{Z}[x_1,\ldots,x_n]$, by any difference of the form $x_i - x_j$ with $1 \leq i < j \leq n$. Then it is divisible by their product as well, hence, by the Vandermonde determinant

$$\prod_{1\leq i<j\leq n} (x_i - x_j) = det\left(x_i^{n-j}\right). \tag{173}$$

Let us denote the above product by a_δ. Now we are ready to define the Schur function $s_\lambda(x_i)$ as a quotient

$$s_\lambda(x_1,\ldots,x_n) \equiv a_{\lambda+\delta}/a_\delta. \tag{174}$$

Note that $s_\lambda(x_i)$ is symmetric and its definition makes sense as long as $\lambda \in \mathbb{Z}^n$ is an integer vector such that $\lambda+\delta$ does not have any negative parts. The Schur functions $s_\lambda(x_i)$ form an

orthonormal basis for the symmetric polynomials which is a subring $\Lambda_n = \mathbb{Z}[x_1, \ldots, x_n]^{S_n}$. The orthonormality requires the definition of the scalar product of symmetric functions. Let us give first the definition and describe later the individual ingredients we use. The scalar product on Λ is a $\mathbb{Z}$-valued bilinear form $\langle u, v \rangle$ such that the bases h_λ and m_μ are dual to each other which is precisely that they satisfy the following relationship:

$$\langle h_\lambda, m_\mu \rangle = \delta_{\lambda\mu} \tag{175}$$

with the Kronecker delta $\delta_{\lambda\mu}$. Given a partition λ, m_λ is defined as the sum over all permutations of the parts of $\lambda = (\lambda_1, \ldots, \lambda_n)$

$$m_\lambda(x_1, \ldots, x_n) = \sum_\alpha x^\alpha. \tag{176}$$

h_λ is defined in terms of the complete symmetric functions h_r as $h_\lambda = h_{\lambda_1} h_{\lambda_2} \ldots$, with

$$h_r = \sum_{|\lambda|=r} m_\lambda \tag{177}$$

where r is the degree of h_r. Finally, Λ is the free $\mathbb{Z}$ module which is generated by the bases m_λ for all λ. Any symmetry function can be written as a linear combination of the Schur functions with the coefficients calculable having the scalar product defined.

The skew Schur function $s_{\lambda/\mu}$ is defined by

$$\langle s_{\lambda/\mu}, s_\nu \rangle = \langle s_\lambda, s_\mu s_\nu \rangle \tag{178}$$

where λ interlaces μ. We can use the fact that the Schur functions form an orthonormal basis and write the skew Schur function in another form

$$s_{\lambda/\mu} = \sum_\nu c^\lambda_{\mu\nu} s_\nu \tag{179}$$

where the $c^\lambda_{\mu\nu}$'s are defined by

$$s_\mu s_\nu = \sum_\lambda c^\lambda_{\mu\nu} s_\lambda \tag{180}$$

and are integers. An equivalent definition of the skew Schur function can be given in terms of the semi-standard tableau, which is obtained by assigning a positive integer to each box in a skew partition such that the numbers weakly increase along the rows, and strictly increase along the columns.

Having introduced the Schur and skew Schur functions, let us also mention the identities we have made use of. If we sum two Schur functions with two sets of independent variables $x = (x_1, x_2, \dots)$ and $y = (y_1, y_2, \dots)$ over all partitions, we get

$$\sum_{\lambda} s_\lambda(x) s_\lambda(y) = \prod_{i,j} (1 - x_i y_j)^{-1}. \tag{181}$$

Had we changed the partition from λ to λ^t in one of the Schur functions, we would end up with

$$\sum_{\lambda} s_{\lambda^t}(x) s_\lambda(y) = \prod_{i,j} (1 + x_i y_j). \tag{182}$$

The Schur function of the variables $(1, q, q^2, \dots)$ can be expressed in terms of a product of terms which are dependent on the hook length of the partition up to an overall factor:

$$s_\lambda(1, q, q^2, \cdots) = q^{n(\lambda)} \prod_{s \in \lambda} (1 - q^{h_\lambda(s)})^{-1} \tag{183}$$

where $n(\lambda)$ is defined as

$$n(\lambda) \equiv \sum_i (i-1)\lambda_i. \tag{184}$$

It is not hard to show that $n(\lambda)$ can be calculated alternatively using the arm length as well as the leg lengths:

$$n(\nu) = \sum_i (i-1)\nu_i = \frac{1}{2} \sum_i \nu_i^t (\nu_i^t - 1) = \sum_{s \in \nu} a'(s) = \sum_{s \in \nu} a_\nu(s)\,, \tag{185}$$

$$n(\nu^t) = \sum_i (i-1)\nu_i^t = \frac{1}{2} \sum_i \nu_i (\nu_i - 1) = \sum_{s \in \nu} \ell'(s) = \sum_{s \in \nu} \ell_\nu(s)\,, \tag{186}$$

with the same $\ell_\nu(s)$ and $a_\nu(s)$ defined previously in the text, and we introduce $\ell'(s) = j - 1$ and $a'(s) = i - 1$[10].

[10]For the sake of completeness, let us also mention some useful relations among $h(\lambda)$, $n(\lambda)$ and $\kappa(\lambda) = 2\sum_{(i,j)\in\lambda}(j-i)$:

$$\begin{aligned} \sum_{s \in \lambda} h_\lambda(s) &= n(\lambda) + n(\lambda^t) + |\lambda| = 2\,n(\lambda) + \frac{1}{2}\kappa(\lambda) + |\lambda| \\ \kappa(\lambda) &= 2(n(\lambda^t) - n(\lambda))\,. \end{aligned}$$

Two skew Schur functions $s_{\lambda/\nu}(x)$ and $s_{\nu/\mu}(y)$ can be summed over all possible partitions satisfying $\mu \prec \nu \prec \lambda$ to give another skew Schur function

$$s_{\lambda/\mu}(x,y) = \sum_{\nu} s_{\lambda/\nu}(x) s_{\nu/\mu}(y). \tag{187}$$

The above sum can be generalized to multiple sums in the following way

$$s_{\lambda/\mu}(x^{(1)},\ldots,x^{(n)}) = \sum_{(\nu)} \prod_{i=1}^{n} s_{\nu^{(i)}/\nu^{(i-1)}}(x^{(i)}) \tag{188}$$

where the summation is again over all partitions $(\nu) = (\nu^{(0)},\ldots,\nu^{(n)})$ satisfying the same interlacing condition generalized to more partitions, $\mu = \nu^{(0)} \prec \nu^{(1)} \prec \cdots \prec \nu^{(n-1)} \prec \nu^{(n)} = \lambda$.

References

[1] S. Katz, A. Klemm and C. Vafa, "Geometric engineering of quantum field theories," *Nucl. Phys.* **B497**, (1997) 173–195, `hep-th/9609239`.

[2] S. Katz, P. Mayr and C. Vafa, "Mirror symmetry and exact solution of 4D N = 2 gauge theories. I," Adv. Theor. Math. Phys. **1**, 53 (1998) `hep-th/9706110`.

[3] N. A. Nekrasov, "Seiberg-Witten prepotential from instanton counting," Adv. Theor. Math. Phys. 7 (2004) 831-864, `hep-th/0206161`.

[4] M. Aganagic, A. Klemm, M. Marino, C. Vafa, "The Topological Vertex," Commun. Math. Phys. 254 (2005) 425-478, `hep-th/0305132`.

[5] A. Iqbal, "All genus topological string amplitudes and 5-brane webs as Feynman diagrams," `hep-th/0207114`.

[6] A. Iqbal, A. -Kian. Kashani-Poor, "Instanton counting and Chern-Simons theory," Adv. Theor. Math. Phys. 7 (2004) 457-497, `hep-th/0212279`.

[7] A. Iqbal, A. -Kian. Kashani-Poor, "$SU(N)$ geometries and topological string amplitudes," `hep-th/0306032`.

[8] T. J. Hollowood, A. Iqbal, C. Vafa, "Matrix Models, Geometric Engineering and Elliptic Genera", `hep-th/0310272`.

[9] A. Iqbal, A. -Kian. Kashani-Poor, "The vertex on the strip", hep-th/0410174.

[10] H. Nakajima, K. Yoshioka, "Instanton counting on blowup-I: 4-Dimensional pure gauge theory", math.AG/0306198.

[11] H. Nakajima, K. Yoshioka, "Instanton counting on blowup-II: K-theoretic partition function", math.AG/0505553.

[12] H. Nakajima, "Lectures on Hilbert Schemes of Points on Surfaces", University Lecture Series, American Mathematical Society (September 1999).

[13] R. Gopakumar, C. Vafa, "M-Theory and Topological Strings–I", hep-th/9809187,
R. Gopakumar, C. Vafa, "M-Theory and Topological Strings–II", hep-th/9812127.

[14] A. Okounkov, N. Nekrasov, "Seiberg-Witten theory and random partitions," hep-th/0306238.

[15] A. Okounkov, N. Reshetikhin, C. Vafa, "Quantum Calabi-Yau and Classical Crystals", hep-th/0309208.

[16] H. Awata, H. Kanno, "Instanton counting, Macdonald functions and the moduli space of D-branes", hep-th/0502061.

[17] M. Aganagic, R. Dijkgraaf, A. Klemm, M. Marino, C. Vafa, "Topological strings and integrable hierarchies", Commun. Math. Phys. 261 (2006) 451-516 hep-th/0312085.

[18] C. Vafa, "Superstrings and topological strings at large N", J. Math. Phys. **42** (2001) 2798-2817, hep-th/0008142.

[19] S. Gukov, A. Iqbal, C. Kozçaz, C. Vafa, Work in progress.

[20] C. Faber, R. Pandharipande, "Hodge integrals and Gromov-Witten theory", math.AG/9810173.

[21] J. Bryan, R. Pandharipande, "Curves in Calabi-Yau 3-folds and Topological Quantum Field Theory", math.AG/0306316.

[22] A. Okounkov, N. Reshetikhin, "Random skew plane partitions and the Pearcey process", hep-th/0503508.

[23] I. Antoniadis, E. Gava, K. S. Narain and T. R. Taylor, "Topological amplitudes in string theory," Nucl. Phys. B **413**, 162 (1994) `hep-th/9307158`.

[24] M. Bershadsky, S. Cecotti, H. Ooguri and C. Vafa, "Kodaira-Spencer theory of gravity and exact results for quantum string amplitudes," Commun. Math. Phys. **165**, 311 (1994) `hep-th/9309140`.

[25] I. G. Macdonald, "Symmetric functions and Hall polynomials," (second edition, 1995), Oxford Mathematical Monographs, Oxford Science Publications.

[26] S. Gukov, A. Schwarz, C. Vafa, "Khovanov-Rozansky Homology and Topological Strings", Lett. Math. Phys.74:53-74, (2005), `hep-th/0412243`.

[27] M. Haiman, "Notes on Macdonal polynomials and the geometry of Hilbert schemes", In *Symmetric Functions 2001*: Surveys of Developments and Perspectives, Proceedings of the NATO Advanced Study Institute held in Cambridge, June 25-July 6, 2001, Kluwer, Dordrecht (2002) 1-64.

[28] Y. Tachikawa, "Five-dimensional Chern-Simons terms and Nekrasov's instanton counting," JHEP **0402**, 050 (2004), `hep-th/0401184`.